Multi-Connectivity Techniques for Improved Performance in Mobile Communications

A Thesis Submitted to the
Department of Electrical Engineering and Electronics
of the University of Liverpool
in accordance with the requirements for the Degree of

DOCTOR OF PHILOSOPHY

Paul Ushiki Adamu

November 2023

Abstract

Multi-Connectivity (MC) techniques play a significant role in enhancing the performance and reliability of mobile communication systems. These techniques aim to improve network connectivity by utilising multiple simultaneous connections between a mobile device and base stations or access points. Among other multiple benefits, MC techniques can provide increased data rates and enhanced link reliability, both of which are of extreme relevance to the new use cases introduced in the Fifth Generation (5G) of mobile communication systems, namely enhanced Mobile Broadband (eMBB), Ultra-Reliable Low-Latency Communication (URLLC) and massive Machine Type Communication (mMTC). MC techniques are equally important for the future Sixth Generation (6G) technology services and applications, where data rates and link reliability requirements will be even more demanding than in the previous generation. In this context, this thesis proposes some novel MC techniques with the potential to significantly improve both aspects (i.e., data rate and reliability) in mobile communication systems.

First, a MC framework based on Carrier Aggregation (CA) is proposed. CA was originally proposed as a technique to combine spectrum from different bands into a single virtual chunk of spectrum for the higher layers of the protocol stack. In this thesis, a novel framework where CA is exploited as a diversity technique is proposed. The idea is to divide a large block of contiguous spectrum into a number of adjacent sub-blocks, where each of them is treated as an individual Component Carrier (CC) according to CA and therefore runs an independent transmission process. The motivation for this approach is to benefit from the diversity experienced at different frequencies. This idea is evaluated by means of simulations and the obtained results indicate that CA can effectively be exploited as a diversity technique to increase network capacity, with the optimum number of CCs depending on the radio propagation scenario. The simulation results indicate that the use of CA as a diversity technique, as proposed in this thesis, can enhance the obtained data rate up to almost five times with respect to the case where only one CC is employed.

Subsequently, a mathematical model is developed to characterise the performance of CA as a diversity technique. The model is first used to characterise the channel capacity as a function of the number of CCs and other relevant parameters, which is shown to explain and corroborate the findings derived from simulation results. Capitalising on the developed mathematical model, the impact of various relevant configuration parameters on the performance of CA as a diversity technique is then evaluated. In such a study, not only the ergodic capacity but also the secrecy capacity are both considered and investigated. The results demonstrate that the proposed mathematical modelling approach can correctly predict the performance of CA as a diversity technique as well as the impact of various relevant configuration parameters.

Finally, a hybrid transmission scheme for improved link reliability is also proposed. The proposed hybrid system benefits from the range of frequency bands available in mobile communication systems and their complementary characteristics. Higher-frequency bands tend to provide larger bandwidths (i.e., higher data rates) but are also characterised by more challenging propagation conditions (i.e., lower link reliability), while the opposite is true in general for lower-frequency bands. To exploit these complementary characteristics, a hybrid system is proposed that dynamically switches between both bands according to the instantaneous channel quality. The obtained results demonstrate that such a hybrid scheme not only improves dramatically the transmission reliability but also has the potential to simultaneously increase the capacity while efficiently exploiting the resources in both bands. Concretely, for a reliability requirement of 10^{-5}, the proposed scheme can provide an 8/9-fold increase in the communication range of the main link in the higher-frequency bands by only reducing 2%-4% the availability of the backup link in the lower-frequency bands. Moreover, the attained high level of link reliability is not obtained at the expense of the link capacity, which is indeed improved by applying the proposed scheme. These findings suggest that the proposed scheme is a suitable technique to effectively meet the URLLC requirements for 5G/6G in a resource-efficient manner.

In summary, the MC techniques developed in this thesis can provide significant improvements in terms of enhanced data rates and reliability for current and future 5G/6G mobile communication systems.

Acknowledgements

As this part of my study life comes to an end, looking back to the whole journey of my PhD especially during the strange period of the pandemic makes me realise how lucky I am to have reached this point with the support from the people I have met one way or another.

I want to express my deep gratitude and thanks to my supervisor Dr. Miguel López-Benítez for your encouragement, guidance and continuous support over the years. This has build up my analytical skills and the learning process to finding solutions to formulated real life problems. His valuable comments have definitely put me in the right direction and improved the quality of this thesis, I feel deeply indebted. It has been a great pleasure making this journey under your supervision.

I am also grateful to my friends made during my time in Liverpool either from the university or outside the university, thank you for your support and kindness.

Lastly, special thanks to my family (especially my father Engr. Ushiki), siblings and the extended family, you have been the heroes with your unconditional support, I cannot thank you enough. This journey would not be possible without your love and encouragement. I hope I am making you proud.

Table of Contents

List of Figures **xi**

List of Tables **xv**

List of Abbreviations **xvii**

1 Introduction **1**
1.1 Mobile Communication Systems 1
1.2 Evolution of the Mobile Communication Technology from 1G to 4G 2
1.3 The Fifth Generation (5G) 5
1.4 5G Use Cases 8
1.4.1 Enhanced Mobile Broadband (eMBB) 9
1.4.2 Massive Machine Type Communication (mMTC) . . . 11
1.4.3 Ultra-Reliable Low-Latency Communication (URLLC) 11
1.5 The Sixth Generation (6G) and Beyond 13
1.6 Multi-Connectivity Techniques 16
1.7 Research Objectives 20
1.8 Contributions and Thesis Organisation 20
1.9 List of Publications 22

2 Carrier Aggregation as a Diversity Technique: A Simulation Approach **23**
2.1 Introduction 23
2.2 Background and Related Work 25
2.3 System Model 30
2.4 CA Proposed as a Diversity Technique 31

2.5 Evaluation Methodology 34
2.5.1 Simulation Platform 34
2.5.2 Simulation Configuration 35
2.6 Simulation Results and Discussion 38
2.7 Conclusions 44

3 Carrier Aggregation as a Diversity Technique: An Analytical Approach 45
3.1 Introduction 45
3.2 System Model 47
3.3 Models for the Effective SNR 49
3.3.1 Ideal Model for the Effective SNR 49
3.3.2 Average Model for the Effective SNR 51
3.4 Ergodic Capacity Analysis 52
3.5 Secrecy Capacity Analysis 54
3.6 Results 57
3.6.1 Ergodic Capacity Results 58
3.6.2 Secrecy Capacity Results 64
3.7 Conclusions 70

4 Hybrid Transmission Scheme for Improving Link Reliability 73
4.1 Introduction 73
4.2 System Model 76
4.3 Analysis of SNR Statistics 78
4.3.1 Cumulative Distribution Function of the SNR 78
4.3.2 Probability Density Function of the SNR 82
4.4 Performance Analysis 83
4.4.1 Probabilities of Outage and Link Usage 83
4.4.2 Average Bit Error Rate 84
4.4.3 Ergodic Capacity 87
4.5 Results 91
4.5.1 Evaluation Scenario 91
4.5.2 Validation of the SNR Statistics 92
4.5.3 Performance Evaluation 93
4.6 Conclusions 101

5 Conclusions and Future Work 103
5.1 Conclusions 103
5.2 Future Work 106

5.3 Summary 109

Appendix **111**

References **121**

List of Figures

1.1 Evolution of mobile communication systems from 1G to 5G [1]. 3
1.2 IMT global mobile data traffic estimate for 2020-2030 [2]. . . . 7
1.3 Key requirements of IMT-2020 versus IMT-Advanced [3]. . . . 8
1.4 5G usage scenarios of IMT-2020 and beyond [3]. 10
1.5 Some potential new 6G services and applications [4]. 13
1.6 Comparison of key performance requirements of 5G vs. 6G [4]. 14

2.1 Illustration of the Carrier Aggregation (CA) concept aggregating up to 5 Component Carriers (CCs). 26
2.2 Transmission and reception with CA. The transmitter splits the data stream into N CCs and the packets are reordered at the receiver. 27
2.3 The three different CA spectrum scenarios: a) Intra-band contiguous; b) Intra-band non-contiguous; c) Inter-band non-contiguous. 28
2.4 Contiguous and non-contiguous UMa-LOS received throughput compared with the use of single Component Carrier (CC) and the presence of blockage. 39
2.5 Contiguous and non-contiguous UMa-NLOS received throughput. 40
2.6 Contiguous and non-contiguous UMi-LOS received throughput. 41
2.7 Contiguous and non-contiguous InH-Office-NLOS throughput. 41
2.8 One to five component carrier contiguous UMa-NLOS simulation. 42

3.1 System model considered in this chapter. 48
3.2 Ergodic capacity as a function of the number of CCs for various values of bandwidth overhead parameter α (average SNR = 10 dB, $\varepsilon = 3$ dB). 60

3.3 Optimum number of component carriers as a function of the bandwidth overhead parameter α (left) and resulting ergodic capacity (right). 61
3.4 Ergodic capacity as a function of the number of CCs for various values of the average SNR ($\alpha = 0.05$, $\varepsilon = 3$ dB). 63
3.5 Optimum number of component carriers as a function of the average SNR (left) and the resulting ergodic capacity (right). . 64
3.6 Ergodic capacity as a function of the number of CCs for various values of the spread parameter ε (average SNR = 10 dB, α = 0.05). 65
3.7 Ergodic capacity as a function of the number of CCs for various values of the bandwidth overhead parameter α (average SNR = 10 dB, $\varepsilon = 3$ dB). [Counterpart to Fig. 3.2 based on the average model of effective SNR.] 66
3.8 Ergodic capacity as a function of the number of CCs for various values of the average SNR ($\alpha = 0.05$, $\varepsilon = 3$ dB). [Counterpart to Fig. 3.4 based on the average model of effective SNR.] . . . 67
3.9 Secrecy capacity as a function of the number of CCs for various values of the bandwidth overhead parameter α (**ideal effective SNR model**, 10 dB SNR in both main and eavesdropper links). 68
3.10 Secrecy capacity as a function of the number of CCs for various values of the bandwidth overhead parameter α (**ideal effective SNR model**, 20 dB SNR in the main link and 10 dB SNR in the eavesdropper link). 69
3.11 Secrecy capacity as a function of the number of CCs for various values of the bandwidth overhead parameter α (**average effective SNR model**, 20 dB SNR in the main link and 10 dB SNR in the eavesdropper link). 70

4.1 Proposed hybrid transmission scheme. 77
4.2 Validation of the SNR statistics ($d = 1000$ m). 92
4.3 Outage probability versus maximum tolerable BER. 94
4.4 Outage probability versus communication distance. 95
4.5 FR1 link usage probability versus communication distance. 96
4.6 ABER versus communication distance. 97
4.7 Ergodic capacity (top) and FR1 link usage probability (bottom) versus communication distance (transmitter/receiver antenna gains: $G_T = G_R = 40$ dBi. 98

4.8 Ergodic capacity (top) and FR1 link usage probability (bottom) versus communication distance (transmitter/receiver antenna gains: $G_T = G_R = 30$ dBi. 98
4.9 Ergodic capacity (top) and FR1 link usage probability (bottom) versus communication distance (transmitter/receiver antenna gains: $G_T = G_R = 20$ dBi. 99
4.10 Ergodic capacity (top) and FR1 link usage probability (bottom) versus communication distance for various bandwidth configurations with $G_T = G_R = 30$ dBi and $\gamma_T = \gamma_{\text{out}}$. 101

List of Tables

1.1 Comparison of the mobile cellular generations [5]. 6
1.2 Typical IoT applications and characteristics/requirements [6]. 12
1.3 Multi-connectivity techniques in 3GPP standards. 18

2.1 Main simulation parameters. 36
2.2 Carrier frequency and bandwidth allocation for various CCs. . 37
2.3 UMa-NLOS simulation results for 1 CC to 5 CCs. 43

3.1 Best attainable ergodic capacity for various scenarios and levels of bandwidth penalty (α) according to Fig. 3.3. 62

List of Abbreviations

1G	First Generation.
2G	Second Generation.
3G	Third Generation.
3GPP	3G Partnership Project.
4G	Fourth Generation.
5G	Fifth Generation.
5G-NR	Fifth Generation New Radio.
6G	Sixth Generation.
ABER	Average Bit Error Rate.
AI	Artificial Intelligence.
AMPS	Advanced Mobile Phone System.
BER	Bit Error Rate.
BPSK	Binary Phase Shift Keying.
BS	Base Station.
CA	Carrier Aggregation.
CAGR	Compound Annual Growth Rate.
CC	Component Carrier.
CCs	Component Carriers.
CDF	Cumulative Distribution Function.
CDMA	Code-Division Multiple Access.
CoMP	Coordinated Multipoint.
DC	Dual Connectivity.
DL	Downlink.
DPS	Dynamic Point Selection.
E2E	End-to-End.

EDGE	Enhanced Data-rates for GSM Evolution.
eMBB	enhanced Mobile Broadband.
eNB	eNodeB.
FDD	Frequency Division Duplex.
FDMA	Frequency-Division Multiple Access.
FTR	Fluctuating Two-Ray.
gNB	Next Generation Node-B.
GPRS	General Packet Radio Service.
GSM	Global System for Mobile Communication.
HARQ	Hybrid Automatic Repeat Request.
HetNet	Heterogeneous Network.
ICI	Inter-Cell Interference.
IMT	International Mobile Telecommunications.
IoT	Internet of Things.
ITS	Intelligent Transport System.
ITU-R	International Telecommunication Union - Radiocommunication sector.
JT	Joint Transmission.
LOS	Line-of-Sight.
LTE	Long Term Evolution.
LTE-A	Long Term Evolution-Advanced.
LWA	LTE-Wi-Fi Aggregation.
M2M	Machine-to-Machine.
MAC	Medium Access Control.
MC	Multi-Connectivity.
MCS	Modulation and Coding Scheme.
MIMO	Multiple-Input Multiple-Output.
mm-Wave	Millimetre Wave.
MMS	Multimedia Messaging Service.
mMTC	massive Machine Type Communication.
MPTCP	Multipath TCP.
MR-DC	Multi-Radio Dual Connectivity.
MRC	Maximal Ratio Combining.
Multi-RAT	Multi-Radio Access Technology.

NLOS	Non-Line-of-Sight.
NR	New Radio.
O-RAN	Open Radio Access Network.
PDCP	Packet Data Convergence Protocol.
PDF	Probability Density Function.
PHY	Physical.
QoS	Quality of Service.
RAN	Radio Access Network.
RAT	Radio Access Technology.
RLC	Radio Link Control.
RMa	Rural Macro.
SC	Selection Combining.
SMS	Short Message Service.
SNR	Signal-to-Noise Ratio.
TACS	Total Access Cellular System.
TDD	Time Division Duplex.
TDMA	Time-Division Multiple Access.
THz	Tera-Hertz.
UE	User Equipment.
UHD	Ultra-High Definition.
UL	Uplink.
UMa	Urban Macro.
UMi-StreetCanyon	Urban Micro.
URLLC	Ultra-Reliable Low-Latency Communication.
VoIP	Voice Over IP.
VR/AR	Virtual Reality/Augmented Reality.
XR	eXtended Reality.

Chapter 1

Introduction

1.1 Mobile Communication Systems

The 20th century witnessed a revolution in communication systems: they changed dramatically the way humans communicate, freed communication from the constraint of wires as in the previous century to radio waves, and enabled the property of filling spaces and connected points that could not be connected before in any other way, thus enabling broadcast and making information available everywhere by covering large geographical areas. Mobile radio communication systems have become familiar to most people and are nowadays used in everyday life, from garage door openers to remote controllers for home entertainment equipment uses, pagers, cordless telephones, hand-held walkie-talkies and cellular telephones. These examples of mobile radio communication systems are vastly different from each other in terms of the type of services they offer, their performance, cost and complexity. Mobile communication allows users' radio terminals to be connected and in operation while in constant motion or on the move [7, 8].

Mobile radio transmission systems can be classified as simplex, half-duplex or full-duplex systems. The simplex system makes communication possible in one direction only, like the paging systems that receive messages but cannot acknowledge receipt. Half-duplex systems allow communication in two-ways but share the same radio channel for both transmission and reception, a user can only receive or transmit information at any given time like the push-to-talk and release-to-listen hand-held walkie-talkies. The full-duplex system provides two simultaneous and separate channels by means of Frequency Division Duplex (FDD) or Time Division Duplex (TDD) for com-

munication to and from the user. It allows simultaneous radio transmission and reception between a subscriber and the base station [7, 9].

A mobile communication system can in general be described as a group of networks, services and applications that allows users to exchange (transmit and receive) information (voice and data) while moving between and during connections. The ancient radio-telephony systems that are nowadays considered the first mobile communication systems have evolved dramatically through a long and intensive process of evolution and transformation, from the use of bulky (usually vehicle-mounted) analogue technology to providing rudimentary voice services in the First Generation (1G) systems such as the Advanced Mobile Phone System (AMPS) service in 1983, to the small digital devices that can nowadays be carried everywhere by a person allowing universal user mobility while communicating with adequate Quality of Service (QoS) in the subsequent generations [5, 9, 10]. Mobile radio communications have witnessed an exponential growth since the introduction and commercial use of the first systems and it is worth discussing briefly the main features that have characterised such evolution.

1.2 Evolution of the Mobile Communication Technology from 1G to 4G

Few communication systems have been subject to a process of evolution and transformation as intensive and fast-paced as cellular mobile communications [9, 10]. In just a few decades, mobile communication systems have shifted from providing basic voice service to a limited number of subscribers to providing highly sophisticated personal data services to a large number of users. This would not have been possible without the remarkable technological evolution suffered through different so-called generations of mobile communication systems. An overview of the evolution of mobile communication technologies is shown in Figure 1.1 and discussed below.

- **The First Generation Technology** was a set of analogue systems introduced in the 1980s, including the North American AMPS and the Total Access Cellular System (TACS) that followed in the UK, with a bit-rate of up to 2.4 kbps. These systems used Frequency-Division Multiple Access (FDMA) to divide the bandwidth into specific frequencies that were assigned to individual voice calls, which were allowed in one country (i.e., without roaming). It was the first generation of wireless

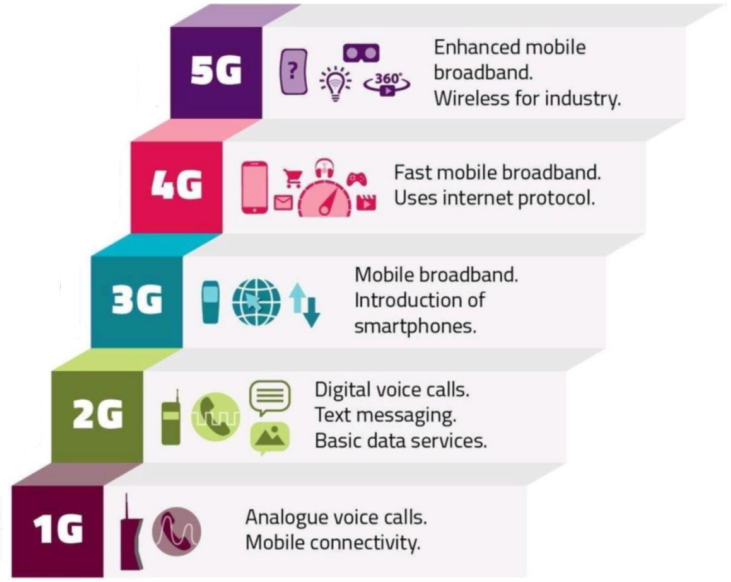

Figure 1.1: Evolution of mobile communication systems from 1G to 5G [1].

telephony technology that used multiple cell sites (i.e., the cellular concept) and had the ability to transfer calls from one site to the next as users travelled between the cells during a conversation (i.e., handovers), which is the main technological development in this generation. The first generation was designed primarily for voice services with basic data capabilities like fax, and supported cell sizes (i.e., coverage distances from a given base station or radio access point) of 2 – 30 km. The first generation technology was limited in terms of available user capacity, was in general not robust to interference as a result of using analogue technology, provided poor voice quality when moving across cells (it was not unusual for voice calls to drop during handovers), lacked of any significant security features, and the different commercial technologies deployed in different countries (and even in the same country by different network operators) were incompatible with each other [5, 8, 9].

- **The Second Generation Technology** was composed of digital mobile systems introduced in the 1990s based on either Time-Division Multiple Access (TDMA) in Europe or Code-Division Multiple Access (CDMA) in the USA. The use of digital modulation offered the advantages of better utilisation of the available bandwidth, more privacy, and the incorporation of error detection and correction. The second gener-

ation of mobile telecommunications commenced operation in Finland, with the first call in 1991 based on the Global System for Mobile Communication (GSM) standard. The official start of GSM commercial network deployments in the summer of 1992 witnessed a rapid increase in the number of subscriber calls in the network to over a million by the following year, 1993. The world-wide adoption of the GSM network standard allowed compatibility with other systems and seamless mobility, allowing roaming across locations and countries. It enabled simple data transmission in the form of text messaging via Short Message Service (SMS) and photo or picture transfer via Multimedia Messaging Service (MMS), but lacked support for more sophisticated and demanding forms of data communication such as the transmission of video. The later versions of this generation, such as General Packet Radio Service (GPRS) and Enhanced Data-rates for GSM Evolution (EDGE), which are often referred to as 2.5G and 2.75G systems, achieved higher data-rates in the order of hundreds of kbps, thus providing better quality, capacity and enhanced security, which improved the system performance [5, 8, 11, 12]. These evolved versions of data transmission in GPRS and EDGE were facilitated by the introduction of some changes in the radio interface in order to support higher bit rate in the wireless link between users and base stations. However, a deeper transformation of the network was required for a full and efficient support of demanding data services, including not only the radio access network but also the rest of the network infrastructure (i.e., the core network), which was successfully accomplished by the next generation.

- **The Third Generation Technology** was introduced in the 2000s to overcome the shortcomings of the second generation. To be able to guarantee global communication interoperability, the 3G Partnership Project (3GPP) was established to combine the effort and collaboration agreement in crucial technical decisions. This technology was able to transmit data at bit-rates of up to 2 Mbps using packet switching. Packet switching was more efficient for data transmission than the circuit switching approach used by the second generation systems, which is more appropriate for the voice communication services for which the second generation systems were originally designed. Third generation systems enabled faster communications, high speed web browsing with more security, video conferencing, 3D gaming, TV streaming, mobile TV, etc., with a user experience similar to or very close to that in a regular desktop computer at that time (this target was motivated by the boost in popularity of the Internet during the 2000s). Third gen-

eration devices also support location-based services, where a service provider sends localised weather or traffic information to the phone based on their current geographical location. Some further advancements were introduced in the later stages of this technology to support the higher data needs of consumers, reaching higher throughput and speed at packet data rates of up to 14.4 Mbps [12, 13].

- **The Fourth Generation Technology** of mobile telecommunication was introduced around 2010 based on the Long Term Evolution (LTE) and Long Term Evolution-Advanced (LTE-A) standards, which are capable of providing 100 Mbps to 1 Gbps speeds with features such as IP telephony, ultra-broadband internet access and advanced communication services like video calling, HDTV streamed multimedia, real-time language translation and video voice mail with high QoS and high security. The 4G network infrastructure is only packet-based (all-IP) for all services, including the legacy voice service which is provided using voice-over-IP technology [14]. This is a significant change with respect to the previous generations of mobile communication systems.

  CA, which is one of the key technologies considered in the research presented in this thesis, was introduced in the advanced releases of Fourth Generation (4G) LTE systems to support ultra-broadband applications [15] by aggregating multiple CCs in order to allow end users to experience higher data rates with lower latency across the network [16, 17, 18]. This technology will be discussed in more detail in Chapter 2, where it will be the focus of one of the technical contributions provided in this thesis.

A comparison of the mobile cellular generations is given in Table 1.1.

1.3 The Fifth Generation (5G)

The fourth generation wireless technology, since its advent and later emergence to 4G/LTE, provided a wide range and diverse broadband services to end-users with an unprecedented scale of smart end-user devices. The higher download speed offered by 4G stimulated the appearance of new services and technologies with high data rates and low latency transmission requirements. The proliferation of these new smart mobile devices, and the adoption of services with vast bandwidth-intensive applications, drove the ever increasing mobile data traffic demands. Figure 1.2 illustrates such evolution, with an estimated data traffic per month of up to 5000 EB by the year

Table 1.1: Comparison of the mobile cellular generations [5].

Generation	Technology	Multiple Access	Data Rate	Applications
1G	AMPS, TACS	FDMA	2.4 kbps	Voice
2G	GSM	FDMA, TDMA, CDMA	10 kbps	Voice + Simple data
2.5G	GPRS		50 kbps	
	EDGE		200 kbps	
3G	UMTS	CDMA	384 kbps	Voice + Data
	CDMA 2000		384 kbps	+ Video calling
3.5G	HSUPA/HSDPA	CDMA	5-30 Mbps	
	EVDO		5-30 Mbps	
3.75G	LTE	OFDMA	100-200 Mbps	Online gaming +
		SC-FDMA		High Definition Television
4G	LTE-A	OFDMA	DL 3 Gbps	Online gaming +
		SC-FDMA	UL 1.5 Gbps	High Definition Television
5G	NR	OFDMA	10-50 Gbps	Ultra High definition video +
				Virtual Reality applications

2030 [2]. New services and devices impose new network requirements, which are nowadays extremely challenging for 4G/LTE. The increase in the number of new heterogeneous wireless services has been relentless, making systems that solely use the 4G technology unable to meet the mixed and stringent service requirements of future wireless networks [19, 20]. The massive volume of mobile data being consumed strains the current mobile network in delivering the required capacity. The 4G network technology, as a result, is unable to effectively meet the demands of the multiple connected devices with their high data rates, low-latency requirements, and low or zero network interference [21, 22]. This calls for a new network design, which motivated the development of the 5G and Radio Access Network (RAN) technology to support high frequency spectrum-based radio connectivity and to ensure it evolves to meet all the expected requirements.

The 5G system design aims to provide the best combination of high capacity, high data speed, communication range, low latency and ultra-reliability [23, 24, 25] in order to meet the requirements of a broad range of services and applications. As such, 5G networks, which have now been in commercial deployment for a few years but still have a very long way to go, intend to provide a unifying mobile connectivity platform capable of supporting not only legacy and traditional services provided by mobile networks but also

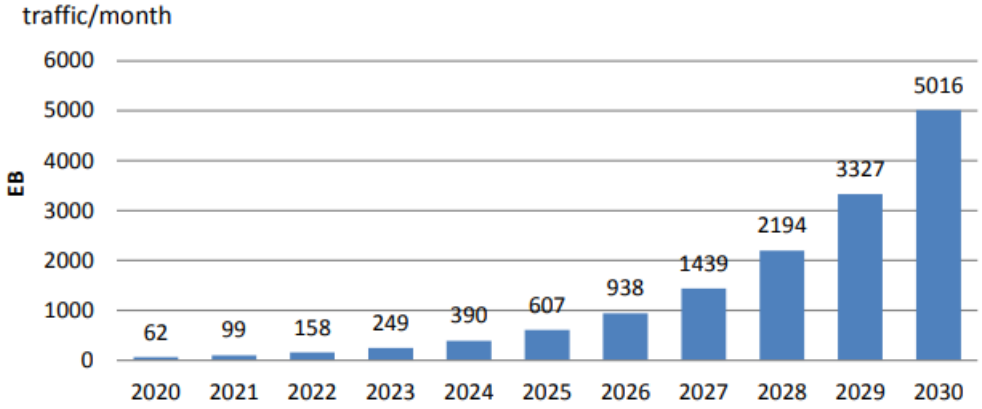

Figure 1.2: IMT global mobile data traffic estimate for 2020-2030 [2].

other new services and applications not supported before and that impose new requirements, hence the ambitious performance and QoS requirements set for 5G networks. This has been shaped by the aim of mobile communication networks to serve as a means of wireless connectivity not only for the Internet of Things (IoT), which typically involves a large number of smart devices connected per user as well as Machine-to-Machine (M2M) communication, and to support as well wireless connectivity in industrial automation processes. This will factor in different usage scenarios in the future mobile communication networks with heterogeneous QoS requirements. Recent forecasts in [26] have estimated that 16.7 billion IoT devices will be connected to the Internet by the end of 2023, which will be expected to continue to grow steadily for many years to come, reaching more than 29 billion IoT connections by 2027, with cellular IoT making around 20% of the global IoT devices connected. More recent forecasts in [27] have estimated that 30.1 billion devices are expected to be connected over the decade by 2030, reaching up to 34.7 billion by 2032. According to [28], the average Compound Annual Growth Rate (CAGR) between 2022 and 2028 will be 18%, with almost 60 percent of cellular IoT connections to be broadband by the end of 2028.

In order to meet the demanding and highly heterogeneous QoS requirements of the various applications envisaged for 5G, a new network technology was developed. The 5G technical performance targets, also known as the International Mobile Telecommunications (IMT)-2020 capabilities as described by the International Telecommunication Union - Radiocommunication sector (ITU-R), are aimed to equip mobile systems with a new radio interface that is more flexible, reliable and secure than the previous generations. The key

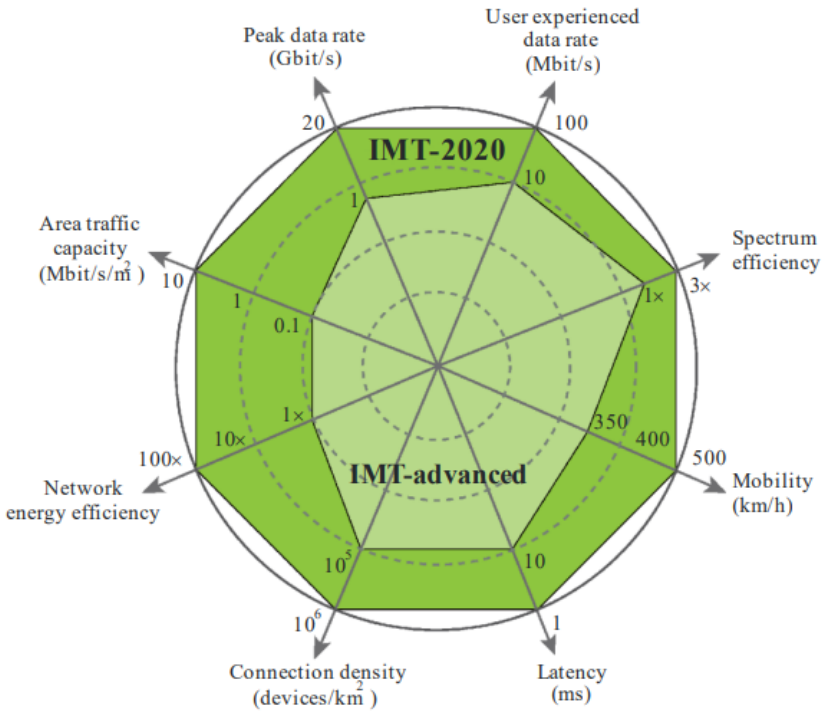

Figure 1.3: Key requirements of IMT-2020 versus IMT-Advanced [3].

capabilities of the IMT-2020 5G technology improvement to support these use cases are shown in Figure 1.3 compared with those of the previous generation IMT-Advanced [29, 3, 30]. It is acknowledged that optimising the mobile network to simultaneously meet the heterogeneous requirements of different services and applications is extremely challenging. As a result, a framework composed of three different use cases is considered, where each use case includes a certain type of application or service characterised by a common set of QoS performance requirements, such that for each use case the aim is to optimise the network for a subset of the performance metrics illustrated in Figure 1.3.

1.4 5G Use Cases

The 5G mobile technology has been proposed to adequately address the insufficiency of 4G networks and to adequately meet the stringent QoS requirements of the broad heterogeneity of services and applications that 5G networks are expected to support today and in the future. According to

ITU-R, the services and applications supported by 5G can be classified into three main use cases or scenarios as follows:

- *eMBB*: This is considered a direct extension of the 4G broadband service which supports stable broadband connections with high peak data rates, and strives to increase the ability of mobile broadband to have access to multi-media contents, services and data at higher data-rates than previous generations.

- *mMTC*: Sometimes referred to as massive Internet of Things (mIoT), this use case aims to provide support for a massive number of IoT/M2M communication types and devices. The main focus here is not on the data rate itself, since the data rate requirements of individual IoT devices are usually low or relatively low. The main focus in this use case is on providing connectivity for a massive number of devices efficiently. Another relevant aspect in the provision of IoT use case scenarios is energy efficiency (since many IoT devices are powered by small, non-rechargeable batteries).

- *URLLC*: This use case supports services and applications that require low-latency transmissions with very high reliability. This includes, for example, the control of the production in industrial processes, long distance medical surgery, intelligent transportation systems, and similar cases. The transmission rate is relatively (but not always necessarily) low and the main requirement is to ensure that the transmitted data packets reach their destination with very high probability (i.e., high reliability) and within a strict timeframe (i.e., low-latency) [31, 32, 33, 34, 35].

The broad range of services and applications that 5G networks were designed to support can be placed somewhere within a triangle whose three corners are defined by each of the three 5G use cases defined above, which is illustrated in Figure 1.4. Notice that some services and applications would be very close, in terms of QoS requirements, to the pure definition of one of the three use cases, while in some other services and applications may combine different aspects of two (perhaps three) of these use case scenarios. A more detailed discussion of each 5G use case scenario is provided below.

1.4.1 Enhanced Mobile Broadband (eMBB)

The eMBB is one of the primary use cases of Fifth Generation New Radio (5G-NR) and it is seen as an extension of the existing services provided

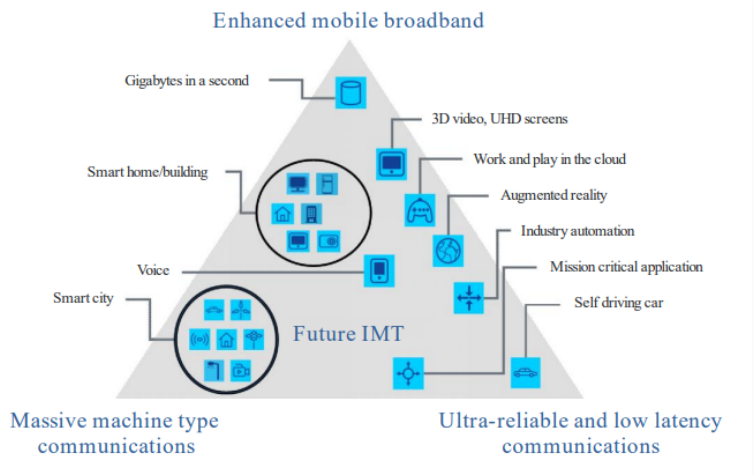

Figure 1.4: 5G usage scenarios of IMT-2020 and beyond [3].

by 4G systems, in the sense that the main focus of eMBB is on increasing data rates, following the same trend that defined the evolution of the Third Generation (3G) and 4G mobile communication systems. Mobile data traffic and video content accessibility will increase significantly in the future with new mobile broadband demanding services, including Ultra-High Definition (UHD) displays, mobile 3D projection, immersive video conferencing, augmented reality, and mixed reality displays and interfaces. This has led to the definition of the eMBB usage scenario, which will include new applications and requirements to the existing mobile broadband for an increasingly seamless user experience and improved overall system performance. This use case scenario intends to address the human-centric broadband access for multi-media content, services and data.

The eMBB use case enables enhanced broadband access in high density areas, in moving vehicles or high-speed trains, by supporting 10000x more traffic. The eMBB services demand high peak data rates greater than 10 Gbps for a good user experience and to provide the required level of QoS that is currently enjoyed in fixed broadband internet services [31].

In order to support these high data rates in eMBB use case scenarios, 5G networks have introduced the use of Millimetre Wave (mm-Wave) bands. mm-Wave communication makes use of the available spectrum and bandwidth in that radio band to provide users with peak data rates in the order of Gbps. The eMBB service is aimed at providing better and enhanced connectivity that includes not only smartphones but also connected IoT devices with high data-rate requirements, thus resolving issues of poor experience in high data rate scenarios in crowded locations [31, 36, 37].

1.4.2 Massive Machine Type Communication (mMTC)

The IoT is set to revolutionise the global world by connecting heterogeneous smart devices. This concept has gained global attention with the goal of connecting physical objects with the ability to communicate with each other in an automated manner with little or no human intervention. This concept is an enabler and inspirer of M2M where data communication between heterogeneous devices without human intervention takes place [6]. Table 1.2 illustrates some typical mMTC/IoT applications and their associated requirements. mMTC/IoT devices are typically characterised by requirements of low power, long battery life and low-cost. Requirements for low latency, high reliability and high data rates may sometimes be relevant in some specific cases, but are not usually associated with this use case scenario.

The large number of connected devices and the ever-increasing demand from a massive number of mMTC devices has resulted in different communication technology types being employed, with diverse features and capabilities, in order to support modern IoT deployments. This includes not only traditional wireless communication technologies that were originally developed for other communication scenarios but that have been proven to be effective in supporting IoT (such as Wi-Fi, Bluetooth or ZigBee) but also other technologies specifically designed and/or optimised to support IoT (such as LoRaWAN). Despite the broad range of wireless technologies for IoT, cellular mobile communication systems are expected to play a key role in providing wireless connectivity to IoT systems, supporting a substantial fraction of the smart devices connected wirelessly to the IoT. For this reason, the mMTC use case scenario has received significant attention in mobile communications.

IoT/M2M applications and devices are expected to be in several orders of magnitude larger than the world population and exponentially increasing, with billions of devices and machines that will potentially utilise the mobile network to access services and connect with other devices. This growing number of connected devices will increase mobile data demand and impose even more challenging requirements for operators. As a driver for the increase in the estimated global mobile data traffic, 5G mobile networks are envisioned to support hyper-connectivity between machines in the current and future IoT landscape and therefore constitute a key supporter of IoT.

1.4.3 Ultra-Reliable Low-Latency Comms (URLLC)

The 5G concept considers URLLC as one of the new application scenarios crucial for enabling mission-critical services such as factory and vehicle

Table 1.2: Typical IoT applications and characteristics/requirements [6].

Applications	Application Domain	Tolerable Delay	Update Frequency	Data Rate
Structural Health	Smart City	30 min	10 min	Low
Waste Management	Smart City	30 min	1 hour	Low
Video Surveillance	Smart City	Seconds	Real Time	High
Air Quality Monitor	Smart Home	5 min	30 min	Low
Monitoring and Supervision	Industrial	Seconds or ms	Seconds	Low
Closed Loop Control	Industrial	Milliseconds	Milliseconds	Low
Interlocking and Control	Industrial	Milliseconds	Milliseconds	Low
Patient's Health Care Delivery and Monitoring	Healthcare	Low (seconds)	1 report per hour/day	High
Real-time emergency response and remote diagnostics	Healthcare	Low (seconds)	Requires Ad-hoc emergency communication	High
Real-time management and accuracy of information across the supply chain	ITS	Low (seconds)	1 report per hour/day	High

automation, wireless control of industrial manufacturing or production processes, remote medical surgery and intelligent transportation systems, among others. This use case scenario includes services and applications that are characterised by a very high reliability requirement, defined by a maximum link failure probability of $1 - 10^{-5}$ (i.e., 99.999% of successfully delivered packets), and a tight user plane latency below $1ms$, as specified in 3GPP Release 17 [30]. In URLLC scenarios, a data packet is usually considered to have been successfully received if it has been delivered within the set latency target. Therefore, both reliability and latency are related and equally important concepts in URLLC communications.

mm-Wave bands were introduced in 5G networks when mobile systems were deployed in the bandwidth-limited sub-6 GHz spectrum and, as a result, mm-Wave bands are usually viewed as a key enabler for the high data rates required by eMBB applications, because of the promising availability of abundant spectrum that it offers. However, due to challenges in propagation, blockage, high path loss, and channel uncertainty, communication in mm-Wave bands is inherently unreliable. This is effectively a practical challenge for URLLC mobile applications that require extremely high reliability.

The advent of new applications with varying data rates in smart factories (Industry 4.0), Virtual Reality/Augmented Reality (VR/AR), and UHD video surveillance applications with strict reliability and latency requirements, all claim for novel approaches that deliver the necessary reliability and low latency without sacrificing the overall system capacity [38, 39].

1.5 The Sixth Generation (6G) and Beyond

While there has been tremendous, noticeable and recorded success in the mobile industry from Second Generation (2G) to 4G, it is still important to ensure the successful commercial deployment of 5G in the coming years, at a time when the 6G technology is on the way. There is no clear, completely closed view of what 6G mobile networks will be, but there is an overall agreement on some of the key ingredients that will be part of future 6G networks and that will shape the evolution of the 6G technology.

Academia and industry have started to look beyond the 5G technology and have started to conceptualise the 6G technology with various aspects of the technology such as mega-trends, services, requirements, the candidate technologies and timeline for standardisation and commercialisation in research. This new generation technology will continue to improve the three 5G use cases and services (i.e, eMBB, mMTC and URLLC) while introducing services emerging from the advancement in other relevant technologies such as sensing, imaging, displaying and Artificial Intelligence (AI) [4, 40, 41, 42]. 6G is expected to introduce new services such as truly immersive eXtended Reality (XR), high-fidelity mobile holograms and digital twins [4] as illustrated in Figure 1.5.

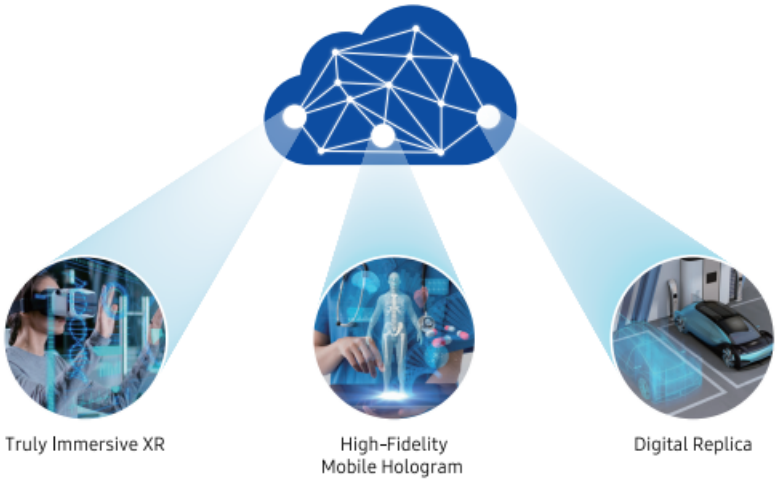

Figure 1.5: Some potential new 6G services and applications [4].

There will be advancements in services in 6G technology that will require a massive amount of real-time data processing, hyper-fast data rates, and extremely low latency. These new services will give a rise to new requirements for the key performance indices, overall architecture and trustworthiness. 6G

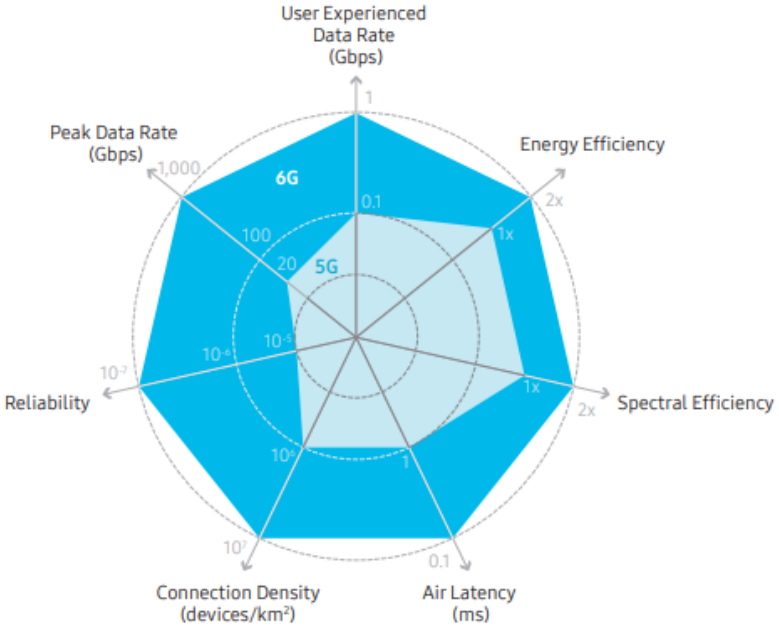

Figure 1.6: Comparison of key performance requirements of 5G vs. 6G [4].

needs to provide a much higher data rate than 5G aiming at a pick data rate of 1000 Gbps and user experienced data rate of 1 Gbps, targeting an air latency below 0.1 ms, an End-to-End (E2E) latency of less than 1 ms and user experienced latency of less than 10 ms. It is intended to also improve the reliability by 100 times compared to 5G. These new expected requirements for 6G are illustrated in Figure 1.6, showing the relative increase with respect to the 5G technology [4], clearly showing the challenges faced by 6G.

The development of the 6G technology is currently in its infancy and the concept of what 6G will finally be will be shaped by still unknown factors. With the exponential growth of advanced technologies in the wireless communication field such as AI, space, robotics and automation, new trends are emerging in the development of the new 6G technology [4, 43, 44, 45, 46]. Transforma Insights has envisioned that by the year 2030, there will be 30.1 billion connected IoT devices [27] which will be three and half times larger than the United Nations expected world population of 8.5 billion by the same year [47]. These connected devices, which are becoming part of our social infrastructure and daily lives, make machines the main user of this technology, which together with the potential benefit of AI and Open Radio Access Network (O-RAN) makes wireless communication in 6G promising.

With the foreseen vision of 6G, new additional spectrum will be necessary to meet all the capacity demands of the new technology. Given the forecasted ultra-high data rates required for new 6G services and the massive amount of spectrum that will be required to support such data rates, spectrum in the Tera-Hertz (THz) bands is being targeted. THz bands currently have large amounts of bandwidth available for mobile communications that could accommodate the volume of traffic expected for some of the more demanding new 6G services. Therefore, 6G is expected to operate at higher frequencies in THz bands. However, along with this enormous availability of bandwidth comes the challenging propagation conditions of THz bands, where the degrading effects of channel fading are substantially more accentuated than in the lower sub-6 GHz and mm-Wave bands employed by preceding generations of mobile communication systems. THz bands pose challenges related to increased susceptibility to atmospheric absorption and blockage by obstacles. Fading models aim to capture the variation or attenuation of the received signal strength due to changes in the transmission medium or path caused by factors such as distance, obstacles, and interference. These models need to account for the mentioned factors in THz bands so that they can be used to design robust communication systems. Traditional fading models widely employed in the legacy sub-6 GHz bands, such as Rayleigh, Nakagami-m, Nakagami-q (Hoyt), Nakagami-n (Rice), η-μ and κ-μ have been shown to be unsuitable for higher frequency bands in the mm-Wave, where the Fluctuating Two-Ray (FTR) model [48] has been proven to be more accurate. Similarly, none of these models can accurately describe the effects of fading in the THz bands suggested for use in 6G, where the α-μ model has been proposed as a more suitable candidate [49]. Thus, in 6G communications, fading models become crucial for understanding and mitigating the impact of the variations on signal quality and reliability, which will play an important role in spectrum exploration for 6G [50, 51].

Novel antenna technologies, comprehensive AI, spectrum sharing and network topology evolution are some of the candidate technologies that will be key enablers to realising 6G [4, 52] in the challenging propagation conditions offered by THz bands. However, it is worth noting that Multi-Connectivity (MC) techniques, which will be the focus of the research presented in this thesis, can also play an important role towards achieving this objective. MC essentially involves the simultaneous connection of a device to its network through multiple communication links. In 6G, MC is potentially seen as a key enabler for seamless and ultra-reliable communications, catering to the diverse requirements imposed by a wide range of demanding applications, including Augmented Reality (AR), Virtual Reality (VR) and autonomous vehicles, among many others. However, implementing MC techniques in

6G requires addressing challenges related to handover mechanisms, network management, and interference mitigation. Advanced algorithms for intelligent link/network selection and seamless switching between connections will also be essential for delivering a seamless user experience. A more detailed discussion of MC techniques will be provided in Section 1.6.

At the moment, there are more open questions than satisfactory answers about 6G. What 6G will be remains uncertain. However, there is no doubt that its evolution, definition and development will be an exciting journey.

1.6 Multi-Connectivity Techniques

A huge number of technological solutions have been proposed and developed over the last decade in order to address the challenging requirements imposed by the three use cases that were introduced in 5G (discussed in Section 1.4) and that will also be a key relevant aspect in the definition of the 6G concept.

The focus of this work is on a subset of solutions that are commonly known and referred to as MC techniques. These techniques aim to improve network connectivity by utilising multiple simultaneous connections or paths between the source of information and its destination. The concept of MC is very broad and essentially embraces any technique that allows the transmission of information (at any level of the protocol stack) through multiple/redundant paths. Such multiple paths are usually, but not necessarily, established between one mobile device and different base stations or access points. However, as it is the case of the MC solutions that will be proposed in this thesis, multiple paths can also be established between one mobile device and one base station or access point through multiple links at the Physical (PHY) and/or Medium Access Control (MAC) layers, through which the data flow from higher layers is split. While the propagation challenges and conditions for wireless communication networks discussed in Section 1.5 can make communication in 6G mobile networks liable to disruption and disconnection, MC techniques as envisioned in this thesis are aimed at improving the network performance by the use of multiple connections, owing to the availability of multiple connected links which reduces interruption in the communication when one individual connected link fails due to fading.

MC techniques play a significant role in enhancing the performance and reliability of mobile communication systems. Some key benefits of MC techniques include the following:

- **Increased data rates:** By aggregating multiple connections, such as combining 4G/5G and Wi-Fi or multiple 4G/5G carriers, the use of

the multi-connectivity principle enables higher data rates for mobile devices. This helps in achieving faster download and upload speeds, supporting bandwidth-intensive applications and services. Therefore, multi-connectivity techniques can be extremely useful in helping eMBB services achieve their required data rates.

- **Enhanced reliability and robustness:** MC techniques enhance network reliability by providing redundancy. If one connection fails or experiences degradation, the device can seamlessly switch to an alternative connection, ensuring uninterrupted communication and minimising service disruptions. This is particularly beneficial in environments with challenging propagation conditions, such as urban areas or crowded venues. Thus, multi-connectivity techniques can be extremely useful in helping URLLC services achieve their required levels of reliability.

- **Latency reduction:** Multi-connectivity techniques can also help in reducing latency, which is crucial for real-time applications such as online gaming, video conferencing, and Voice Over IP (VoIP) calls. By leveraging multiple connections, data can be transmitted and received concurrently, resulting in reduced latency and improved responsiveness. Again, MC techniques can be extremely useful in helping URLLC services, not only to achieve their required levels of link reliability but also to meet the stringent latency requirements.

- **Improved network coverage:** Multi-connectivity allows devices to connect to multiple base stations or access points simultaneously. This helps in extending the coverage area, particularly in scenarios where a single connection may suffer from weak signal strength or limited coverage. The device can maintain a connection with one access point while seamlessly switching to another if necessary, providing a more reliable and consistent user experience.

- **Load balancing and traffic offloading:** Multi-connectivity allows intelligent load balancing and traffic offloading across different connections. This helps optimise network resource usage by distributing traffic among available connections based on factors like signal strength, capacity, and network conditions. By offloading data to Wi-Fi networks or other available connections, the burden on cellular networks can be reduced, leading to improved overall network performance.

MC techniques play a vital role in enhancing network performance, coverage, reliability, and user experience in mobile communication systems. These

Table 1.3: Multi-connectivity techniques in 3GPP standards.

Name	Location	Form of MC	RAT	Standard
CoMP (JT)	inter-site	intra-freq.	LTE	3GPP Rel. 11
CA	intra-site	intra-freq. or inter-freq	LTE	3GPP Rel. 10
DC	inter-site	intra-freq. or inter-freq	LTE	3GPP Rel. 12
LWA	intra-site or inter-site	inter-RAT	LTE and Wi-Fi	3GPP Rel. 13
Multi-RAT DC	inter-site	inter-RAT	LTE and 5G	3GPP Rel. 15

techniques leverage the capabilities of different network technologies and provide a flexible and robust communication environment for mobile devices. In this thesis, the interest is mainly in realising the first two aspects itemised above, and the proposed technical contributions are mainly aimed at achieving them (i.e., enhanced data rates and/or reliability).

MC techniques have been paid significant attention as a promising technique not only to increase the system capacity but also to effectively achieve high reliability in URLLC [53]. As a result, different MC techniques have been introduced in successive 3GPP releases in the PHY layer (e.g, coordinated multi-point), MAC layer (e.g., carrier aggregation), Packet Data Convergence Protocol (PDCP) (e.g., dual connectivity and LTE-WiFi aggregation) and higher layers [53, 54, 55]. Some of the main existing MC techniques are summarised in Table 1.3 and discussed below.

In the PHY layer, Coordinated Multipoint (CoMP) was introduced in Release 11 with two basic modes. In the Joint Transmission (JT) mode, multiple base stations send the same data simultaneously on the same carrier and the receiver combines the data streams at the PHY layer by means of some appropriate diversity combination technique, thereby improving the signal strength received at the User Equipment (UE) Downlink (DL), while in the Uplink (UL) multiple base stations will receive the signal sent by the UE and jointly process it. In the Dynamic Point Selection (DPS) mode, the UE is connected to multiple base stations but data transmission occurs only with one of them at a time, which is dynamically switched according to the experienced channel quality conditions [54, 56, 57, 58]. The CoMP transmission/reception specified in 3GPP is a method of Multiple-Input Multiple-Output (MIMO) that reduces interference in transmission and enables features such as network synchronisation, feedback of multi-cell channel state information, and synchronous data transfer between base stations [59]. CoMP can be designed to eliminate Inter-Cell Interference (ICI), which is relevant in LTE and 5G

Heterogeneous Network (HetNet) designs, thus improving cell throughput, spectral and energy efficiency due to reduced ICI [57, 60, 61, 62].

In the MAC layer, the concept of CA consists of the aggregation of multiple CCs or blocks of contiguous and/or non-contiguous spectrum with the aim of achieving higher data rates. In Release 10 specifications, where CA was introduced in the 3GPP standard, the aggregation of up to five CCs was supported and, later on, extended to support a theoretical maximum of 32 CCs in Releases 13-14. CA has been shown to improve the system peak date rate and performance with the aggregation of multiple carriers of different HetNet links, effectively benefiting from the different coding schemes and utilising the spectrum effectively [63, 64]. The aggregation is typically done for CCs of different spectrum bands (inter-band aggregation), even though the possibility of aggregating CCs in the same bands (contiguous or non-contiguous aggregation) is also contemplated in the standard [15, 54, 58, 65].

In the PDCP layer, multiple MC approaches have been standardised. Dual Connectivity (DC) was first specified in Release 12 to allow UEs to be simultaneously connected to two eNodeB (eNB) via a non-ideal back-haul. In this scenario, the UE is configured to use the radio resources provided by the two distinct schedulers. In Release 13, 3GPP introduced LTE-Wi-Fi Aggregation (LWA) to merge data streams transmitted through different Radio Access Technology (RAT) at the PDCP layer, for both collocated and non-collocated nodes, to enhance throughput and exploit the availability of more than one connectivity technology at the same location such as LTE and Wi-Fi, which is a common scenario in malls, airports and other similar hot spots [54, 58]. The same concept is preserved in Release 15 where DC is specified for operations between 5G-NR Next Generation Node-B (gNB) and LTE eNB nodes in Multi-Radio Dual Connectivity (MR-DC) [66]. In Release 15 Multi-Radio Access Technology (Multi-RAT) DC was introduced to enable DC in different RATs, combining LTE carriers and 5G-NR carriers in order to enhance data rates. Aside from data split, packets are duplicated in the PDCP layer for the transmission of the same packet over both paths to improve reliability [54, 58, 67]. This MC technique in 5G-NR can split or duplicate data traffic considering the different 5G-NR features, with a trade off between services tailored to eMBB and URLLC requirements [68, 69].

The concept of MC can be extended to higher layers, including, for example, Multipath TCP (MPTCP) as a popular example at the transport layer. However, the focus of this work is mainly on the radio interface of mobile communication systems, which typically addresses the lower layers of the protocol stack. As a result, the technical contributions provided in this thesis belong to the PHY and MAC layers. Therefore, MC techniques for higher layers have not been included in this discussion.

1.7 Research Objectives

MC techniques have been tremendously successful in improving the performance of mobile communication systems and enhancing various relevant performance metrics for a wide variety of services and applications (i.e., 'use cases' according to 5G/6G terminology). This motivates the research work presented in this thesis to further explore novel approaches based on the principle of MC. The main objective of this work is to propose novel MC techniques suitable for their use in existing and future mobile communication systems that can improve the performance of existing and new service applications in 5G/6G use case scenarios. Concretely, the objective of this thesis is to contribute to the enhanced provision of eMBB and/or URLLC services in 5G/6G networks by means of novel MC techniques that can effectively enhance the user data rates and/or reliability of the wireless mobile communication links in order to meet the requirements of these services more effectively and more efficiently.

1.8 Contributions and Thesis Organisation

This thesis provides three main novel contributions, which will be presented and discussed in subsequent chapters as follows:

- Chapter 2 proposes a novel framework for the use of CA as a MC technique. The main idea proposed in this chapter is to divide a contiguous block of spectrum (that could, in principle, be used as a single carrier) into a number of sub-blocks and treat each of them as different CCs that are combined via CA. The motivation for this is to benefit from the frequency diversity experienced by each CC when the spectrum is divided in such a way. Notice that CA was originally proposed as a technique to increase data rates by incorporating additional bandwidth into the system. Therefore, the concept of CA in a traditional sense inherently implies the use of additional bandwidth as a way to increase data rates. On the other hand, the framework proposed in Chapter 2 proposes a different approach that does not require additional bandwidth, but simply splits the existing spectrum into blocks in order to benefit from frequency diversity, thus effectively exploiting CA as an MC technique, which is a novel point of view that, to the best of the author's knowledge, has not been considered in the literature before. The proposed CA-based MC method is implemented in detail in the ns-3 simulator in order to evaluate its performance based on system

level simulations. The performance of CA under various propagation scenarios is then evaluated and analysed. The obtained results indicate that CA can effectively be exploited as a diversity technique to optimise the overall system performance and increase the network capacity. Moreover, it is found that the optimum number of CCs into which the spectrum should be divided depends on the radio propagation distance. Such an optimum number of CCs is determined by the trade-off between the diversity gain and the bandwidth penalty incurred by each CC.

- Chapter 3 further explores the framework proposed in Chapter 2 from an analytical perspective. More specifically, Chapter 3 develops a mathematical model aimed at characterising the performance of CA as a diversity technique. The main objective is to develop a mathematical model that can explain the behaviour and performance of the CA-based MC technique presented in Chapter 2. Given the high complexity of this problem, the concept of *effective Signal-to-Noise Ratio (SNR)* is proposed, which is defined as the equivalent SNR experienced in a single carrier that would lead to the same throughput performance as the one obtained when the same amount of spectrum available is split into several CCs that are then combined according to CA. Mathematical models for such effective SNR are then elaborated, which are then exploited to derive the statistical distribution of the effective SNR under various assumptions. Such statistics are finally employed to obtain closed-form expressions for the overall system performance in terms of both ergodic and secrecy capacities as a function of the number of CCs and other relevant parameters. The obtained numerical results demonstrate that the developed mathematical model can explain and corroborate the findings derived from simulation results in Chapter 2.

- Chapter 4 proposes a novel hybrid transmission scheme for improved link reliability. The proposed hybrid system benefits from the range of frequency bands available in mobile communication systems and their complementary characteristics. Higher-frequency bands tend to provide larger bandwidths (i.e., higher data rates) but are also characterised by more challenging propagation conditions (i.e., lower link reliability), while the opposite is true in general for lower-frequency bands. To exploit these complementary characteristics, a hybrid system is proposed that dynamically switches between both bands according to the instantaneous channel quality. The proposed hybrid transmission system is studied analytically. Concretely, the SNR statistics observed at the receiver are first determined, which are then employed to calculate

closed-form expressions for relevant system performance metrics such as the outage probability, bit-error rate and channel capacity. The obtained results demonstrate that the proposed hybrid transmission scheme not only improves dramatically the transmission reliability but also has the potential to simultaneously increase the capacity while efficiently exploiting the resources in both bands.

This thesis is finally concluded in Chapter 5, where the main findings derived from this research are summarised. Some directions to further extend the research ideas explored in this thesis are suggested as well.

1.9 List of Publications

The research work presented in this thesis has led to the following outcomes:

1. P. U. Adamu and M. López-Benítez, "Performance Evaluation of Carrier Aggregation as a Diversity Technique in mmWave Bands," in Proceedings of the *IEEE 93rd Vehicular Technology Conference* (VTC 2021-Spring), Helsinki, Finland, 25-28 April 2021.
   DOI: 10.1109/VTC2021-Spring51267.2021.9448984

2. P. U. Adamu, M. López-Benítez and J. Zhang, "Hybrid Transmission Scheme for Improving Link Reliability in mmWave URLLC Communications," *IEEE Transactions on Wireless Communications*, vol. 22, no. 9, pp. 6329-6340, September 2023.
   DOI: 10.1109/TWC.2023.3241792

3. P. U. Adamu and M. López-Benítez, "Analysis of Carrier Aggregation as a Diversity Technique for Improved Spectral Efficiency and Secrecy Performance in Mobile Communications," submitted to *MDPI Sensors* (under review).

Chapter 2

Carrier Aggregation as a Diversity Technique: A Simulation Approach

2.1 Introduction

As wireless communication is becoming more of a commodity just like electricity and water, it has given rise to a large array of emerging high data rate hungry devices and services [70]. The fifth generation mobile communication network is evolving and will be characterised by an increase in the number of mobile wireless devices and service types, the availability of different radio access technologies, and the ability to transmit at a high data rate which is expected to meet the data requirement of various high speed multimedia applications [17, 71, 72]. In order to meet the requirements of various high-speed multimedia applications, wireless communication systems in the next generation are expected to reach the data rate characteristics of 1 Gbps. Boosting the transmission rate in these systems is achieved by using larger bandwidth but due to the practical constraints, large segments of the continuous spectrum may not be available for most wireless network operators which makes the effective use of a plurality of non-continuous frequency spectrum an alternative option [17, 71]. This has also motivated the international research community to carry out research on spectrum expansion technologies

to increase a single user's peak data rates and improve network performance with techniques such as CA, which is the focus of the study presented in this chapter. CA traditionally aggregates multiple blocks of contiguous and non-contiguous spectrum in the licensed and unlicensed bands, referred to as CCs in 3GPP, with the aim to enable the use of larger amounts of spectrum and therefore achieve higher data rates. This technique plays an important role in current 5G wireless networks with an air interface based on millimetre wave (mm-Wave) bands as well as for future 6G networks and beyond with air interfaces based on higher spectrum such as THz bands.

While CA brings multiple benefits, it also poses various technical challenges that need to be addressed for successful implementation. Some of these challenges include: i) *management of interference between aggregated carriers* (i.e., CCs), because combining multiple carriers can potentially introduce interference between them when they belong to adjacent spectrum bands, thus requiring proper interference management techniques to minimise the impact on signal quality and overall network performance; ii) *CA control*, because synchronisation and precise timing must be maintained between carriers for an effective CA; iii) *dynamic radio resource allocation*, because the efficient allocation of resources across multiple carriers is a complex task and therefore efficient radio resource management algorithms are needed to adapt to changing network conditions in order to optimise the use of the available frequency bands; iv) *handover and mobility management*, because the transfer between cells and across larger geographical areas of a communication established simultaneously over multiple carriers is more complex, thus requiring effective mechanisms to ensure a smooth and seamless handover process to avoid interruptions in service; v) *backward compatibility*, since older devices may not be compatible with CA and network operators need to manage the transition period as newer devices are introduced; vi) *increased power consumption*, because using multiple carriers may increase power consumption in user devices and therefore efficient power management strategies are needed to balance the benefits of CA with the impact on device battery life; vi) *hardware and software upgrades*, because implementing CA may require upgrades to both network infrastructure and user devices, and coordinating these upgrades across a network is typically a logistically challenging task; and vii) *compatibility with spectrum regulations*, since CA may in some cases involve the combination of different spectrum bands, which may pose issues to the compliance with spectrum regulations. Addressing these challenges is crucial for the successful deployment and operation of CA in mobile communication networks. Since its introduction in the context of mobile communication systems, continuous research and development efforts have been ongoing to enhance the efficiency and performance of CA technologies.

The remainder of this chapter is organised as follows. First, relevant background and related work are presented in Section 2.2. The considered system model is then introduced in Section 2.3, which relies on the implemented `mm-Wave` module integrated into the ns-3 simulator employed in this chapter. Section 2.4 presents in detail the proposed use of CA as a diversity technique. The evaluation methodology followed in this chapter is then explained in Section 2.5, where the simulation platform and the relevant simulation configurations are detailed. The simulation results obtained for the different scenarios considered in this study are presented and analysed in Section 2.6. Finally, Section 2.7 summarises the main conclusions derived from this study and concludes the chapter. The research findings and results of this chapter have been published in [64].

2.2 Background and Related Work

The idea of CA was originally introduced for the first time in 3GPP Release 8 in the context of UMTS/HSPA+ (referred to as Dual Cell), enabling two downlink carriers assigned to one user. However, the concept that is commonly known as CA in mobile communication systems was reintroduced as a new feature in LTE-A 3GPP Release 10 [73] enabling the combination of two or multiple CCs seamlessly to higher layers of the protocol stack as illustrated in Figure 2.1 in order to increase the overall bandwidth used for communication and thus the throughput experienced by the users of wireless mobile networks. This technique was motivated by the limited per-channel bandwidth defined for mobile networks at that time and the demand for higher data rates that were not achievable with such an amount of spectrum per single channel (or CC). It is a relatively new technology that enhances mobile data capacity, throughput and improves network performance by allowing the combination of two or more CCs of the same or different frequency bands into a single aggregated channel as a means of efficient spectrum utilisation that increases the bandwidth of the mobile broadband and the system reliability [17, 18, 74]. When CA is activated, the transmitter's MAC layer splits the sequence of data packets generated at higher layers into N data flows, each of which is sent over one of the N available CCs as shown in Figure 2.2. The CA-enabled receiver reorders the recovered packets at the MAC layer so that the process is transparent to the higher layers of the protocol stack. The total data rate observed at higher layers is the sum of the individual rates experienced in each CC. It is worth noting that the number of CCs was initially limited to a maximum of 5 CCs in Release 10 thereby

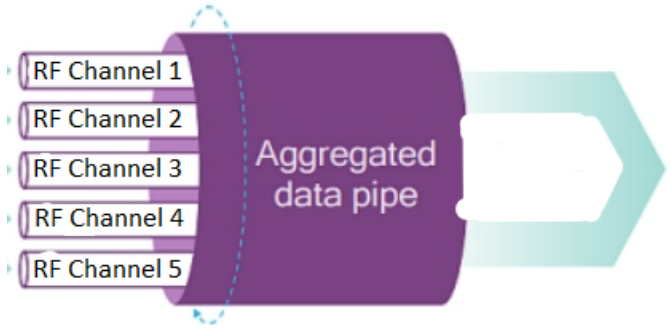

Figure 2.1: Illustration of the CA concept aggregating up to 5 CCs.

effectively increasing the maximum user bandwidth fivefold [75, 76]. Later on, this limit was extended to a maximum of 8 CCs in Release 11, and further extended to a maximum of 32 CCs in Releases 13-14. 5G supports a maximum of 16 CCs in Phase 1 (3GPP TS 38.133).

Generally, carriers (i.e., CCs) can be aggregated in three different spectrum scenarios briefly explained below and illustrated in Figure 2.3.

- **Intra-band Contiguous CA**: It is the aggregation of neighbouring CCs in the same spectrum band. It is a less practical scenario given the frequency allocation in the real world, as the availability of large contiguous spectrum for network operators is impossible to get in lower frequency bands. The contiguous channels in this scenario are of the same size and they are spaced with a lesser frequency guard in between.

- **Intra-band Non-Contiguous CA**: It is the aggregation of CCs in the same band in a non-contiguous manner. This is a more practical scenario where spectrum allocation is non-contiguous within the same band. In the example shown in Figure 2.3 the middle carrier is allocated to other users or other instances of network sharing while the two CCs at the extremes of the spectrum are aggregated. Different channel sizes are allowed.

- **Inter-band Non-contiguous CA**: In this scenario, multiple CCs of different spectrum bands are being aggregated. This is the most practical scenario due to the unavailability of a contiguous wide spectrum to achieve the desired peak data rates. The different radio propagation characteristics for the different spectrum bands can be exploited to potentially improve mobility robustness for the low-latency and high reliability 5G challenging scenarios.

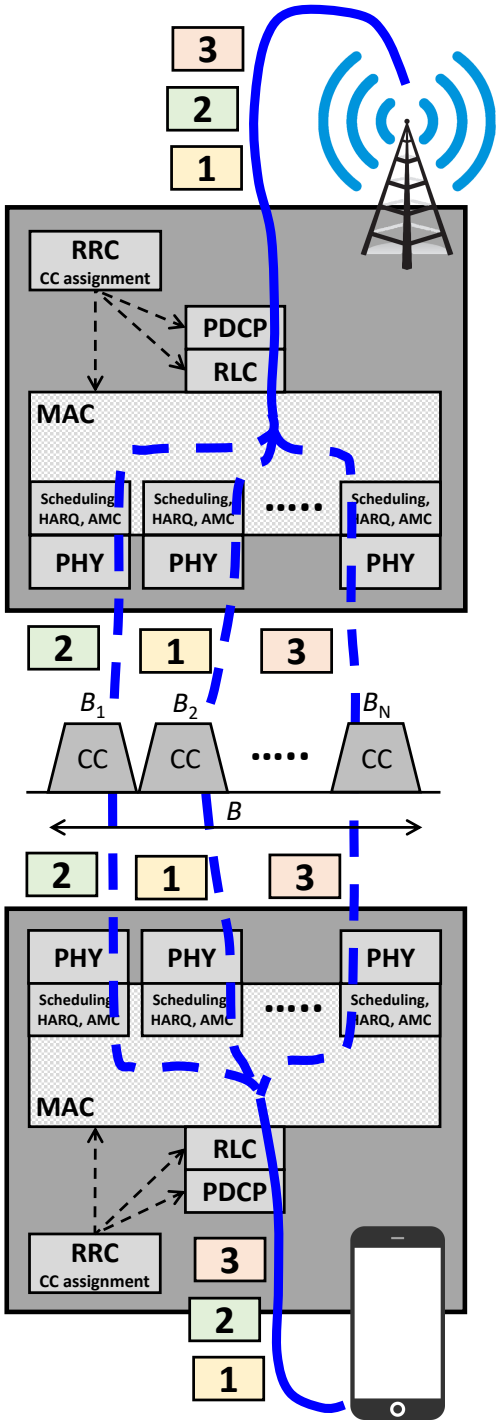

Figure 2.2: Transmission and reception with CA. The transmitter splits the data stream into N CCs and the packets are reordered at the receiver.

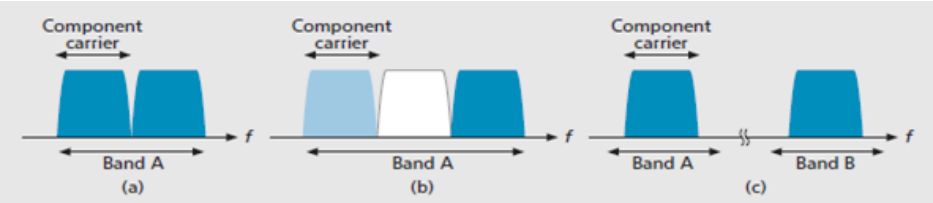

Figure 2.3: The three different CA spectrum scenarios: a) Intra-band contiguous; b) Intra-band non-contiguous; c) Inter-band non-contiguous.

CA technology is crucial in allowing the coexistence of the previous generation 4G network and the fifth generation network, allowing operators to combine different 4G carriers with 4G carriers or 4G with 5G carriers as well. It has evolved into dual connectivity to allow the coexistence of 4G and 5G mobile networks with reduced latency and the ability to achieve higher data rates in the order of Gbps with aggregated bandwidths in the most recent 3GPP releases. 5G networks support two frequency ranges, the sub-6 GHz microwave 4G carriers (frequency range 1) and millimetre wave or mm-Wave 5G carriers (frequency range 2) in the 5G RAN, both in the licensed and unlicensed frequency bands. Initial 3GPP releases allowed the combination of up to 5 CCs when using CA, while more recent releases have extended this limit to a theoretical maximum of up to 32 CCs. This is aimed at increasing the bandwidth in order to facilitate multi-gigabit data rates (contiguous or non-contiguous aggregation) with multiple numbers of CCs to be aggregated in more recent releases, with the mm-Wave band being viewed as the key enabler for the enhanced mobile broadband eMBB [16, 77, 78].

However, communication in mobile mm-Wave bands is characterised by several challenges, mainly related to the harsh propagation environment at such a high frequency. mm-Wave has a high isotropic propagation loss, which is experienced in the band and increases with the square of the carrier frequency. The use of MIMO techniques, spatial multiplexing, beam-forming and other techniques has been widely deployed in mm-Wave frequency bands to tackle these challenges, hence increasing the link budget and increasing the range of communication. This is made possible with many antenna elements packed in a small area [79, 80, 81]. Communications in mm-Wave bands are also affected by blockage, which prevents a direct Line-of-Sight (LOS) communication in the presence of obstacles such as buildings and the human body. However, communication is made possible in the Non-Line-of-Sight (NLOS) scenario as well (e.g., in urban environments with a rich scattering environment as shown in [82]) and by increasing the density of mm-Wave base station deployments as a way to decrease the outage probability, providing

extended coverage ranges approximately in the order of hundreds of metres [83]. Mobile communications shifted towards higher frequency bands with the aim to obtain larger bandwidths as a way to increase the network capacity, however communication in mm-Wave bands also introduced challenges, requiring new access protocols in the MAC layer, fast network procedures for timely base station updates in the event of blockages and intermittency of the channel availability, thus causing the emergence of buffer-bloat and under-utilising the available resources to some extent [84, 85, 86].

It has been shown in different research studies that CA can be employed in a wide variety of scenarios in order to enhance data rates, increase capacity and improve the overall system performance. CA is shown in [87] to provide higher data rates, enable flexibility and utilise the frequency resources optimally. Simulation results provided in [76] with aggregated schemes and bandwidth structure show the effect of CA on the system performance in terms of throughput, with a higher throughput gain in an LTE-A system with 5 CCs than in the counterparts with 2 CCs, 3 CCs and 4 CCs, and also a higher throughput performance of CA when compared to the non-aggregated scenario. CA is also seen as a critical enabler of 5G-NR, where the enhancements of the latest 3GPP releases improve the system performance while increasing the throughput and reducing its power usage needs [88, 89]. It has also been shown that with different access technology configurations, the principle of CA also has the potential to improve the system performance with packet duplication in 5G-NR CA/DC [90]. The study in [91] also confirms that the use of CA increases the data rate significantly. For details, the reader is referred to [92], where a systematic literature review is presented, summarising network parameters, relevant methods and findings.

In summary, CA in 5G provides some important benefits by efficiently using the available spectrum and leveraging the underutilised spectrum, despite some challenges associated with the use of higher frequency bands such as mm-Wave (e.g., higher path loss compared to lower frequency bands, atmospheric absorption caused by oxygen and water vapour, and more accentuated blockage caused by solid objects). CA helps aggregate carrier frequencies (referred to as CCs in the CA jargon) irrespective of spectrums (i.e., it can be used to aggregate licensed and unlicensed spectrum). It will also be beneficial for network carrier load balancing, enabling intelligent and dynamic load balancing with real-time network loaded data. Carrier aggregation has been stated to increase the system throughput to the range of Gbps in 5G networks and beyond, providing better network performance and enhancing the scalability for carriers with expanded coverage. Moreover, it can also increase network reliability with the use of aggregated back-up carriers and can thus reduce latency in the context of URLLC communication scenarios.

2.3 System Model

The system model considered in this chapter assumes that a block of contiguous spectrum with bandwidth size B is available, which would normally be exploited as a single carrier (i.e., single CC) but is however split into N adjacent CCs. When CA is activated, the transmitter's MAC layer splits the sequence of data packets generated at higher layers into N data flows, each of which is sent over one of the N available CCs, as shown in Figure 2.2. The CA-enabled receiver reorders the recovered packets at the MAC layer so that the process is transparent to the higher layers of the protocol stack.

The specific aspects of CA in particular, and the considered mobile communication system and its environment in general, are determined by the implementation of CA in the `mm-Wave` module of the ns-3 simulator employed in this work, which will be discussed in more detail in Section 2.5. The modelling of CA in the `mm-Wave` module for ns-3 relies on the implementations of the ns-3 `LTE` module and is compliant with the 3GPP specifications for New Radio (NR). The implementation of the data plane includes the lower layers of the protocol stack involved in the operation of CA (i.e., PHY and MAC) and is transparent to the functionalities offered by higher layers (i.e., Radio Link Control (RLC) and PDCP). The control functionalities are carried out by the Radio Resource Control (RRC) layer, which shares the information for setting up the CCs between the UE and the Base Station (BS). To this end, the BS broadcasts information on the primary CC, and when the UE connects to it, the RRC entity at the BS instructs the UE to add the relevant number of CCs with its different parameters as configured in each simulation (i.e., numerology, frequency and bandwidth for each CC). Once the desired number of CCs have been set up and configured, a separate instance of the MAC/PHY entities is run in each CC for data transmission, with all the data packets in each CC being re-combined at the receiver's MAC layer as discussed above and illustrated in Figure 2.2.

A detailed description of the CA model and its implementation in the employed ns-3 simulator is beyond the scope of this work, but the interested reader can find all the relevant details in [93]. The system models for other relevant aspects of the mobile communication system and its environment considered in this chapter are those of the `LTE` module for ns-3 and can be found in the module's documentation provided for the simulator (some of these aspects will be discussed in more detail in Section 2.5).

2.4 CA Proposed as a Diversity Technique

The main purpose of CA is to allow operators combine multiple chunks of (possibly non-contiguous) spectrum in a transparent manner for higher layers of the protocol stack so that it can be seen as a single block of spectrum by higher layers. CA techniques have been widely investigated from this perspective as this is how the idea of CA originally emerged.

However, it is worth noting that CA may also be exploited as a diversity technique, which is the fundamental idea proposed and investigated in this chapter. The motivation to consider this idea stems from the fact that each CC that is aggregated through CA runs an individual instance of the associated layers of the protocol stack and therefore the employed transmission parameters are adapted individually to each of the CCs. This means that the transmission process in each individual CC can benefit from the diversity obtained through the use of different CCs. In general, the transmission through each CC will experience independent propagation conditions – this is particularly true when the CCs are located at very distant carrier frequencies given the different path loss associated with different frequencies, however this is also true (to a lower extent) even if the CCs are in adjacent carrier frequencies given that instantaneous channel fading is essentially a random process with significant variations across slightly different wavelengths (i.e., frequencies). Notice that such diversity exists in principle in any frequency band that is suitable for mobile communications, including the sub-6 GHz bands where 4G mobile systems were deployed, the mm-Wave bands where 5G mobile systems are currently being deployed and also the THz bands where 6G mobile systems are expected to be deployed.

The observation above suggests the possibility of exploiting CA as a diversity technique, even in the case where a contiguous block of spectrum is available, where the use of CA would not really be necessary in order to exploit that spectrum and where it would not normally be used in the classical scenario of CA. Notice that the original idea and motivation of CA was to aggregate frequency bands or CCs where the use of a large chunk of spectrum was not possible because of existing frequency allocations or other practical limitations. On the other hand, the idea in this chapter is to force the use of CA in a large block of spectrum in order to benefit from the diversity experienced by the transmission process at different frequencies. The idea is to divide a relatively large block of contiguous spectrum into a number of adjacent CCs, divide the original data stream into the same number of data sub-streams (each with a lower data rate), then transmit each data sub-stream through one of the CCs and then combine these data sub-streams via CA (concretely, via intra-band contiguous CA as shown in Figure 2.3a).

To be more specific, the idea proposed in this chapter is discussed now in more detail. Assume that a mobile operator has a relatively large block of contiguous spectrum that can be exploited for transmission as a single channel (CC in CA terminology). According to the original formulation of the CA concept, in this scenario CA would not be necessary given that in this scenario there is only one block or chunk of spectrum, and therefore there is no other block of spectrum with which it could be aggregated. The idea explored in this chapter is that such a large block of contiguous spectrum is artificially divided into a number N of smaller sub-blocks where each sub-block receives a fraction $1/N$ of the total available bandwidth and then each of these sub-blocks is treated as an independent carrier (i.e., CC) that is aggregated to the other CCs via the use of the CA concept. Notice that the use of CA in this case is artificial, since transmission over the whole chunk of spectrum (used as a single channel) would be possible. However, the available spectrum is artificially divided into a number of CCs that are recombined via CA in order to benefit from the frequency diversity that would normally be expected in channels with a large bandwidth. This is possible because the data stream transmitted through each CC will undergo an individual instance of the associated layers of the protocol stack. As a result, the data transmitted through each CC will have its own dedicated instance of scheduler, transmission power control, adaptation of the Modulation and Coding Scheme (MCS), etc. All these parameters will be adapted individually to the instantaneous conditions experienced in each CC and therefore can be expected to be optimised accordingly. If, on the other hand, the whole chunk of available spectrum was exploited as a single channel or CC, then a single instance of scheduler, transmission power control, adaptation of the modulation and coding scheme, etc., would be run over the whole block of spectrum, which would not be optimum for the conditions experienced at each frequency interval. Thus, by artificially forcing separate data streams via different CCs in the available spectrum, the aim is to exploit the diversity in each frequency interval. As a result, in this context, CA can be effectively employed as a diversity technique to improve the overall performance.

Notice that CA was originally proposed as a technique to increase data rates by incorporating additional bandwidth into the system. Therefore, the concept of CA in a traditional sense inherently implies the use of additional bandwidth as a way to increase data rates. On the other hand, the framework proposed in this chapter as discussed above does not require additional bandwidth, but simply splits the existing spectrum into blocks in order to benefit from frequency diversity, thus effectively exploiting CA as a MC technique, which is a novel point of view that, to the best of the author's knowledge, has not been considered in the literature before. For instance, a mobile operator

with a spectrum block of 20 MHz using CA in a traditional sense would seek to find other blocks of spectrum to be aggregated to the existing 20 MHz block. On the other hand, the framework proposed in this chapter would not seek to increase the amount of existing spectrum but instead would exploit the existing block of 20 MHz, not as a single carrier of 20 MHz, but instead as 2 CCs of 10 MHz each, or 4 CCs of 5 MHz each, which would then be combined via CA. The number of possibilities is much larger, in particular if the new bands introduced for 5G are considered. In Frequency Range 1 (FR1), a block of 100 MHz could be exploited with the proposed framework as 2 CCs $\times$ 50 MHz, 4 CCs $\times$ 25 MHz, 5 CCs $\times$ 20 MHz or 10 CCs $\times$ 10 MHz (the option of 20 CCs $\times$ 5 MHz is not allowed by the standard given that up to 16 CCs can be aggregated). In Frequency Range 2 (FR2), a block of 400 MHz could be exploited as 2 CCs $\times$ 200 MHz, 4 CCs $\times$ 100 MHz or 8 CCs $\times$ 50 MHz. Therefore, while traditional CA aims to increase capacity by increasing the bandwidth available (i.e., Hz), the proposed CA-based MC framework aims to increase the capacity by increasing the spectrum efficiency within the available spectrum (i.e., bit/s/Hz).

The proposed CA-based method faces similar technical challenges as those discussed in Section 2.1, with some new specific considerations that are worth discussing. Firstly, managing the interference between the CCs is important in the proposed method because all the CCs aggregated via CA will always be adjacent. Therefore, the underlying allocation of radio resources should carefully take this aspect into account to minimise interference between adjacent CCs and optimise the overall performance achieved with the application of this technique. This technique will also incur in additional power consumption as well as additional complexity in the handover process. This is because, using multiple CCs will consume more power and need to be transferred to a new cell, whereas if the proposed technique was not used, only a single CC would have been used. Backward compatibility with older devices that do not support CA would, of course, be an issue, as it would also be for lower-end inexpensive user terminals that may not support CA either. On the positive side, the proposed technique should not have any implications from a spectrum regulation point of view, since the spectrum used would be exactly the same if only one CC were to be employed. However, each CC has its own associated signalling traffic, which would increase with the number of CCs employed and, as a result, the proposed technique would result in a higher signalling overhead. To fairly evaluate the joint effect of the above technical aspects on the network performance of the proposed CA method, simulations were carried out with a sophisticated network simulator, as discussed below in Section 2.5.

Before concluding this section, it is worth mentioning that the concept of CA, as defined by 3GPP, was envisaged to be implemented between one BS and one UE. Therefore, any CA-based method, including the one proposed in this section, applies to the physical connections between one BS and one UE. The counterpart 3GPP technique that exploits diversity across multiple BSs is Dual Connectivity (DC), which shares some similarities with CA and allows the combination of different bands through multiple BSs. One of the main differences is that DC aggregates the split traffic at a higher layer of the protocol stack, namely the PDCP layer, to enable the use of multiple BSs for the same UE. The underlying idea on which the CA method proposed in this section relies might be adapted in order to be exploited in the context of DC, however this new scenario would pose new questions, such as the need to allocate each CC to a specific BS. This scenario is beyond the scope of the work presented in this chapter and is suggested as future work.

2.5 Evaluation Methodology

2.5.1 Simulation Platform

This work investigates the performance of the proposed CA-based diversity strategy over mm-Wave bands by means of system level simulations. Discrete-event network simulators are fundamental in the development and analysis of complex networks. Having a full-stack simulation capability, modelling all layers of the protocol stack with models of real life scenarios, and an end-to-end cellular system with mm-Wave CA integrated into the simulation model is crucial for the study presented in this chapter. To this end, it is important to have an end-to-end simulation system that can exploit the capabilities of mm-Wave links across all the layers of the communication protocol stack.

The need for a cross-layer design solution and the analysis of the performance of an end-to-end environment in mm-Wave cellular networks motivated the introduction of a mm-Wave module for the widely used open source ns-3 simulator [94]. In [95], a full stack mm-Wave simulation model is presented, integrated into ns-3, which includes a significant number of detailed statistical channel models and the ability to incorporate measurements or ray tracing data. The end-to-end simulation system in [95] has a modular and highly customisable design of the PHY and MAC layers that adapts to the large bandwidth available in mm-Wave bands, with ray tracing, 3GPP statistical channel modelling like path-loss, blockage, etc., implements the

higher layers of the LTE network in the RLC layer and interfaces with the LTE core network ns-3 module for the full stack end-to-end connectivity. Therefore, the mm-Wave module for the ns-3 simulator presented in [95] is a suitable candidate to carry out the simulations required in this study.

The performance of mobile communication networks with CA over two CCs was simulated in contiguous and non-contiguous allocations in [93]. Relying on the same simulation model, the work presented in this chapter extends the ns-3 simulator developed in [95] and employed in [93] in order to implement the proposed CA-based diversity technique. The code of the ns-3 simulator with the integrated mm-Wave module was refactored in order to implement the diversity technique based on the CA proposed in Section 2.4. Moreover, the simulation code was also extended to a broader range of propagation scenarios and channel models as defined by 3GPP [96] and the number of component carriers was also increased beyond two (as implemented in [93]) in order to explore and exploit the full potential of the diversity strategy proposed in this chapter. This enabled this simulation study to investigate the impact of various levels of CA (i.e., combining different numbers of CCs) in different propagation scenarios and determine the optimum configuration as a function of the propagation and communication context. Further details on the simulator and employed scratch file are provided in the Appendix.

2.5.2 Simulation Configuration

The employed simulation platform is used to assess the performance of CA in a mm-Wave mobile communication system, when employed not only in the classical approach (i.e., as a way to increase the total data rate by aggregating several CCs) but also as proposed in Section 2.4 (i.e., as a diversity technique to improve the system performance with the same amount of available bandwidth). For the latter case, different data streams can be transmitted in each link/CC using different frequencies. The transmission in each CC can be adapted to the channel independently by using different scheduling instances, MCS and retransmission processes.

The main simulation parameters are summarised in Table 2.1. The considered simulation scenario is composed of one base station eNB and one mobile terminal UE, as this is the scenario for which CA was originally defined. The UE is assumed to be placed at a fixed distance from the eNB in each simulation run, however different distances ranging from 10 m up to 5.5 km are considered in different simulation runs. Simulating several static scenarios rather than one mobile scenario where the BS-UE distance changes dynamically allows the analysis of the results without the complex-

Table 2.1: Main simulation parameters.

Parameter	**Value**	
Number of eNB	1	
Number of UE	1	
BS-UE distance	10 m – 5500 m	
Propagation scenarios	UMa, RMa, UMi, InH-Office	
Propagation conditions	LOS/NLOS	
Total amount of spectrum	1 GHz	
Number of CC's	1-5	
CC bandwidth	1/no. of CC's	
Simulation time	5 min.	
Contiguous Freq.(GHz)	$f_0 = 40$	($f_0 = 39.75$, $f_1 = 40.25$)
Non-contiguous Freq.(GHz)	$f_0 = 73$	($f_0 = 32.5$, $f_1 = 73$)

ity introduced by dynamic mobility. As it will be shown in Section 2.6, the performance and optimum configuration of the proposed CA method depends on the BS-UE distance, and this is an important aspect that would have been difficult (or even impossible) to appreciate in a dynamic mobile scenario. For a more detailed performance evaluation, and in order to validate the obtained conclusions over different communication scenarios, various 3GPP propagation environments are considered, namely Urban Macro (UMa), Rural Macro (RMa), Urban Micro (UMi-StreetCanyon) and Indoor Home Office (InH-Office) as detailed in [97]. For each considered propagation environment, both LOS and NLOS conditions are evaluated.

The eNB and UE can communicate over a total amount of available spectrum with a bandwidth of 1 GHz. Communication can be achieved either by using the contiguous block of spectrum as a single link that uses the total available bandwidth of 1 GHz as a single carrier, or by using CA. When CA is considered, the total bandwidth of 1 GHz is subdivided into a number of contiguous chunks, each of which is managed as a separate CC that is aggregated to the other CCs in the same 1 GHz spectrum block. In this case,

Table 2.2: Carrier frequency and bandwidth allocation for various CCs.

No of CC	**BW per CC (MHz)**	**Carrier Frequency (GHz)**				
1	1000	40				
2	500	39.75	40.25			
3	333.3	39.67	40	40.33		
4	250	39.63	39.88	40.13	40.38	
5	200	39.6	39.8	40	40.2	40.4

a total maximum of up to five CCs can be aggregated using the principle of CA. The contiguous block of 1 GHz of the spectrum is assumed to be centred around a central carrier frequency of 40 GHz, coinciding with one of the mm-Wave bands defined by 3GPP. Thus, when a single link is considered, the carrier frequency is 40 GHz as shown in Table 2.1. If two CCs are considered, then the block of 1 GHz is divided into two sub-blocks of 500 MHz each, with carrier frequencies at the centre of each block (i.e., f_0 = 39.75 GHz and f_1 = 40.25 GHz as shown in Table 2.1). For a higher number of CCs, a similar process is followed, which results in the bandwidth allocations and carrier frequencies shown in Table 2.2.

For comparison purposes, when the performance is evaluated considering two CCs, a non-contiguous scenario is also considered, with central carrier frequencies of f_0 = 32.5 GHz and f_1 = 73 GHz as shown in Table 2.1. This non-contiguous CA scenario is introduced with a CC of 73 GHz, which coincides with one of the mm-Wave bands defined by 3GPP, in order to illustrate more clearly the impact of the carrier frequency on the obtained performance results. The performance is assessed in terms of the throughput experienced at the Radio Link Control RLC layer of the protocol stack.

2.6 Simulation Results and Discussion

This section presents simulation results assessing the performance of CA in mm-Wave bands not only as a way to allow mobile operators to aggregate several spectrum bands in order to gain additional capacity but also as a diversity technique to improve the performance of the already allocated spectrum, following the strategy proposed in Section 2.4.

The impact of CA is firstly evaluated considering a total amount of spectrum of 1 GHz bandwidth, which the operator can exploit as a single block with a single CC or two blocks with a spectrum split ratio of 0.5 between the primary and secondary CCs, with central frequencies of 39.75 GHz and 40.25 GHz for contiguous CA and 32.5 GHz and 73 GHz for non-contiguous CA. The user is placed at a fixed distance from the base station under both LOS and NLOS conditions. The possibility of blockage is considered as well, thus expanding the range of propagation scenarios of the 3GPP models.

Figure 2.4 shows the system performance under UMa propagation scenario with LOS. As it can be expected, CA helps increase the overall system throughput. Both configurations with two CCs provide a significantly greater throughput than both configurations with only one CC. One can also notice that the experienced throughput is highly dependent on the centre frequency considered, with transmissions at lower frequencies experiencing higher throughputs because of the reduced path loss. However, it is also interesting to note that the use of CA can help reduce the impact of path loss throughput degradation, since this affects to a larger extent when only one CC is considered. Notice that, when only one CC is employed, the difference between the throughput at 40 GHz and 73 GHz can be up to around 400 Mbit/s (more than 20 % performance degradation). However, when two CCs are considered, the throughput difference between the configurations using CCs at 40.25 GHz and 73 GHz gives a more similar throughput. The throughput is slightly higher when both CCs are contiguous at lower frequencies (39.75 GHz and 40.25 GHz), but if one of the CCs is moved to a higher carrier frequency (73 GHz) then throughput degradation is quite light and significantly lower than that observed if the same change of carrier frequency is applied when only one CC is used. This can be explained by the propagation diversity offered by CA. On the other hand, the presence of blockage appears to have a slightly more severe impact on the throughput when two CCs are used instead of only one, however such degradation is not very significant; notice that the CA case considers blockage in the lower-frequency CC where its effect is more severe (even with full blockage in both CCs the throughput would still be similar). In general, the use of CA with two CCs in the presence of blockage still provides significantly higher throughput than

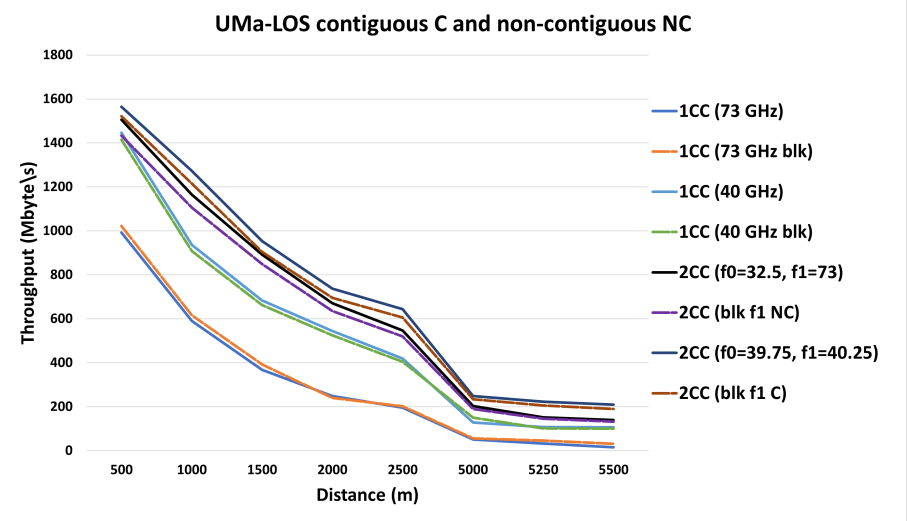

Figure 2.4: Contiguous and non-contiguous UMa-LOS received throughput compared with the use of single CC and the presence of blockage.

the use of one single CC even if it is not experiencing any blockage. Therefore, it can be seen that CA not only provides a higher overall throughput compared to the use of a single CC but also makes the obtained throughput performance less sensitive to the particular radio propagation frequencies of the CCs as a result of the propagation diversity from combining several CCs.

Figure 2.5 shows the counterpart to Figure 2.4, also considering an UMa propagation scenario, but in this case under NLOS conditions. It can be observed that, in this other case, the performance difference between the use of CA with two CCs and the use of a single CC with no CA is not so significant. In fact, while there is still a clear difference between using a single CC at 40 and 73 GHz, there is no practical difference between the two configurations with two CCs (contiguous and non-contiguous spectrum). In fact, the use of two CCs in both configurations leads virtually to a very similar performance, which is indeed very similar to the performance attained with the use of one single CC at 40 GHz and, at some distances, even slightly lower. This slightly lower performance of CA can be explained based on the fact that under NLOS conditions the practical propagation distances are reduced significantly (as it can be noticed by comparing the abscissas axes of Figure 2.4 and 2.5) and at such shorter distances the path loss does play such an important role, therefore the potential gain that CA could provide as a diversity technique is not large enough to compensate for the overhead associated with the use of CA (mainly, the use of guard bands between CCs

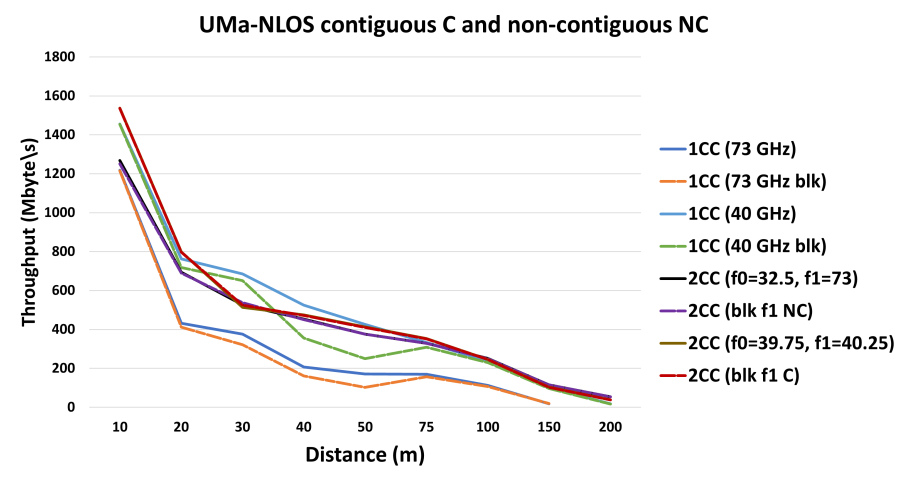

Figure 2.5: Contiguous and non-contiguous UMa-NLOS received throughput.

that reduce the overall spectrum efficiency and the extra signalling overhead involved in the use of CA). In this case, under NLOS conditions, it seems that the use of the whole spectrum available as a single chunk with one single CC, where possible, should provide a better throughput performance.

It is worth noting that the observations made above for the UMa scenario are in general applicable to other propagation scenarios as well. The same trends were observed for other macro scenarios such as the RMa propagation model, micro scenarios (see, as an example, the results obtained for UMi-StreetCanyon-LOS in Figure 2.6) and even indoor environments (see, as an example, the results obtained for InH-Office in Figure 2.7). It can be noticed that the full potential of CA as a diversity technique can be exploited in macro scenarios and under LOS conditions, with the experienced blockage being a secondary aspect.

To further explore the performance of CA as a diversity technique, we now consider a single contiguous block of spectrum with a bandwidth of 1 GHz where the operator can opt to exploit it as a single block of spectrum with one single CC or, by using the principles of CA, as multiple blocks of spectrum each with its own CC, where the available spectrum is divided into a number of contiguous CCs with carrier frequencies as shown in Table 2.2. Notice that in this scenario there would be no need to use CA techniques since the whole block of spectrum is contiguous and the operator could use a single CC. However, we investigate here the possibility of splitting the block into a number of contiguous CCs that are exploited using CA according to the strategy proposed in this chapter and explained in Section 2.4. The

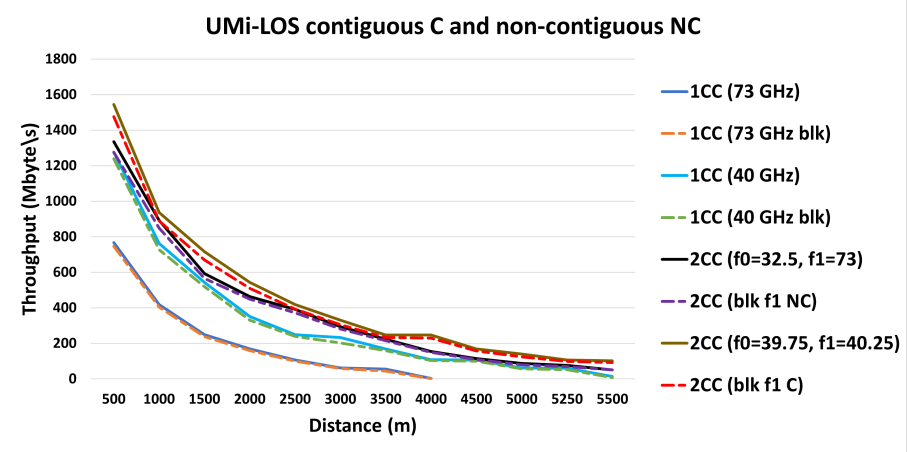

Figure 2.6: Contiguous and non-contiguous UMi-LOS received throughput.

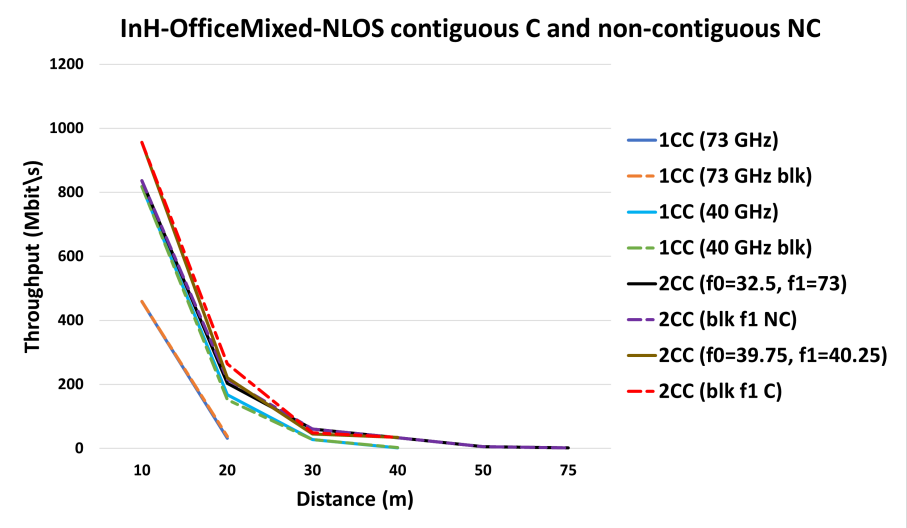

Figure 2.7: Contiguous and non-contiguous InH-Office-NLOS throughput.

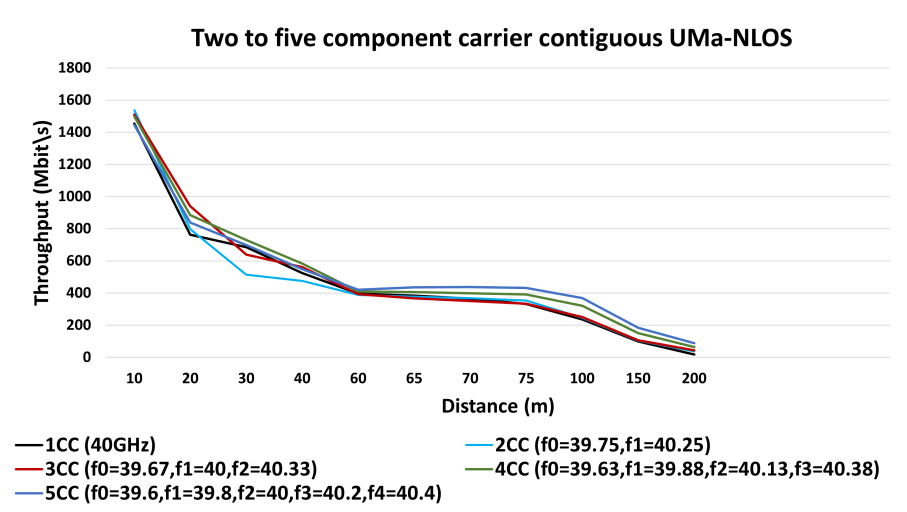

Figure 2.8: One to five component carrier contiguous UMa-NLOS simulation.

motivation to consider this approach is to explore the potential benefits that CA could bring as a diversity technique, which is the focus of the study presented in this chapter.

Figure 2.8 shows the throughput performance observed under an UMa-NLOS propagation scenario when the number of CC is increased from one to five. The UMa-NLOS propagation scenario is selected here because it provides more accurate results than the other available scenarios, however similar conclusions should be drawn for other scenarios as well. The results in Figure 2.8 indicate that the optimum number of CCs increases with the distance, which is shown more clearly in Table 2.3. In general, increasing the number of CCs increases the ability of the system to exploit any available radio propagation diversity since each CC is handled individually with its own scheduler instance, retransmission process, transmission power control, adaptive MCS, etc. However, a higher number of CCs also incurs in a higher overhead resulting from the higher signalling required to handle each CC along with the presence of some guard bands between CCs (which contributes to a decrease in the overall spectrum efficiency). It is worth noting that CA, because of the individual processes running independently for each CC, incurs in a penalty, since part of the bandwidth available for each CC must be used to transmit the CC signalling traffic, and part of it must also be used as a guard band to protect from adjacent channel interference from the neighbouring CCs. For CA to be beneficial as a diversity technique, the gain obtained from channel diversity needs to outperform the penalty associated with a higher number of CCs. The trade-off between both aspects determines

Table 2.3: UMa-NLOS simulation results for 1 CC to 5 CCs.

Dist (m)	**1 CC (Mbps)**	**2 CCs (Mbps)**	**3 CCs (Mbps)**	**4 CCs (Mbps)**	**5 CCs (Mbps)**	**Improvement w.r.t. 1 CC**
10	1455.5	**1537.2**	1510.4	1499.7	1445	5.61%
20	762.1	797.6	**941**	884.4	839.4	23.47%
30	684.9	513.8	639.3	**730.5**	698	6.66%
40	524.2	474.5	560.9	**583.2**	547.9	11.26%
60	397.5	388.7	392.2	410	**421**	5.91%
65	383.7	377.8	367.9	405.5	**435.6**	13.53%
70	364.8	368.3	351	398.3	**437.7**	19.98%
75	332.7	352.5	334.5	390.5	**432.5**	30.00%
100	236.7	245.5	250.9	320.6	**369.1**	55.94%
150	99.2	104.4	106.5	150.3	**184.9**	86.39%
200	18.3	38	44.2	64.7	**87.9**	380.32%

the optimum number of CCs for each propagation distance as observed in Figure 2.8 and Table 2.3. At shorter distances, the channel diversity is not significant (e.g., the path loss experienced at different CCs over short distances is very similar) and therefore a lower number of CCs provides the highest throughput, while at longer distances the radio propagation gain diversity increases and therefore the optimum number of CCs increases. These results indicate that CA can therefore be exploited as a diversity technique to optimise the overall system performance, with the optimum number of CCs depending on the radio propagation distance. The results shown in Table 2.3 indicate that the use of CA as a diversity technique, as proposed in this chapter, can enhance the obtained data rate up to almost five times with respect to the case where only one CC is employed.

2.7 Conclusions

Carrier Aggregation (CA) was originally proposed as a technique to allow mobile operators to combine spectrum from different bands into a single virtual chunk of spectrum that could be seen by the higher layers of the protocol stack as a single block of spectrum. Each aggregated Component Carrier (CC) runs its own instance of the scheduler, retransmission process, transmission power control, adaptive MCS, etc., and therefore adapts each transmission individually according to the CC's propagation conditions. This allows CA to be potentially seen as a diversity technique. In this chapter, a different focus has been considered where the suitability of CA as a diversity technique has been explored. The performance of CA under various propagation scenarios has been evaluated and analysed. The obtained results indicate that CA can effectively be exploited as a diversity technique to optimise the overall system performance and increase the network capacity, with the optimum number of component carriers depending on the radio propagation distance. Such optimum number of CCs is determined by the trade-off between diversity gain (the higher the number of CCs, the higher the diversity gain) and bandwidth penalty incurred by each CC (the higher the number of CCs, the higher the amount of bandwidth that needs to be sacrificed to accommodate guard bands between CCs and to transmit the signalling traffic associated to the processes run individually in each CC).

Chapter 3

Carrier Aggregation as a Diversity Technique: An Analytical Approach

3.1 Introduction

The performance of CA as a diversity technique was evaluated in Chapter 2 by means of simulations carried out with the ns-3 simulator [98, 99], where it was demonstrated that CA can be exploited as a diversity technique to enhance the overall system performance and increase the network capacity without increasing the total amount of spectrum. Simulation studies can be valuable tools for exploring the performance of a particular technique. In fact, the simulation study presented in Chapter 2 was instrumental in understanding and demonstrating the effectiveness of CA when used as a diversity technique. However, an analytical study is also necessary to provide a comprehensive understanding of the technique being investigated. In this context, this chapter presents an analytical study of CA as a diversity technique that complements the simulation study presented in Chapter 2 by developing a mathematical model and a corresponding set of closed-form expressions that can characterise the operation of CA as a diversity technique, thus providing a theoretic basis that supports and explains the findings of the simulation study presented in Chapter 2.

The following contributions are provided in this chapter:

- In order to investigate the performance of CA as a diversity technique, the concept of *effective SNR* is introduced, which is defined as the equivalent SNR at which a single channel achieves the same performance as the considered CA scenario with the same total bandwidth. This concept provides a simple yet powerful tool for the mathematical analysis of CA. Two models for the effective SNR are proposed, namely an ideal model and an average model. For both models, two scenarios are considered where the SNR is distributed homogeneously and heterogeneously across the aggregated CCs. Closed-form expressions for the statistical distribution of the effective SNR are then derived for the four possible cases.

- Capitalising on the developed model of effective SNR, the ergodic capacity of a system with CA as a diversity technique is analysed and mathematical expressions are thus derived for both homogeneous and heterogeneous SNR scenarios.

- Similarly, the secrecy capacity of a system using CA as a diversity technique is also investigated and mathematical expressions are derived as well for the homogeneous and heterogeneous SNR scenarios. By considering both the ergodic and secrecy capacities, a robust communication system design can be achieved.

The remainder of this chapter is organised as follows. First, the system model is described in Section 3.2. Afterwards, Section 3.3 introduces and provides a formal definition of the concept of effective SNR along with mathematical expressions for its statistical distribution under both homogeneous and heterogeneous SNR scenarios, considering an ideal modelling approach as well as an average modelling approach. Based on the developed effective SNR model, analytical results for the performance of CA as a diversity technique in terms of the ergodic and secrecy capacities are presented in Sections 3.4 and 3.5, respectively. Numerical results are then presented and discussed in Section 3.6. Finally, Section 3.7 summarises and concludes this chapter.

The findings and results of this chapter have been submitted for consideration for possible publication as a journal paper, which is under review at the time of submitting this thesis (see publication number 3 in Section 1.9).

3.2 System Model

Let B denote the total bandwidth of a contiguous block of spectrum whose size is appropriate to be exploited as a single 5G-NR or 6G carrier. The mobile operator divides the bandwidth B into N adjacent sub-blocks[1], each of which is physically exploited as a separate CC and combined with the rest of the sub-blocks at the receiver by means of CA. The transmitter's MAC layer splits the sequence of data packets generated at higher layers into N data flows, each of which is transmitted over one of the N available CCs as shown in Figure 3.1. The CA-enabled receiver reorders the recovered packets at the MAC layer so that the process is transparent to the higher layers. The total data rate observed at higher layers is the sum of the individual rates experienced in each CC.

When CA is employed, each CC runs its own instance of the MAC and PHY layers and their associated processes, which are dynamically adapted to the instantaneous channel quality conditions experienced in each CC. This requires the use of L1/L2 control signalling to exchange control and feedback information for each CC. The signalling overhead introduced by each CC together with the guard bands required between adjacent CCs can both be jointly characterised by a fraction α ($0 < \alpha \ll 1$) of the total bandwidth. As a result, a bandwidth αB needs to be sacrificed for each employed CC and the total bandwidth W available for data transmission when N CCs are used is $W = B(1-\alpha N)$. Notice that the overhead parameter α refers to the fraction of total available bandwidth B and not to the bandwidth allocated to each individual CC. In order to obtain a positive data rate, the requirement $B(1-\alpha N) > 0$ must be met, which implies that the number of CCs that can be used is constrained by the upper bound $N \leq N_{max} = \lfloor 1/\alpha \rfloor$.

The data transmitted through each CC experience an independent fading process. The Rayleigh fading model is a popular fading model commonly used to characterise wireless communication scenarios under NLOS and is

[1]An operator may divide the total bandwidth into CCs with the same or different bandwidths. This chapter does not make any specific assumptions on the bandwidth allocated to each individual CC and the analytical results here presented do not take this aspect into account. The study of the impact of equal/unequal CC bandwidth allocations and the optimum configuration that maximises the total aggregated capacity is out of the scope of this chapter and is left as future work. However, the simulation results in [99] suggest that a homogeneous bandwidth allocation where the total bandwidth is equally divided across the used CCs may maximise the total aggregated capacity.

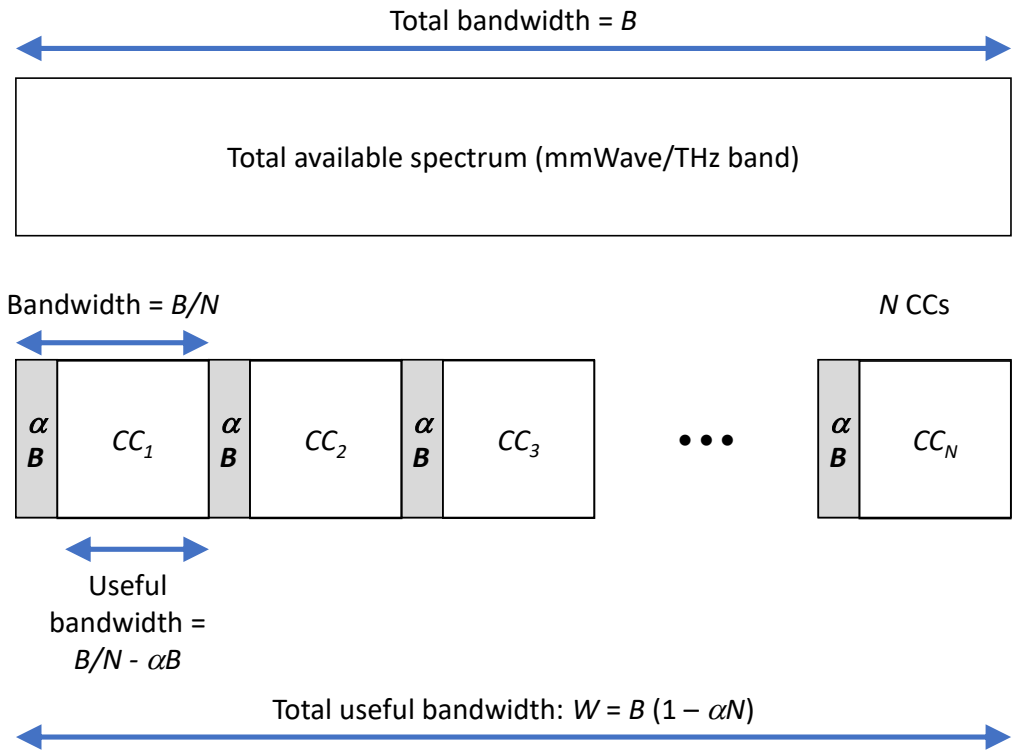

Figure 3.1: System model considered in this chapter.

chosen here to ensure that the obtained performance takes into account a rather unfavourable propagation scenario (i.e., better performance may be achieved in practice). Accordingly, the Probability Density Function (PDF) of the instantaneous SNR at the receiver is:

$$f_{\gamma_n}(x) = \frac{1}{\overline{\gamma}_n} \exp\left(-\frac{x}{\overline{\gamma}_n}\right), \quad \text{for } n = 1, \ldots, N \tag{3.1}$$

and its Cumulative Distribution Function (CDF) is:

$$F_{\gamma_n}(x) = 1 - \exp\left(-\frac{x}{\overline{\gamma}_n}\right), \quad \text{for } n = 1, \ldots, N \tag{3.2}$$

where $\overline{\gamma}_n$ is the average SNR in the nth CC. Two frequency diversity scenarios are considered, namely a homogeneous SNR scenario where all CCs experience the same average SNR ($\overline{\gamma}_n = \overline{\gamma}$ for $n = 1, \ldots, N$) and a heterogeneous SNR scenario where each CC experiences a different SNR ($\overline{\gamma}_n \neq \overline{\gamma}_k$ for $n \neq k$) with an overall average SNR $\overline{\gamma} = (1/N) \sum_{n=1}^{N} \overline{\gamma}_n$.

3.3 Models for the Effective SNR

The capacity of CA has usually been investigated in the literature by characterising the capacity of each CC individually as an independent channel and then adding up the individual capacity of each CC. This approach may be suitable to calculate numerically the aggregate sum-rate in optimisation based studies (e.g., [100, 101]), however the involved mathematical expressions provide little insights into how the total capacity depends on each relevant parameter. In order to investigate the capacity of CA as a diversity technique, the analysis carried out in this chapter considers a different approach based on the concept of *effective SNR*, which is defined in this study as the equivalent SNR at which a single channel with bandwidth B achieves the same performance as the considered CA scenario with a total aggregated bandwidth B divided across N CCs and instantaneous channel quality conditions represented by the set $\{\gamma_n\}_{n=1}^{N}$ of SNR values in each CC.

The introduction of this definition of effective SNR provides a convenient and useful new tool for the analysis of CA in general, and as a diversity technique in particular. However, this concept also raises the question of how to map a set $\{\gamma_n\}_{n=1}^{N}$ of N SNR values in each CC into a single effective SNR γ_{CA} that results in the same performance in the case of a single channel. This is an extremely challenging problem given the broad range of processes at the MAC and PHY layer that determine the performance of CA (packet scheduler, Hybrid Automatic Repeat Request (HARQ) retransmission process, transmission power control, dynamic adaptation of the MCS, etc.) and the many different algorithms that can be implemented for each of such MAC/PHY processes. For this reason, an exact mapping of the individual SNR in each CCs into a single effective SNR, while highly desirable, seems unfeasible. To overcome this limitation, this chapter considers two different models for the effective SNR, which are presented below.

3.3.1 Ideal Model for the Effective SNR

The maximum effective SNR that would be achievable in an ideal scenario would be equal to the sum of the SNR of all the individual CCs, $\gamma_{\text{CA}}^{\text{ideal}} = \sum_{n=1}^{N} \gamma_n$. Notice that when there are N SNRs, the very best possible diversity combination is the sum of all of them. However, such an outcome would not be possible in a passive wireless communication link where the received signal symbols are not explicitly processed at the PHY layer so that they are combined constructively. Thus, the model presented in this section is referred to as *ideal* to reflect the fact that it represents a situation that is highly de-

sirable but extremely unlikely (i.e., in practice, the effective SNR is expected to be lower than the sum-value predicted by this model). This model characterises the maximum possible diversity gain across the N available CCs that could hypothetically be achieved in an ideal diversity propagation scenario and can be used to derive theoretical upper bounds on the CA performance.

Proposition 3.1 (Ideal SNR model for CA with homogeneous SNR)**.** *The PDF and CDF of the instantaneous effective SNR under an ideal CA scenario with homogeneous SNR are given, respectively, by:*

$$f_{\gamma_{\mathrm{CA}}}(x) = \frac{1}{(N-1)!}\frac{x^{N-1}}{\overline{\gamma}^{N}}\exp\left(-\frac{x}{\overline{\gamma}}\right) \tag{3.3}$$

$$F_{\gamma_{\mathrm{CA}}}(x) = \frac{\gamma(N, x/\overline{\gamma})}{\Gamma(N)} \tag{3.4}$$

where $\Gamma(\cdot)$ and $\gamma(\cdot,\cdot)$[2] in (3.4) represent the gamma function [102, eq. (8.310.1)] and the lower incomplete gamma function [102, eq. (8.350.1)], respectively.

Proof. The effective SNR in this case is calculated as the sum of N i.i.d. exponential random variables, therefore it follows an Erlang distribution (i.e., a gamma distribution with integer shape parameter). Refer to [103, chap. 12] for the PDF; the CDF follows from the direct integration of the PDF with the help of [102, eq. (3.351.1)], noting that $(N-1)! = \Gamma(N)$ □

Proposition 3.2 (Ideal SNR model for CA with heterogeneous SNR)**.** *The PDF and CDF of the instantaneous effective SNR under an ideal CA scenario with heterogeneous SNR are given, respectively, by:*

$$f_{\gamma_{\mathrm{CA}}}(x) = \sum_{n=1}^{N}\frac{\Omega_n}{\overline{\gamma}_n}\exp\left(-\frac{x}{\overline{\gamma}_n}\right) \tag{3.5}$$

$$F_{\gamma_{\mathrm{CA}}}(x) = 1 - \sum_{n=1}^{N}\Omega_n\exp\left(-\frac{x}{\overline{\gamma}_n}\right) \tag{3.6}$$

[2]The lower incomplete gamma function has two parameters and is denoted as $\gamma(\cdot,\cdot)$, with the two parameters between brackets and separated by a comma, and it should not be confused with the average SNR, which is denoted as $\overline{\gamma}$, with an overline above it.

where

$$\Omega_n = \prod_{\substack{j=1 \\ j \neq n}}^{N} \frac{1}{1 - \overline{\gamma}_j / \overline{\gamma}_n}. \tag{3.7}$$

Proof. The effective SNR in this case is calculated as the sum of N i.n.i.d. exponential random variables, therefore it follows a generalised Erlang (hypoexponential) distribution. Refer to [104, eq. (7)] for the PDF; the CDF readily follows from the direct integration of the PDF, noting that $\sum_{n=1}^{N} \Omega_n = 1$. □

3.3.2 Average Model for the Effective SNR

The ideal model for the effective SNR proposed in Section 3.3.1 assumes an optimistic, best-case scenario and, as such, the expressions provided in Propositions 3.1 and 3.2 represent upper bounds to the actual performance of CA. A model that can provide a closer approximation to the actual performance would be desirable. However, as discussed in Section 3.3, an exact mathematical model for the effective SNR in such case is unlikely to be feasible. Thus, this section proposes a simple approximation where the effective SNR is obtained as the average of the SNR in each CC, $\gamma_{\text{CA}}^{\text{avg}} = \frac{1}{N} \sum_{n=1}^{N} \gamma_n$. The average is commonly employed as an approximation due to its ability to provide a representative value that reflects the overall trend or central tendency of a set of values. This approach allows us to summarise the set of SNR values in each CC in a concise and meaningful way, making it possible to obtain results that can be expected to be closer to the actual effective SNR than the ideal model of Section 3.3.1. While this approach may not accurately capture the impact of all the MAC/PHY processes that determine the performance of CA, the average is in general a widely accepted measure that offers a reliable estimation in many practical scenarios. Moreover, it provides a simple yet powerful model that can be conveniently employed in subsequent analytical manipulations.

Proposition 3.3 (Average SNR model for CA with homogeneous SNR)**.** *The PDF and CDF of the instantaneous effective SNR under an average CA*

scenario with homogeneous SNR are given, respectively, by:

$$f_{\gamma_{\mathrm{CA}}}(x) = \frac{N^N}{(N-1)!}\frac{x^{N-1}}{\overline{\gamma}^N}\exp\left(-N\frac{x}{\overline{\gamma}}\right) \tag{3.8}$$

$$F_{\gamma_{\mathrm{CA}}}(x) = \frac{\gamma(N, Nx/\overline{\gamma})}{\Gamma(N)}. \tag{3.9}$$

Proof. Note that $\gamma_{\mathrm{CA}}^{\mathrm{avg}} = \gamma_{\mathrm{CA}}^{\mathrm{ideal}}/N$. If X and Y are random variables related as $Y = X/N$, then their PDFs are related as $f_Y(z) = Nf_X(Nz)$, which yields (3.8) from (3.3). The CDF in (3.9) follows from the direct integration of the PDF in (3.8) following the same steps as in the proof of Proposition 3.1. □

Proposition 3.4 (Average SNR model for CA with heterogeneous SNR)**.** *The PDF and CDF of the instantaneous effective SNR under an average CA scenario with heterogeneous SNR are given, respectively, by:*

$$f_{\gamma_{\mathrm{CA}}}(x) = N\sum_{n=1}^{N}\frac{\Omega_n}{\overline{\gamma}_n}\exp\left(-N\frac{x}{\overline{\gamma}_n}\right) \tag{3.10}$$

$$F_{\gamma_{\mathrm{CA}}}(x) = 1 - \sum_{n=1}^{N}\Omega_n\exp\left(-N\frac{x}{\overline{\gamma}_n}\right) \tag{3.11}$$

with Ω_n defined in (3.7).

Proof. Same as for Proposition 3.2, applied to (3.5) and (3.6). □

Remark 3.1. *Note that if $N = 1$ then (3.3)–(3.4), (3.5)–(3.6), (3.8)–(3.9) and (3.10)–(3.11) reduce to (3.1)–(3.2), respectively.*

Proof. By substitution, noting where appropriate that $\Omega_1 = 1$ and $\gamma(1, x) = 1 - \exp(-x)$ [102, eq. (8.350.1)]. □

3.4 Ergodic Capacity Analysis

Based on the concept of effective SNR, the ergodic capacity of a CA scenario can be obtained in bits per second as:

$$C = W\int_0^\infty \log_2(1+x) f_{\gamma_{\mathrm{CA}}}(x)dx \tag{3.12}$$

where W is the total aggregated bandwidth effectively available for data transmission and $f_{\gamma_{\mathrm{CA}}}(x)$ is the effective SNR PDF. In this section, analytical results will be provided only for the average SNR model presented in Section 3.3.2. The counterparts for the ideal model of Section 3.3.1 can be obtained by simply replacing $\overline{\gamma}/N$ with $\overline{\gamma}$ (homogeneous SNR scenario) and $\overline{\gamma}_n/N$ with $\overline{\gamma}_n$ (heterogeneous SNR scenario).

Theorem 3.1 (Ergodic capacity of single carrier scenario)**.** *The ergodic capacity of the single carrier scenario is given by:*

$$C = B(1-\alpha)\log_2(e)\exp\left(\frac{1}{\overline{\gamma}}\right)E_1\left(\frac{1}{\overline{\gamma}}\right) \tag{3.13}$$

where $E_1(x) = \int_x^\infty e^{-t}t^{-1}dt$ *denotes the exponential integral function [105, eq. (5.1.1)].*

Proof. Since the control signalling overhead introduced by a single carrier requires a capacity equivalent to a bandwidth αB, the bandwidth effectively available for data transmission is $W = B(1-\alpha)$. Introducing (3.1) in (3.12) and noting that $\log_2(x) = \log_2(e)\ln(x)$, the resulting integral can be solved with the help of [102, eq. (4.337.2)] and [105, eq. (5.1.7)]. □

Theorem 3.2 (Ergodic capacity of CA with homogeneous SNR)**.** *The ergodic capacity of CA with homogeneous SNR is:*

$$C = B(1-\alpha N)\log_2(e)\exp\left(\frac{N}{\overline{\gamma}}\right)\sum_{n=1}^{N}\frac{\Gamma\left(n-N,\frac{N}{\overline{\gamma}}\right)}{\left(\frac{N}{\overline{\gamma}}\right)^{n-N}} \tag{3.14}$$

where $\Gamma(\cdot,\cdot)$ *represents the upper incomplete gamma function defined in [102, eq. (8.350.2)].*

Proof. The control signalling overhead introduced by N CCs requires a capacity equivalent to a bandwidth αNB, thus $W = B(1-\alpha N)$. Introducing (3.8) in (3.12) and noting that $\log_2(x) = \log_2(e)\ln(x)$, an integral of the form [106, eq. (15.24)] is obtained, which can be resolved with the help of [106, eq. (15B.7)] to obtain the expression shown in (3.14). □

Theorem 3.3 (Ergodic capacity of CA with heterogeneous SNR)**.** *The ergodic capacity of CA with heterogeneous SNR is:*

$$C = B(1-\alpha N)\log_2(e)\sum_{n=1}^{N}\Omega_n \exp\left(\frac{N}{\overline{\gamma}_n}\right) E_1\left(\frac{N}{\overline{\gamma}_n}\right). \tag{3.15}$$

Proof. For N CCs, $W = B(1-\alpha N)$. Introducing (3.10) in (3.12) yields a sum of integrals, each of which can be resolved as discussed in the proof of Theorem 3.1. □

Remark 3.2. *Note that if $N = 1$ then both (3.14) and (3.15) reduce to the single carrier expression in (3.13).*

Proof. By substitution, noting where appropriate that $\Omega_1 = 1$ and $\Gamma(0, x) = E_1(x)$ [105, eq. (5.1.1)] [102, eq. (8.350.2)]. □

3.5 Secrecy Capacity Analysis

The ergodic capacity analysed in Section 3.4 represents the maximum theoretically achievable data rate over a wireless channel, which is an important aspect to achieve efficient data transmission and optimise the system performance. However, in practical scenarios, the communication security is also extremely relevant and therefore analysing the secrecy capacity becomes equally important. The secrecy capacity represents the maximum theoretically achievable data rate at which information can be transmitted reliably over a wireless channel while maintaining the confidentiality of communication against attackers (commonly referred to as eavesdroppers). By considering both the ergodic and secrecy capacities, a robust communication system design can be accomplished. The analysis presented for the ergodic capacity in Section 3.4 is here complemented by analysing the secrecy capacity.

The instantaneous secrecy capacity of a wiretap channel [107] is defined as $C_s(\gamma_m, \gamma_e) = C_m - C_e$ if $C_m > C_e$ and zero otherwise, where γ_m and γ_e represent the instantaneous SNR of the main and eavesdropper links, respectively, and their instantaneous capacities are given by $C_m = W\log_2(1+\gamma_m)$ and $C_e = W\log_2(1+\gamma_e)$, respectively. Notice that the eavesdropper needs to use the same configuration as the main link in order to attempt to successfully decode its information. If the main link transmits over a bandwidth B

using CA with N CCs, then the eavesdropper must do exactly the same. As a result, the bandwidth penalty parameter α will be the same for both links and so will be the net bandwidth available for data transmission, hence the presence of the same bandwidth W in the expressions of both C_m and C_e.

The (average) secrecy capacity can be calculated in bits per second as [108, Eqs. (38)–(41)]:

$$\begin{aligned} C_s &= \int_0^\infty \int_0^\infty C_s(x,y) f_{\gamma_m}(x) f_{\gamma_e}(y) dx dy \\ &= W \log_2(e) \left[\mathcal{I}_1 + \mathcal{I}_2 - \mathcal{I}_3\right], \end{aligned} \tag{3.16}$$

where $f_{\gamma_m}(\cdot)$ and $f_{\gamma_e}(\cdot)$ denote the PDF of the instantaneous SNR in the main and eavesdropper links, respectively, and:

$$\mathcal{I}_1 = \int_0^\infty \ln(1+x) F_{\gamma_e}(x) f_{\gamma_m}(x) dx \tag{3.17}$$

$$\mathcal{I}_2 = \int_0^\infty \ln(1+x) F_{\gamma_m}(x) f_{\gamma_e}(x) dx \tag{3.18}$$

$$\mathcal{I}_3 = \int_0^\infty \ln(1+x) f_{\gamma_e}(x) dx \tag{3.19}$$

with $F_{\gamma_m}(\cdot)$ and $F_{\gamma_e}(\cdot)$ denoting the CDF of the instantaneous SNR in the main and eavesdropper links, respectively.

Based on the expressions shown above and capitalising on the effective SNR models proposed in Section 3.3, this section analyses the secrecy capacity of CA when used as a diversity technique. Similar to Section 3.4, analytical results will be provided for the average model of the effective SNR. The equivalent expressions for the ideal effective SNR model can be obtained by simply replacing $\overline{\gamma}_m/N$ and $\overline{\gamma}_e/N$ with $\overline{\gamma}_m$ and $\overline{\gamma}_e$, respectively (for the homogeneous SNR scenario) and by replacing $\overline{\gamma}_{m,n}/N$ and $\overline{\gamma}_{e,n}/N$ with $\overline{\gamma}_{m,n}$ and $\overline{\gamma}_{e,n}$, respectively (for the heterogeneous SNR scenario).

Theorem 3.4 (Secrecy capacity of single carrier scenario)**.** *The secrecy capacity of the single carrier scenario is given by:*

$$\begin{aligned} C_s = B(1-\alpha)\log_2(e) \Bigg\{ &\exp\left(\frac{1}{\overline{\gamma}_m}\right) E_1\left(\frac{1}{\overline{\gamma}_m}\right) \\ &- \exp\left(\frac{1}{\overline{\gamma}_m} + \frac{1}{\overline{\gamma}_e}\right) E_1\left(\frac{1}{\overline{\gamma}_m} + \frac{1}{\overline{\gamma}_e}\right) \Bigg\} \end{aligned} \tag{3.20}$$

where $E_1(\cdot)$ is the exponential integral function.

Proof. Since the control signalling overhead introduced by a single carrier requires a capacity equivalent to a bandwidth αB, the bandwidth effectively available for data transmission is $W = B(1-\alpha)$. Introducing (3.1)–(3.2) in (3.16)–(3.19) and noting that $\log_2(x) = \log_2(e)\ln(x)$, the resulting integrals can be solved with the help of [102, eq. (4.337.2)] [105, eq. (5.1.7)]. □

Theorem 3.5 (Secrecy capacity of CA with homogeneous SNR)**.** *The secrecy capacity of CA with homogeneous SNR is:*

$$\begin{aligned} C_s = B(1-\alpha N)\log_2(e) \Bigg\{ & \exp\left(\frac{N}{\overline{\gamma}_m}\right) \sum_{n=1}^{N} \frac{\Gamma\left(n-N, \frac{N}{\overline{\gamma}_m}\right)}{\left(\frac{N}{\overline{\gamma}_m}\right)^{n-N}} \\ & - \exp\left(N\left[\frac{1}{\overline{\gamma}_m} + \frac{1}{\overline{\gamma}_e}\right]\right) \sum_{n=1}^{N} \frac{(n+N-2)!}{(n-1)!(N-1)!} \\ & \times \left(\frac{N}{\overline{\gamma}_m \overline{\gamma}_e}\right)^{n+N-1} \left(\overline{\gamma}_m^{n-1}\overline{\gamma}_e^{N} + \overline{\gamma}_e^{n-1}\overline{\gamma}_m^{N}\right) \\ & \times \sum_{k=1}^{n+N-1} \frac{\Gamma\left(k-n-N+1, N\left[\frac{1}{\overline{\gamma}_m} + \frac{1}{\overline{\gamma}_e}\right]\right)}{\left(N\left[\frac{1}{\overline{\gamma}_m} + \frac{1}{\overline{\gamma}_e}\right]\right)^{k}} \Bigg\} \end{aligned} \tag{3.21}$$

where $\Gamma(\cdot,\cdot)$ *represents the upper incomplete gamma function.*

Proof. The overhead introduced by N CCs requires a capacity equivalent to a bandwidth $\alpha N B$, thus $W = B(1-\alpha N)$. Introducing (3.8)–(3.9) in (3.16)–(3.19), substituting the lower incomplete gamma function with its equivalent form in [102, eq. (8.352.1)] and noting that $\log_2(x) = \log_2(e)\ln(x)$, integrals of the form [106, eq. (15.24)] are obtained, which can be resolved with the help of [106, eq. (15B.7)]. After reorganising and grouping terms, the expression shown in (3.21) is obtained. □

Theorem 3.6 (Secrecy capacity of CA with heterogeneous SNR)**.** *The secrecy capacity of CA with heterogeneous SNR is:*

$$C_s = B(1-\alpha N)\log_2(e)\left\{\sum_{n=1}^{N}\Omega_{m,n}\exp\left(\frac{N}{\overline{\gamma}_{m,n}}\right)E_1\left(\frac{N}{\overline{\gamma}_{m,n}}\right)\right.$$
$$-\sum_{i=1}^{N}\sum_{j=1}^{N}\Omega_{m,i}\Omega_{e,j}\exp\left(N\left[\frac{1}{\overline{\gamma}_{m,i}}+\frac{1}{\overline{\gamma}_{e,j}}\right]\right)$$
$$\left.\times E_1\left(N\left[\frac{1}{\overline{\gamma}_{m,i}}+\frac{1}{\overline{\gamma}_{e,j}}\right]\right)\right\} \tag{3.22}$$

Proof. For N CCs, $W = B(1-\alpha N)$. Introducing (3.10)–(3.11) in (3.16)–(3.19) yields a sum of integrals, each of which can be resolved as discussed in the proof of Theorem 3.1. □

Remark 3.3. *By comparing (3.20), (3.21) and (3.22) to (3.13), (3.14) and (3.15), respectively, it can be noted that the secrecy capacity is equivalent to the ergodic capacity minus a term that quantifies the amount of information that can be transmitted through the channel but not in a confidential manner due to the presence of an eavesdropper (i.e., the secrecy capacity is lower than the ergodic capacity as expected).*

3.6 Results

The performance of CA as a diversity technique is evaluated numerically in this section based on the analytical results obtained in Sections 3.4 and 3.5. The main aim is to determine whether the mathematical model and closed-form expressions derived in this chapter can correctly predict the trends observed by simulations in Chapter 2 and to determine the impact of various relevant parameters on the system performance. As discussed in Section 3.2, two frequency diversity scenarios are considered, namely a homogeneous SNR scenario where all CCs experience the same average SNR ($\overline{\gamma}_n = \overline{\gamma}$ for $n = 1, \ldots, N$) and a heterogeneous SNR scenario where each CC experiences a different average SNR ($\overline{\gamma}_n \neq \overline{\gamma}_k$ for $n \neq k$) with an overall average SNR $\overline{\gamma} = (1/N)\sum_{n=1}^{N}\overline{\gamma}_n$. In the heterogeneous SNR scenario, the average SNR

of each individual CC is selected from the interval $10\log_{10}\overline{\gamma}_n \in [10\log_{10}\overline{\gamma} - \varepsilon, 10\log_{10}\overline{\gamma} + \varepsilon]$, where ε (in dB) is a spread parameter that determines the level of potential frequency diversity (the larger the value of ε, the higher the level of diversity in the propagation scenario). For simplicity, the performance is mainly investigated for the ideal model of effective SNR. The numerical results obtained for such model show more pronounced trends that illustrate more clearly the impact of different relevant parameters. Some examples illustrating the impact of considering the average model of effective SNR are also shown, corroborating that the same trends are observed (just with different numerical values) and the same conclusions are therefore obtained.

3.6.1 Ergodic Capacity Results

Figure 3.2 shows the ergodic capacity of CA (in terms of the spectral efficiency, i.e., bit/s/Hz) as a function of the number of CCs for various values of the bandwidth overhead parameter α. The first relevant observation is that these results corroborate that CA can be effectively employed as a diversity technique to increase the data rate of the system without increasing the available bandwidth, which can be confirmed by noting that the curves for CA can lead to a higher spectral efficiency than the single carrier scenario (in certain regions of the figure if the number of CCs is correctly configured, which will be discussed later on). It can also be noted that the performance of CA tends to be slightly higher in the heterogeneous SNR scenario than in the homogeneous counterpart. This can be explained by the fact that the level of frequency diversity in the heterogeneous scenario is higher and in such a case the proposed method, based on the use of CA as a diversity technique, can benefit from it to a greater extent. The bandwidth overhead parameter α is also observed to have a significant impact on the resulting performance. As expected, if the use of CA incurs in a higher bandwidth penalty (i.e., higher value of α), a lower amount of net bandwidth is available for data transmission, which leads to lower data rates. Notice that in the hypothetical case of $\alpha = 0$ (i.e., if no bandwidth penalty is incurred by using CA) then the capacity would monotonically increase indefinitely with the number of CCs, as this would increase the frequency diversity gain without any bandwidth penalties. However, in a realistic case with $\alpha > 0$, the curves in Figure 3.2 become convex. This indicates the existence of an optimum number of CCs that maximises the data rate for each value of α. As explained in Section 2.6, increasing the number of CCs will initially increase the data rate as a result of increasing the frequency diversity in the system. However, this also increases the total amount of signalling traffic and band-

width reserved for guard bands (i.e., bandwidth penalty), which reduces the total amount of bandwidth available for data transmission. If the number of CCs is sufficiently high, the bandwidth penalty incurred by a high number of CCs will exceed the gain obtained from the frequency diversity, thus effectively reducing the data rate. In fact, if the number of CCs is made arbitrarily large, it can be seen in Figure 3.2 that the data rate of CA can indeed fall below that of the single carrier scenario, and this will occur sooner (i.e., for a lower number of CCs) when the bandwidth penalty α is higher. The optimum number of CCs thus depends on the bandwidth penalty parameter. From Figure 3.2, it can be determined that the optimum number of CCs that maximises the data rate for $\alpha = \{0.01, 0.02, 0.03, 0.04, 0.05\}$ is 16, 9, 7, 5 and 4, respectively, which is in line with the observations above[3].

The impact of the bandwidth penalty α on the optimum number of CCs and the resulting capacity is more clearly illustrated in Figure 3.3, where three scenarios are considered, namely a 4G LTE scenario with a maximum of 5 CCs, a 5G-NR scenario with a maximum of 16 CCs, and an ideal scenario where the number of CCs that can be aggregated is unconstrained (i.e., unlimited). Table 3.1 shows the capacity achieved by CA for various levels of bandwidth penalty (α) and the improvement with respect to the single carrier scenario where no CA is used. Notice that, according to Figure 3.3, 4G LTE and 5G-NR can achieve the same performance as the unconstrained CA scenario as long as the bandwidth penalty does not exceed the limits $\alpha < 0.04$ and $\alpha < 0.01$, respectively, in which cases the capacity improvement with respect to the single carrier scenario is equal to 64% for 4G LTE and 120% for 5G-NR. Nevertheless, even if the bandwidth penalty exceeds these limits and the maximum number of CCs permitted by the 3GPP standard is taken into account, the use of CA as a diversity technique can still provide substantial capacity improvements with respect to the single carrier scenario as evidenced by the results shown in Table 3.1.

[3]From a mathematical point of view, the bandwidth penalty parameter must be comprised within the interval $\alpha \in [0, 1]$ since it represents a fraction of a certain amount of bandwidth. In practice, this value should remain low since communication protocols are designed to be efficient, and therefore, the signalling load should remain low compared to the total volume of data traffic. The range of values $\alpha \in [0, 0.05]$ assumes that the network is signalling-efficient (i.e., up to 5% of the bandwidth allocated to a CC is consumed by the associated signalling traffic). Higher values of α could be considered, however this should lead to similar conclusions as those obtained with the presented results.

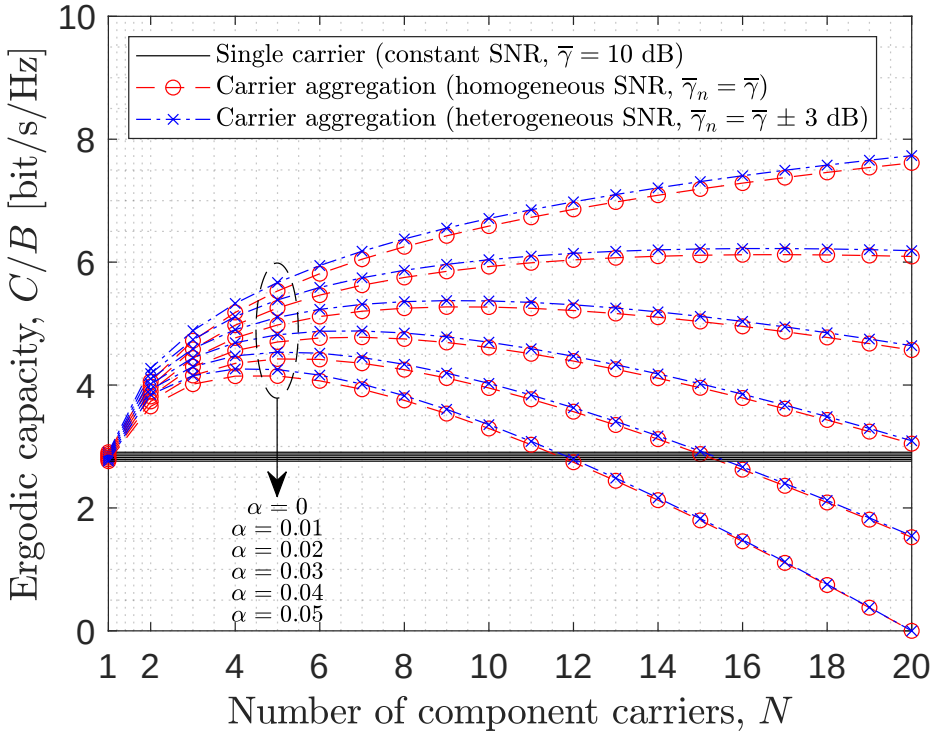

Figure 3.2: Ergodic capacity as a function of the number of CCs for various values of bandwidth overhead parameter α (average SNR = 10 dB, $\varepsilon = 3$ dB).

Figure 3.4 shows the ergodic capacity of CA as a function of the number of CCs for various values of the average SNR experienced in the different considered scenarios. This figure also corroborates the main observations made when discussing Figure 3.2, namely that: i) CA can be effectively employed as a diversity technique in order to improve the spectral efficiency with respect to the traditional single carrier scenario based on the same communication bandwidth (provided that the number of CCs is correctly configured); ii) the performance of CA as a diversity technique tends to increase in the heterogeneous SNR scenario compared to the homogeneous SNR counterpart as a result of a richer diversity; and iii) there exists an optimum number of CCs that maximises the total capacity, in this case, for each considered average SNR. Regarding the last observation, it can be seen in Figure 3.4 that the optimum number of CCs decreases as the average SNR increases. More concretely, for the numerical example shown in Figure 3.4,

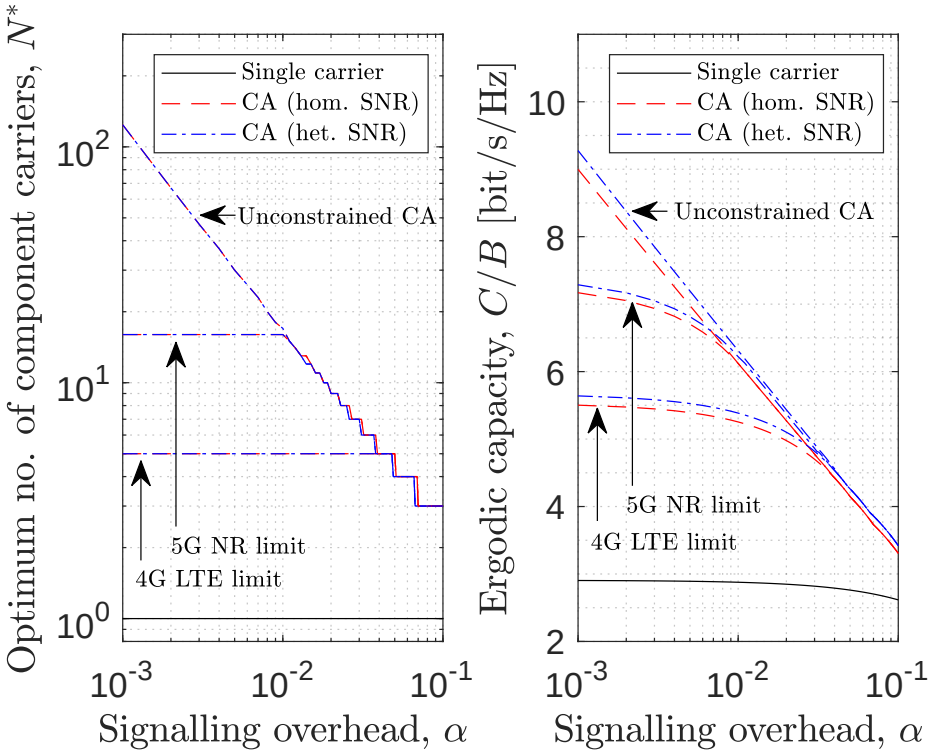

Figure 3.3: Optimum number of component carriers as a function of the bandwidth overhead parameter α (left) and resulting ergodic capacity (right).

the data rate is maximised with 6, 4 and 3 CCs when the average SNR is 0, 10 and 20 dB, respectively. This trend can be explained intuitively based on the fact that a higher average SNR can be associated with a shorter communication distance, where the level of diversity can be expected to be lower than in a longer distance link (where the signal can find a larger number of diverse paths between transmitter and receiver). Thus, a lower diversity gain means that a lower number of CCs can be used while guaranteeing that the bandwidth penalty associated with the number of CCs does not exceed the diversity gain. The optimum number of CCs as a function of the average SNR for a broader range of average SNR values is illustrated in Figure 3.5 along with the capacity obtained when the optimum number of CCs is used for every average SNR. This figure shows clearly how the use of CA as a diversity technique can significantly improve the spectral efficiency in order to increase the system capacity without increasing the amount of spectrum employed. Taking an average SNR of 10 dB as a reference, the results in

Table 3.1: Best attainable ergodic capacity for various scenarios and levels of bandwidth penalty (α) according to Fig. 3.3.

	$\alpha = \mathbf{10^{-3}}$		$\alpha = \mathbf{10^{-2}}$	
Scenario	**Capacity**	**Improvement**	**Capacity**	**Improvement**
No CA	2.90 bit/s/Hz	—	2.88 bit/s/Hz	—
4G LTE CA	5.64 bit/s/Hz	94%	5.41 bit/s/Hz	88%
5G NR CA	7.29 bit/s/Hz	151%	6.34 bit/s/Hz	120%
Unconst. CA	9.28 bit/s/Hz	220%	6.45 bit/s/Hz	124%

Figure 3.5 indicate that the spectral efficiency of 2.74 bit/s/Hz in the single carrier scenario can be improved to around 4 bit/s/Hz with the use of CA as a diversity technique, which represents a 55% increment in the system capacity without increasing the available bandwidth.

The results presented above indicate that CA can provide a slightly better performance in the heterogeneous SNR scenario than in the homogeneous SNR scenario as a result of a higher level of diversity. To illustrate this aspect more clearly, Figure 3.6 shows the impact of the spread parameter ε, which determines the width of the interval of SNR values in each individual CC, on the capacity as a function of the number of CCs. The results show that the capacity gain of using CA increases with the spread of SNR values over the different CCs. This means that, for the same average SNR across the different CCs, the higher the standard deviation of the SNR in the individual CCs, the higher the capacity gain obtained by using CA (with respect to the single carrier scenario). A higher SNR spread can somehow be seen as an additional form of channel diversity that benefits the use of CA as a diversity technique.

The results presented so far have been obtained based on the ideal model of effective SNR presented in Section 3.3.1. As discussed at the beginning of Section 3.6, this choice is preferred because the numerical results obtained from such a model show more pronounced trends that illustrate more clearly the impact of different relevant parameters on the performance of CA as a diversity technique. However, the ideal model for effective SNR assumes an

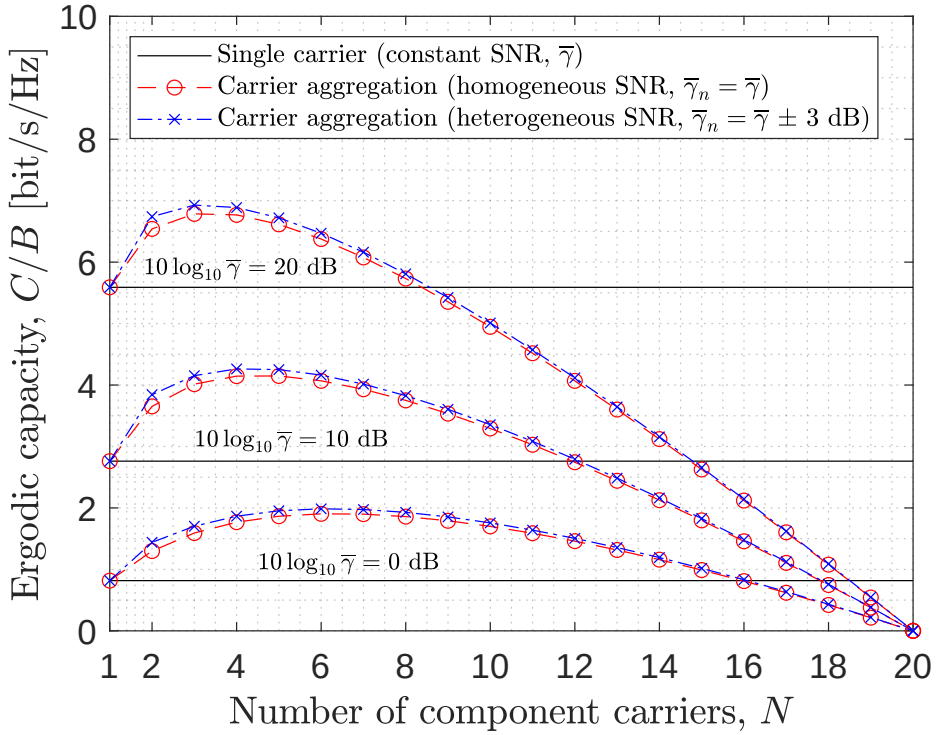

Figure 3.4: Ergodic capacity as a function of the number of CCs for various values of the average SNR ($\alpha = 0.05$, $\varepsilon = 3$ dB).

optimistic best-case scenario and the results obtained from that model should be interpreted as performance upper bounds. The reader may naturally wonder whether the main conclusions obtained from the results presented in this section are also valid under a more realistic SNR model. To corroborate this, some illustrative results based on the average model of effective SNR proposed in Section 3.3.2 are presented here as well. Figure 3.7 and 3.8 show the counterparts to Figure 3.2 and 3.4, respectively, based on the average model of effective SNR. Taking into account that the average effective SNR model is more conservative and provides a scaled version of the ideal effective SNR model, the effective SNR value obtained under the former model will always be lower than the latter. This explains the lower numerical values of capacity obtained in Figure 3.7 and 3.8 (average model) compared to Figure 3.2 and 3.4 (ideal model). However, besides the mere numerical differences between both models, it can be seen that the qualitative performance trends are preserved when the average model of effective SNR is considered and that

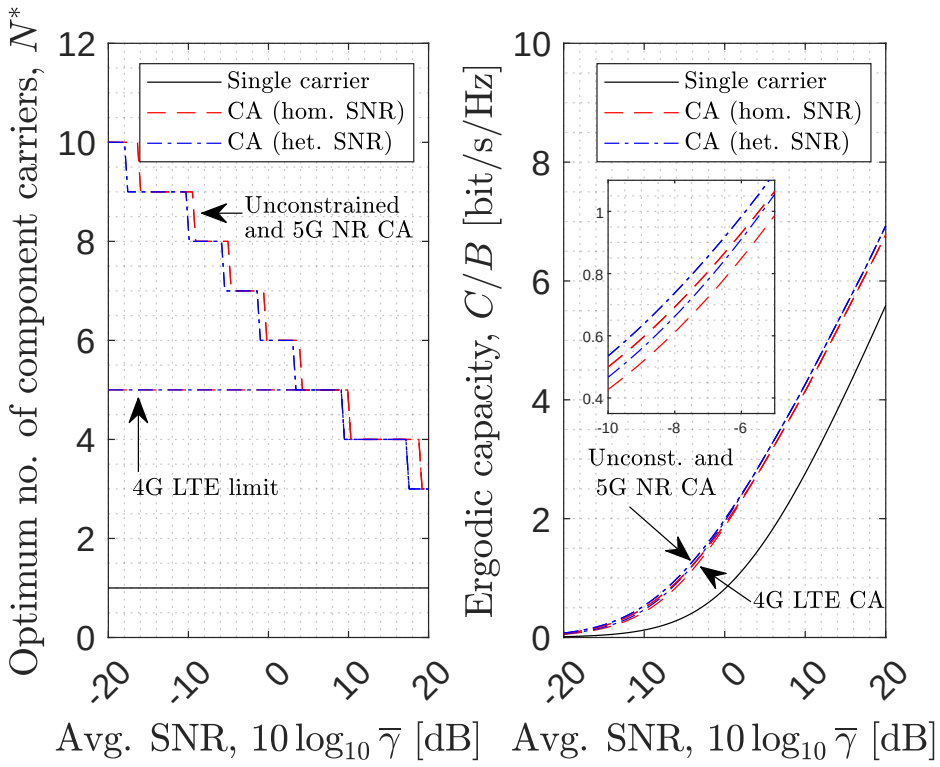

Figure 3.5: Optimum number of component carriers as a function of the average SNR (left) and the resulting ergodic capacity (right).

the main conclusions derived from the analysis presented in this section for the ideal model of effective SNR are still valid. In summary, it can thus be concluded that the mathematical model and closed-form expressions derived in Section 3.4 can correctly predict the trends observed by simulations in Chapter 2 and constitute a useful tool to analyse the performance of CA when used as a diversity technique and to determine the (qualitative) impact of various relevant parameters on the system performance.

3.6.2 Secrecy Capacity Results

The performance of CA as a diversity technique in terms of secrecy capacity was also evaluated as part of this study. It is worth noting that the secrecy capacity was observed to follow the same qualitative trends as the ergodic capacity, being affected in the same way by variations of the bandwidth overhead parameter, number of CCs and average SNR. This is in line with

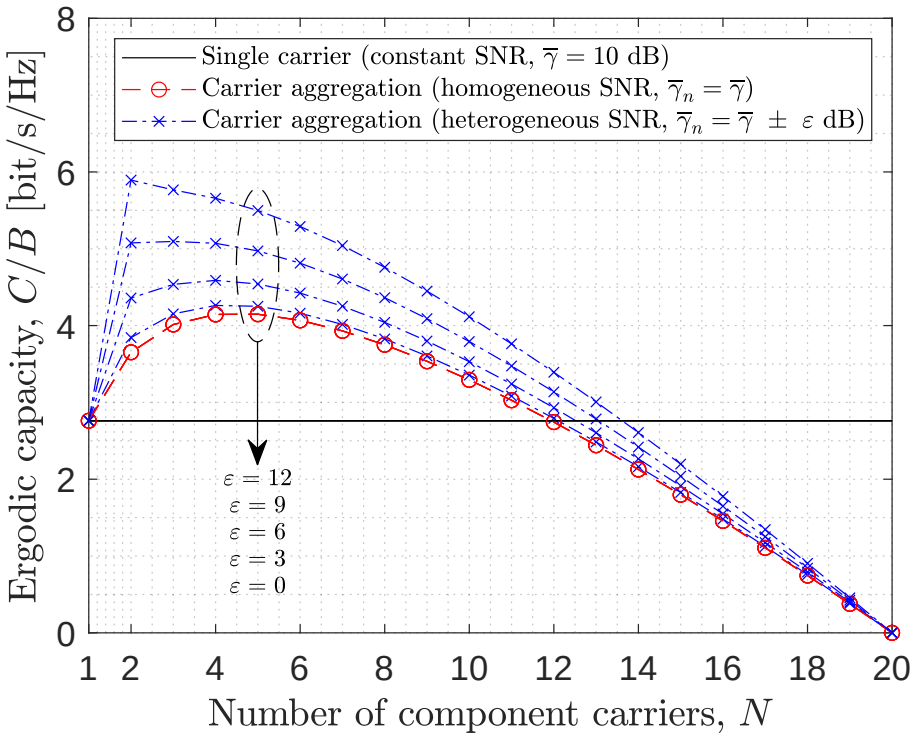

Figure 3.6: Ergodic capacity as a function of the number of CCs for various values of the spread parameter ε (average SNR = 10 dB, $\alpha = 0.05$).

the observation pointed out in Remark 3.3, which highlights the fact that the numerical value of the secrecy capacity is a reduced version of the ergodic capacity as a result of the presence of an eavesdropper. This means that the figures shown in Section 3.6.1 for the ergodic capacity would look very similar when calculated for the secrecy capacity, except for the fact that numerical values in the case of the secrecy capacity would be slightly lower.

The analysis presented in this section focuses on the impact of the eavesdropper on the secrecy capacity, which is the main aspect that determines the difference between ergodic and secrecy capacities. As explained in Section 3.5, the eavesdropper needs to use the same configuration as the main link (i.e., same B, N and α), however it may experience a different average SNR depending on its location with respect to the transmitter and receiver in the main link. Hence, the impact of the eavesdropper can be analysed in terms of its average SNR with respect to the average SNR in the main link.

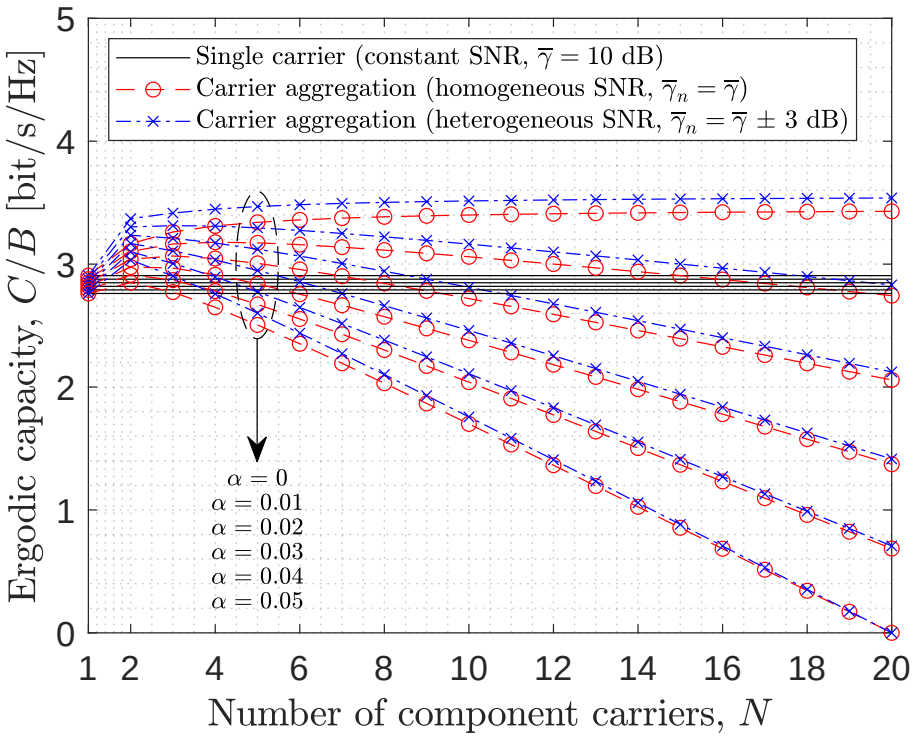

Figure 3.7: Ergodic capacity as a function of the number of CCs for various values of the bandwidth overhead parameter α (average SNR = 10 dB, $\varepsilon = 3$ dB). [Counterpart to Fig. 3.2 based on the average model of effective SNR.]

Figure 3.9 shows the secrecy capacity of a system with CA as a diversity technique as a function of the number of CCs for various values of the bandwidth overhead parameter α, when both the main and eavesdropper links experience the same average SNR of 10 dB (based on the ideal model of effective SNR). These results suggest that the use of CA as a diversity technique, while improving the ergodic capacity with respect to the single carrier scenario (see Section 3.6.1), may actually lead to a lower secrecy capacity compared to the case of single carrier transmission. In other words, while CA allows the system to transmit a higher quantity of bits per second in the same bandwidth (ergodic capacity), it reduces the level of confidentiality of the link at the physical layer (secrecy capacity). This means that the use of CA not only benefits the transmission of data in the main link, but also the transmission of data in the (undesired) link between the same transmitter and the eavesdropper, thus potentially reducing the level of confidentiality

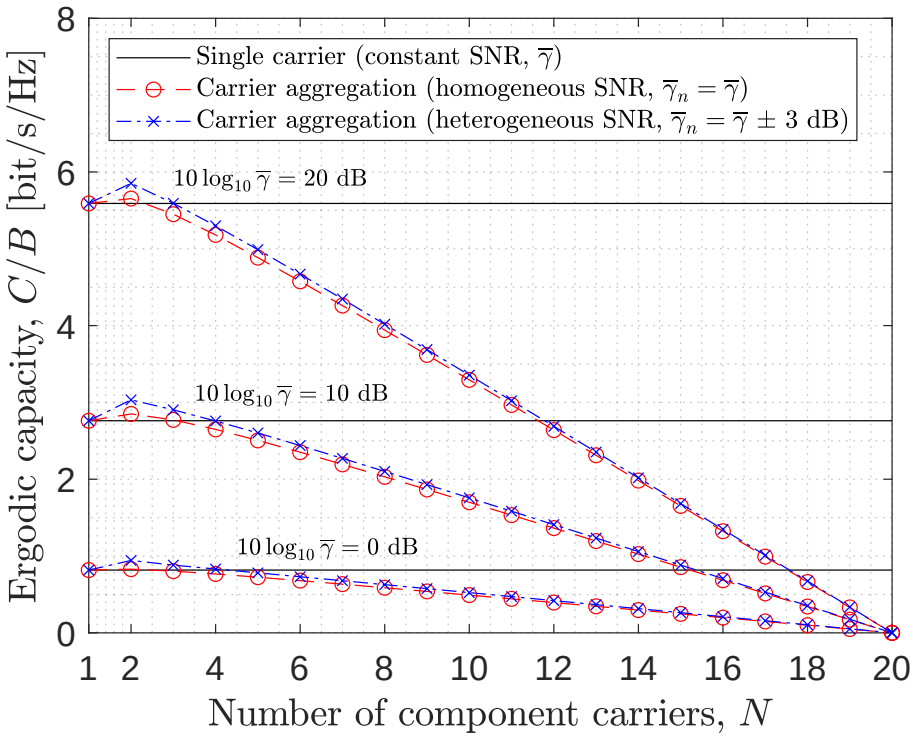

Figure 3.8: Ergodic capacity as a function of the number of CCs for various values of the average SNR ($\alpha = 0.05$, $\varepsilon = 3$ dB). [Counterpart to Fig. 3.4 based on the average model of effective SNR.]

between the transmitter and the legitimate receiver. However, it is worth noting that this is due to the rather favourable propagation conditions in the eavesdropper link, which in the example of Figure 3.9 enjoys the same average SNR as the main link. In a more realistic setup, the main link can typically be expected to experience a higher average SNR than the eavesdropper link, in particular with modern communication systems where the use of multiple antenna technologies and beam-forming techniques are used to direct the transmitted signal towards the desired recipient. This should lead to a much lower SNR at any potential eavesdroppers (unless they are perfectly aligned in the same direction as the transmitter and the legitimate receiver, which is rather unlikely in practical scenarios). When the legitimate receiver in the main link experiences a higher average SNR than the eavesdropper link, then the use of CA can effectively result in an improvement of secrecy capacity as illustrated in Figure 3.10, where the eavesdropper link remains at an average

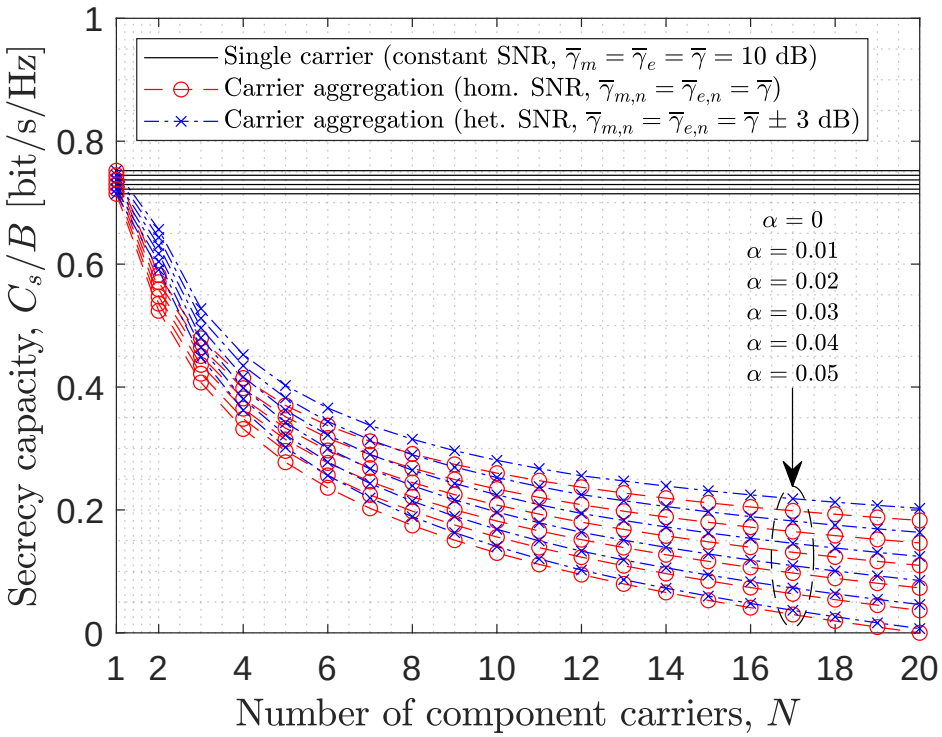

Figure 3.9: Secrecy capacity as a function of the number of CCs for various values of the bandwidth overhead parameter α (**ideal effective SNR model**, 10 dB SNR in both main and eavesdropper links).

SNR of 10 dB and the main link experiences a higher average SNR of 20 dB. By only increasing the average SNR in the main link by 10 dB with respect to the eavesdropper link, the secrecy performance of CA can be substantially improved (if the number of CCs is correctly configured). This is true not only when assuming the ideal effective SNR model (Figure 3.10) but also the more realistic average effective SNR model (Figure 3.11).

From the discussion above, it can be concluded that the secrecy capacity can potentially be improved with the use of CA as a diversity technique when compared to the single carrier scenario, however it may also be degraded depending on the average SNR of the eavesdropper links, which in practical scenarios may or may not be known. In a worst-case scenario, the use of CA would lead to a degraded secrecy capacity compared to the equivalent single carrier scenario, however this does not mean that confidential communication may not be achievable. A degraded secrecy capacity means that the

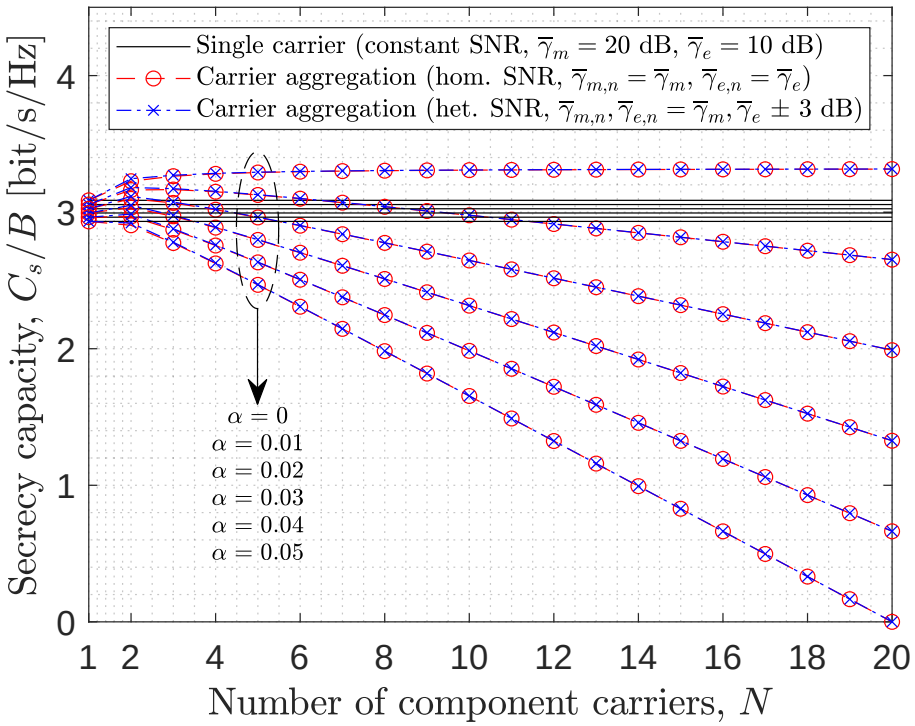

Figure 3.10: Secrecy capacity as a function of the number of CCs for various values of the bandwidth overhead parameter α (**ideal effective SNR model**, 20 dB SNR in the main link and 10 dB SNR in the eavesdropper link).

level of confidentiality is reduced at the physical layer, from an information-theoretic point of view. However, confidentiality can still be guaranteed by taking appropriate measures at higher layers of the protocol stack, which usually involves the use of encryption techniques. The results presented and discussed in this chapter suggest that CA can be used as a diversity technique to increase the user data rates and system ergodic capacity; however, when doing so, special attention should be paid to higher layer techniques for communication confidentiality since the secrecy capacity may in some cases be degraded when using CA as a diversity technique. With an adequate consideration of both ergodic and secrecy capacities, a robust system design for CA as a diversity technique can be obtained. In this context, the analytical results presented in this chapter constitute a useful tool to achieve this end.

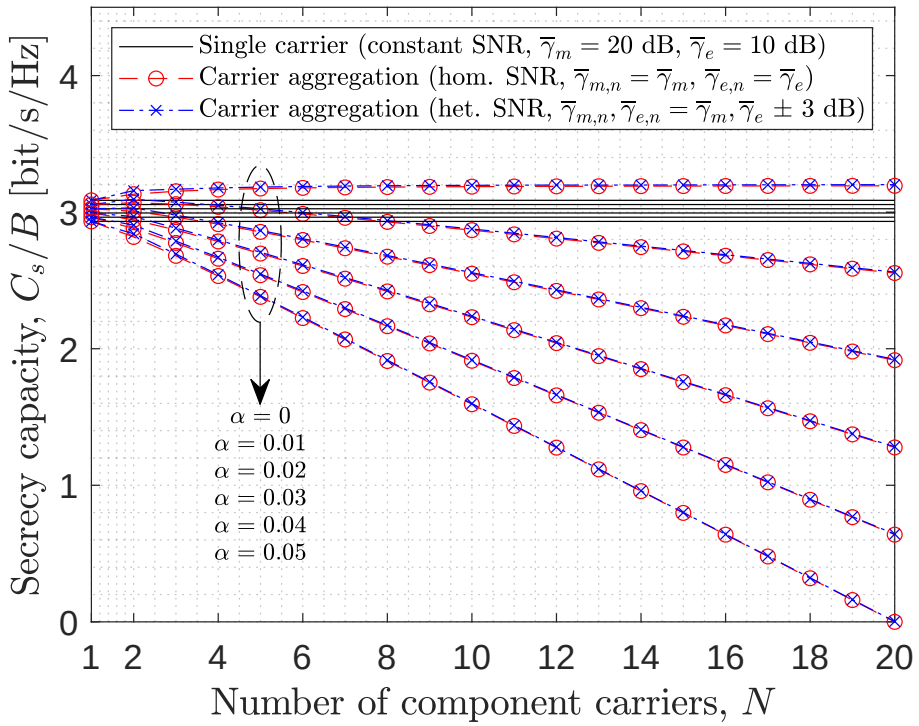

Figure 3.11: Secrecy capacity as a function of the number of CCs for various values of the bandwidth overhead parameter α (**average effective SNR model**, 20 dB SNR in the main link and 10 dB SNR in the eavesdropper link).

3.7 Conclusions

Carrier Aggregation (CA) was originally proposed as a way to increase data rates in mobile communication systems by increasing the amount of spectrum available to users through the aggregation of different spectrum bands. This chapter has shown that CA can also lead to increased data rates without requiring additional spectrum when used as a diversity technique. By dividing a block of the existing spectrum into sub-blocks and treating each of them as a Component Carrier (CC) via regular CA, the channel frequency diversity can be exploited, which results in a higher spectral efficiency and therefore in a higher user data rate with the same amount of available spectrum. In this context, a set of mathematical models and analytical expressions have

been proposed to characterise the performance of CA as a diversity technique in terms of both the ergodic and secrecy capacities. It has been shown that the proposed mathematical modelling approach can correctly predict the performance of CA as a diversity technique as well as the impact of various relevant configuration parameters. The obtained numerical results are in line with previous simulation studies and demonstrate that CA can be effectively exploited as a diversity technique to improve the performance of mobile communication systems. However, it has also been shown that both the ergodic and secrecy capacities should be taken into account to provide a robust system design. In this context, the mathematical models and expressions presented in this chapter are a useful tool to achieve this end.

Chapter 4

Hybrid Transmission Scheme for Improving Link Reliability

4.1 Introduction

The principles of MC can be implemented at different levels of the protocol stack, as discussed in Section 1.6. Chapters 2 and 3 explored the feasibility of exploiting CA (a MAC layer MC technique) as a diversity method, and this chapter extends that work by moving down the protocol stack to propose a novel MC technique for the PHY layer. The interest of this chapter is on the URLLC use case for 5G/6G (see Section 1.4.3), which is related to applications such as the communication among machines and robots for the monitoring, control and automation of industrial processes in the context of the Industry 4.0 paradigm, automotive scenarios in Intelligent Transport System (ITS), tactile Internet, remote healthcare, mission-critical services and ad-hoc disaster/emergency relief among others [109, 110, 111].

The three 5G use cases, also relevant in 6G, are characterised by vastly heterogeneous and often mutually conflicting requirements. For URLLC, a general reliability requirement of $1-10^{-5}$ (i.e., 99.999%) with a user plane latency below 1 ms is specified in [112]. This high reliability requirement makes the wireless access design very challenging in terms of protocols and associated transmission techniques [113, 114, 115]. The main problem addressed in this chapter is how to improve the link reliability in order to meet as closely as possible the strict reliability requirements set for URLLC services. To this end, a novel method inspired by the principles of MC techniques is proposed.

With the aim to enable URLLC, a broad range of techniques have been proposed at the physical [116, 117, 118], link [119, 120, 121, 122, 123, 124, 125] and network [126, 127, 128] layers. However, given the existence of system trade-offs [129], the introduction of techniques to improve the reliability and latency of URLLC services reduces the capacity available for eMBB [130], which has motivated the development of solutions specifically designed to handle eMBB/URLLC coexistence scenarios [131, 132, 133, 134]. The main challenge is how to improve the link reliability without sacrificing the overall system capacity. Most solutions proposed so far in the literature to improve the link reliability achieve their objective at the expense of sacrificing the system capacity quite significantly. The trade-off between the conflicting interests of eMBB and URLLC services (capacity vs. reliability/latency) is efficiently addressed by the technique proposed in this chapter.

A well-known strategy to improve the communication reliability is to create simultaneous connections over multiple communication paths and transmit over them in parallel to achieve redundancy. This concept, referred to as Multi-Connectivity (MC), has been paid significant attention as a promising technique not only to increase the system capacity but also to effectively achieve high reliability in URLLC [53]. As a result, different MC techniques have been introduced in successive 3GPP releases in the PHY (e.g., coordinated multi-point), MAC (e.g., carrier aggregation), PDCP (e.g., dual connectivity and LWA) and higher layers [53] (a discussion was provided in Section 1.6). While PHY layer MC techniques are usually constrained to transmitting the same data simultaneously over the multiple paths available, MC techniques at the MAC and higher layers can transmit different data streams in each path, which can be scheduled according to various principles such as load balancing, packet duplication and packet splitting [53].

In this context, the solution proposed in this chapter is a novel PHY layer MC technique based on diversity reception that exploits and benefits from the complementary characteristics of the multiple frequency bands available in 5G-NR, which are divided into two frequency ranges. Frequency Range 1 (FR1) includes the sub-6 GHz bands traditionally used by previous mobile communication standards along with some new bands introduced to cover the spectrum from 410 MHz to 7125 MHz [135, Table 5.1-1]. On the other hand, Frequency Range 2 (FR2) embraces millimetre wave mm-Wave bands from 24.25 GHz to 52.6 GHz [136, Table 5.1-1]. Given the limited capacity available in FR1 bands, new FR2 bands were introduced with the aim of meeting the capacity requirements of eMBB. The larger bandwidths available in the mm-Wave spectrum and its comparatively lower level of usage make FR2 bands a preferred choice for the provision of eMBB. However, path loss and signal blockage are more pronounced at higher frequencies, which makes

radio propagation in mm-Wave bands more challenging and gives rise to unstable connectivity and unreliable communication [137, 138, 139]. To benefit from the complementary characteristics of both bands (i.e., reliability of FR1 bands and capacity of FR2 bands), this chapter proposes a novel technique for hybrid FR1/FR2 transmission with adaptive combining at the receiver. In the proposed scheme, an FR2 link is used as the main communication link to provide high capacity, whereas an FR1 link is used as a backup to provide improved reliability when needed. As long as the instantaneous Signal-to-Noise Ratio (SNR) in the FR2 link remains above a certain threshold that ensures an acceptable communication quality, the FR2 link is used alone and the FR1 link either remains in standby mode or is used for other data transmissions. However, when the FR2 link quality becomes unacceptable (i.e., its instantaneous SNR falls below a set threshold), the FR1 link is activated and the same signal is transmitted in both FR1 and FR2 links in order to benefit from the increased reliability offered by the FR1 bands (while both links are simultaneously active, a diversity reception technique is used at the receiver). As soon as the signal quality in the FR2 link increases above the threshold, the system switches back to the FR2 link to enjoy the higher data rates available in mm-Wave bands and puts the FR1 link in standby mode (to save energy and reduce interference to the environment) or employs it for other data transmissions (to increase resource efficiency). This dynamic transmission approach allows the proposed hybrid scheme to simultaneously benefit from the reliability of FR1 bands and the capacity of FR2 bands. Moreover, compared to the static diversity scenario of dual-link transmission where both FR1/FR2 links are used continuously [140], the proposed scheme conserves energy and prevents unnecessary interference to the environment (if the FR1 link is put on standby) or increases resource efficiency (if the FR1 link is also used for other data transmissions).

The contributions of this chapter are summarised below:

- An analysis of the SNR statistics at the receiver is provided when two popular diversity techniques, namely Selection Combining (SC) and Maximal Ratio Combining (MRC) [106], are employed. These analytical results are useful to derive various important performance metrics.

- Based on the obtained SNR statistics, the probability of outage and the probability of using the FR1 link under both diversity techniques are evaluated as a function of the received signal quality (represented in terms of the communication distance). The optimum configuration of the FR1/FR2 switching threshold that ensures the highest level of communication reliability is subsequently determined.

- Analytical expressions are derived and used to evaluate the bit-error performance of the proposed hybrid scheme under SC/MRC diversity for various configurations.

- Analytical expressions are also derived for the ergodic capacity of the proposed scheme under SC/MRC diversity, which are used to evaluate its performance for various configurations and operating conditions.

The obtained analytical, simulation and numerical results demonstrate that the proposed hybrid FR1/FR2 transmission scheme can achieve the same level of reliability (in terms of outage probability and bit-error rate) as the continuous dual-link transmission scheme, however with a significantly lower level of usage of the FR1 link, thus resulting in a much more efficient use of the available spectral resources. Moreover, this high level of link reliability is not obtained at the expense of the link capacity, which is indeed improved by the application of the proposed scheme, thus making it an ideal candidate for URLLC in heterogeneous scenarios with eMBB services.

The remainder of this chapter is organised as follows. First, Section 4.2 presents the system model considered in this work along with the proposed hybrid transmission scheme. Then, Section 4.3 derives analytical expressions for the SNR statistics at the receiver under both diversity techniques, which are used in Section 4.4 to derive further analytical expressions for the outage probability, FR1 link usage probability, bit-error rate and ergodic capacity of the proposed scheme. The obtained analytical expressions are used in Section 4.5 to evaluate the performance of the proposed transmission scheme. The focus of Sections 4.3 and 4.4 is on the mathematical analysis of the proposed hybrid transmission scheme rather than the discussion of its behaviour and performance, which is actually presented in Section 4.5 along with logic explanations. Finally, Section 4.6 summarises and concludes this chapter.

The research findings of this chapter have been published in [69].

4.2 System Model

As shown in Figure 4.1, the hybrid transmission system operates over two links in the FR1 (sub-6 GHz) and FR2 (mm-Wave) bands. The FR1 link is used as a backup for the FR2 link, which is the main communication link and remains always active. The FR1 link will remain in standby mode as long as the instantaneous SNR in the FR2 link, γ_2, is above a certain SNR threshold, γ_T, which is defined as the minimum SNR required to provide the desired link performance, for instance in terms of the Bit Error Rate (BER). When

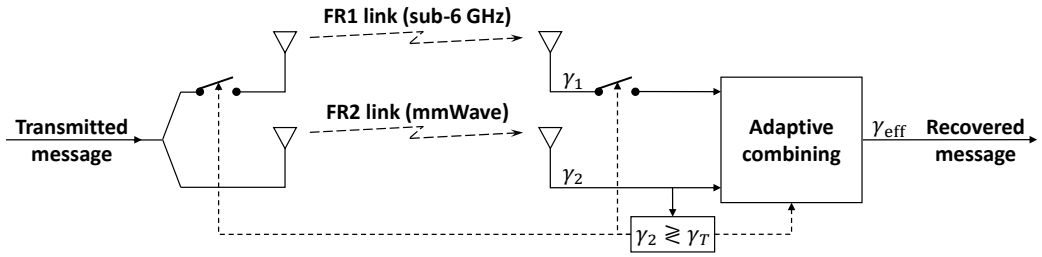

Figure 4.1: Proposed hybrid transmission scheme.

γ_2 falls below γ_T, the receiver sends a feedback signal to the transmitter to activate the FR1 link and transmit simultaneously the same data in both links. The receiver will then employ a diversity technique to combine the information received in both links. As soon as γ_2 increases above γ_T, the receiver sends a feedback signal to the transmitter to deactivate the FR1 link and communication resumes in the FR2 link only.

In this chapter, two diversity combining techniques (SC and MRC) are considered to combine the signals received in the FR1 and FR2 links when both links are activated simultaneously. In MRC, the signals in both links are averaged, weighted by their respective channel impulse responses. This diversity technique is known to be optimal since it maximises the effective SNR, which is given by $\gamma_1 + \gamma_2$ [141, eq. (6.22)]. However, MRC requires the knowledge of all channel fading parameters for each individual link, which results in a higher complexity. On the other hand, SC selects the signal with the highest instantaneous SNR, which leads to a much simpler receiver design at the expense of a lower SNR performance, which in this case is given by $\max(\gamma_1, \gamma_2)$ [141, eq. (6.6)]. While other diversity techniques have been proposed in the literature, SC and MRC are selected in this study owing to their popularity and the representative levels of trade-off that they provide between complexity and performance.

In the FR1 link, the instantaneous SNR per symbol, denoted by γ_1, follows a Rayleigh fading process. Its PDF and CDF are given, respectively, by [106, eq. (2.7)]

$$f_{\gamma_1}(x) = \frac{1}{\overline{\gamma}_1} \exp\left(-\frac{x}{\overline{\gamma}_1}\right), \tag{4.1}$$

$$F_{\gamma_1}(x) = 1 - \exp\left(-\frac{x}{\overline{\gamma}_1}\right), \tag{4.2}$$

where $\overline{\gamma}_1$ is the average SNR in the FR1 link. Rayleigh fading is commonly employed in sub-6 GHz bands to model NLOS conditions and is chosen here

for the FR1 link so that any performance improvement shown in this analysis for the proposed scheme corresponds to an unfavourable propagation scenario (i.e., better performance may be achieved in practice).

For the FR2 link, the Fluctuating Two-Ray (FTR) model is more realistic [142]. According to this model, the instantaneous SNR per symbol, γ_2, is distributed as [143, eq. (6)–(8)]

$$f_{\gamma_2}(x) = \frac{m^m}{\Gamma(m)} \sum_{j=0}^{\infty} \frac{K^j d_j}{(j!)^2} \frac{x^j}{(2\sigma^2)^{j+1}} \exp\left(-\frac{x}{2\sigma^2}\right), \tag{4.3}$$

$$F_{\gamma_2}(x) = \frac{m^m}{\Gamma(m)} \sum_{j=0}^{\infty} \frac{K^j d_j}{(j!)^2} \gamma\left(j+1, \frac{x}{2\sigma^2}\right), \tag{4.4}$$

where m is the fading severity index, K is the ratio between the average powers in the specular (i.e., dominant) and the diffuse (i.e., scattered) multipath components, $2\sigma^2$ is the total power of the diffuse components, $\Gamma(\cdot)$ is the (standard) gamma function [102, eq. (8.310.1)], $\gamma(\cdot,\cdot)$ is the lower incomplete gamma function [102, eq. (8.350.1)], and d_j is [144, eq. (13)]

$$d_j \triangleq \sum_{k=0}^{j} \binom{j}{k} \left(\frac{\Delta}{2}\right)^k \sum_{l=0}^{k} \binom{k}{l} \frac{\Gamma(j+m+2l-k)}{\left((m+K)^2-(K\Delta)^2\right)^{\frac{j+m}{2}}} \times (-1)^{2l-k}\ P_{j+m-1}^{k-2l}\left(\frac{m+K}{\sqrt{(m+K)^2-(K\Delta)^2}}\right), \tag{4.5}$$

where the parameter $\Delta \in [0,1]$ characterises the similarity of the two dominant waves (for $\Delta = 0$ one of them is zero and for $\Delta = 1$ both are equal) and $P_\nu^\mu(\cdot)$ is the associated Legendre function (or spherical function) of the first kind [102, eq. (8.702)]. An alternative expression for d_j is given by [144, eq. (19)]. In the FTR model, the average SNR is obtained as $\overline{\gamma}_2 = (E_b/N_0)2\sigma^2(1+K)$, where E_b/N_0 is the energy per bit to noise power spectral density ratio.

4.3 Analysis of SNR Statistics

4.3.1 Cumulative Distribution Function of the SNR

Based on the operation of the proposed hybrid scheme, the instantaneous effective SNR at the receiver, denoted by γ_{eff}, will be equal to γ_2 when $\gamma_2 > \gamma_T$

or the result of combining γ_1 and γ_2 (according to the employed diversity technique) when $\gamma_2 \leq \gamma_T$. Thus, one can write the CDF of the SNR as

$$F_{\gamma_{\text{eff}}}(x) = P\big(g(\gamma_1, \gamma_2) \leq x, \gamma_2 \leq \gamma_T\big) + P\big(\gamma_2 \leq x, \gamma_2 > \gamma_T\big), \tag{4.6}$$

where $g(\gamma_1, \gamma_2)$ characterises the effective SNR at the output of the selected diversity technique as a function of the SNR for each individual input signal: $g(\gamma_1, \gamma_2) = \max(\gamma_1, \gamma_2)$ for SC [141, eq. (6.6)] and $g(\gamma_1, \gamma_2) = \gamma_1 + \gamma_2$ for MRC [141, eq. (6.22)]. Equation (4.6) is particularised below for the SC and MRC diversity schemes considered in the study presented in this chapter.

Theorem 4.1 (CDF of SNR under SC)**.** *The CDF of SNR for the proposed hybrid system under SC is given by*

$$F_{\gamma_{\text{eff}}}(x) = \begin{cases} \left[1 - \exp\left(-\dfrac{x}{\overline{\gamma}_1}\right)\right] \dfrac{m^m}{\Gamma(m)} & \text{(4.7a)} \\ \times \displaystyle\sum_{j=0}^{\infty} \frac{K^j d_j}{(j!)^2}\, \gamma\left(j+1, \frac{x}{2\sigma^2}\right), \qquad x \leq \gamma_T, & \\ \dfrac{m^m}{\Gamma(m)} \displaystyle\sum_{j=0}^{\infty} \frac{K^j d_j}{(j!)^2} \left[\gamma\left(j+1, \frac{x}{2\sigma^2}\right)\right. & \text{(4.7b)} \\ \left. - \exp\left(-\dfrac{x}{\overline{\gamma}_1}\right) \gamma\left(j+1, \frac{\gamma_T}{2\sigma^2}\right)\right], \quad x > \gamma_T. & \end{cases}$$

Proof. The expression in (4.6) can be rewritten in terms of the associated conditional probabilities as

$$F_{\gamma_{\text{eff}}}(x) = P(g(\gamma_1, \gamma_2) \leq x \,|\, \gamma_2 \leq \gamma_T) P(\gamma_2 \leq \gamma_T) \tag{4.8}$$

$$+ P(\gamma_2 \leq x \,|\, \gamma_2 > \gamma_T) P(\gamma_2 > \gamma_T). \tag{4.9}$$

When $\gamma_2 \leq \gamma_T$, then $g(\gamma_1, \gamma_2) = \max(\gamma_1, \gamma_2)$ under SC, thus the conditional probability in (4.8) can be expressed as

$$\begin{aligned} P(g(\gamma_1, \gamma_2) \leq x \,|\, \gamma_2 \leq \gamma_T) =& P(\max(\gamma_1, \gamma_2) \leq x \,|\, \gamma_2 \leq \gamma_T) \\ =& P(\gamma_1 \leq x) P(\gamma_2 \leq x \,|\, \gamma_2 \leq \gamma_T) \\ =& F_{\gamma_1}(x) \cdot \min\left(1, \frac{F_{\gamma_2}(x)}{F_{\gamma_2}(\gamma_T)}\right). \end{aligned} \tag{4.10}$$

The conditional probability in (4.9) can be expressed as

$$P(\gamma_2 \leq x \,|\, \gamma_2 > \gamma_T) = \mathbf{1}_{(\gamma_T,\infty)}(x) \cdot \frac{F_{\gamma_2}(x) - F_{\gamma_2}(\gamma_T)}{1 - F_{\gamma_2}(\gamma_T)}, \tag{4.11}$$

where $\mathbf{1}_A(x)$ is the indicator function of A, which is equal to one when $x \in A$ and zero otherwise. Introducing (4.10) in (4.8) and (4.11) in (4.9) yields

$$\begin{aligned} F_{\gamma_{\text{eff}}}(x) = & F_{\gamma_1}(x) \cdot \min\left(1, \frac{F_{\gamma_2}(x)}{F_{\gamma_2}(\gamma_T)}\right) F_{\gamma_2}(\gamma_T) \\ & + \mathbf{1}_{(\gamma_T,\infty)}(x) \cdot \frac{F_{\gamma_2}(x) - F_{\gamma_2}(\gamma_T)}{1 - F_{\gamma_2}(\gamma_T)} \left[1 - F_{\gamma_2}(\gamma_T)\right], \end{aligned} \tag{4.12}$$

which can be simplified to the more compact form

$$\begin{aligned} F_{\gamma_{\text{eff}}}(x) = & F_{\gamma_1}(x) \cdot \min\left(F_{\gamma_2}(x), F_{\gamma_2}(\gamma_T)\right) \\ & + \mathbf{1}_{(\gamma_T,\infty)}(x) \cdot \left[F_{\gamma_2}(x) - F_{\gamma_2}(\gamma_T)\right]. \end{aligned} \tag{4.13}$$

The expression in (4.13) can be rewritten as

$$F_{\gamma_{\text{eff}}}(x) = \begin{cases} F_{\gamma_1}(x)F_{\gamma_2}(x), & x \leq \gamma_T, \quad \text{(4.14a)} \\ F_{\gamma_1}(x)F_{\gamma_2}(\gamma_T) + F_{\gamma_2}(x) - F_{\gamma_2}(\gamma_T), & \\ & x > \gamma_T. \quad \text{(4.14b)} \end{cases}$$

Introducing (4.2) and (4.4) in (4.14a) yields (4.7a). Similarly, introducing (4.2) and (4.4) in (4.14b) and simplifying yields (4.7b). □

Theorem 4.2 (CDF of SNR under MRC)**.** *The CDF of SNR for the proposed hybrid system under MRC is given by*

$$F_{\gamma_{\text{eff}}}(x) = \begin{cases} \dfrac{m^m}{\Gamma(m)} \displaystyle\sum_{j=0}^{\infty} \frac{K^j d_j}{j!(2\alpha\sigma^2)^{j+1}} \left[1 - \exp\left(-\frac{x}{\overline{\gamma}_1}\right)\right. & \text{(4.15a)} \\ \left. - \dfrac{2\sigma^2}{\overline{\gamma}_1} \displaystyle\sum_{k=0}^{j} \frac{(2\alpha\sigma^2)^k}{k!} \gamma\left(k+1, \frac{x}{2\sigma^2}\right)\right], & x \leq \gamma_T, \\ \dfrac{m^m}{\Gamma(m)} \displaystyle\sum_{j=0}^{\infty} \frac{K^j d_j}{(j!)^2} \left[\gamma\left(j+1, \frac{x}{2\sigma^2}\right)\right. & \text{(4.15b)} \\ \left. - \exp\left(-\dfrac{x}{\overline{\gamma}_1}\right) \dfrac{\gamma(j+1, \alpha\gamma_T)}{(2\alpha\sigma^2)^{j+1}}\right], & x > \gamma_T, \end{cases}$$

where $\alpha = (2\sigma^2)^{-1} - (\overline{\gamma}_1)^{-1}$.

Proof. When $\gamma_2 \leq \gamma_T$ under MRC, $g(\gamma_1, \gamma_2) = \gamma_1 + \gamma_2$ and the PDF of γ_{eff} can be calculated as [145, eq. (6-45)]

$$f_{\gamma_{\text{eff}}}(x) = \int_0^x f_{\gamma_1}(x-y) f_{\gamma_2}(y) dy \tag{4.16}$$

$$= \frac{1}{\overline{\gamma}_1} \exp\left(-\frac{x}{\overline{\gamma}_1}\right) \frac{m^m}{\Gamma(m)} \sum_{j=0}^{\infty} \frac{K^j d_j}{(j!)^2} \frac{1}{(2\sigma^2)^{j+1}} \times \int_0^x y^j \exp\left(-y\left[\frac{1}{2\sigma^2} - \frac{1}{\overline{\gamma}_1}\right]\right) dy, \quad x \leq \gamma_T. \tag{4.17}$$

The integral in (4.17) can be solved with the assistance of [102, eq. (3.381.1)], which yields

$$f_{\gamma_{\text{eff}}}(x) = \frac{1}{\overline{\gamma}_1} \exp\left(-\frac{x}{\overline{\gamma}_1}\right) \frac{m^m}{\Gamma(m)} \sum_{j=0}^{\infty} \frac{K^j d_j}{(j!)^2} \frac{\gamma(j+1, \alpha x)}{(2\alpha\sigma^2)^{j+1}}, \quad x \leq \gamma_T, \tag{4.18}$$

where $\alpha = (2\sigma^2)^{-1} - (\overline{\gamma}_1)^{-1}$. The solution in [102, eq. (3.381.1)] is valid for $\alpha > 0$, which implies $\overline{\gamma}_1 > \overline{\gamma}_2[(E_b/N_0)(1+K)]^{-1}$. This requirement is met in practice since $\overline{\gamma}_1 > \overline{\gamma}_2$ due to the higher path loss at higher frequencies (i.e., lower signal power) and larger bandwidths (i.e., higher noise power) in FR2.

The corresponding CDF when $\gamma_2 \leq \gamma_T$, $F_{\gamma_{\text{eff}}}(x)$, can be calculated based on (4.18) as

$$F_{\gamma_{\text{eff}}}(x) = \int_0^x f_{\gamma_{\text{eff}}}(y) dy = \frac{1}{\overline{\gamma}_1} \frac{m^m}{\Gamma(m)} \sum_{j=0}^{\infty} \frac{K^j d_j}{(j!)^2} \frac{1}{(2\alpha\sigma^2)^{j+1}} \times \int_0^x \exp\left(-\frac{y}{\overline{\gamma}_1}\right) \gamma(j+1, \alpha y) dy, \quad x \leq \gamma_T. \tag{4.19}$$

By replacing the lower incomplete gamma function in (4.19) with its equivalent form in [102, eq. (8.352.1)] and solving the integral with the aid of [102, eq. (3.381.1)], (4.15a) is obtained.

When $\gamma_2 > \gamma_T$ under MRC, the CDF of the output SNR γ_{eff} can be expressed as

$$F_{\gamma_{\text{eff}}}(x) = G(x) + F_{\gamma_2}(x) - F_{\gamma_2}(\gamma_T), \qquad x > \gamma_T, \tag{4.20}$$

where $G(x)$ can be calculated as [145, eqs. (6-38) and (6-42)]

$$G(x) = \int_0^{\gamma_T} \int_0^{x-z} f_{\gamma_1}(y) f_{\gamma_2}(z) dy dz \tag{4.21}$$

$$= \int_0^{\gamma_T} f_{\gamma_2}(z) \left[\int_0^{x-z} f_{\gamma_1}(y) dy \right] dz \tag{4.22}$$

$$= \int_0^{\gamma_T} F_{\gamma_1}(x-z) f_{\gamma_2}(z) dz \tag{4.23}$$

$$= \int_0^{\gamma_T} f_{\gamma_2}(z) dz - \overline{\gamma}_1 \int_0^{\gamma_T} f_{\gamma_1}(x-z) f_{\gamma_2}(z) dz \tag{4.24}$$

$$= F_{\gamma_2}(\gamma_T) - \exp\left(-\frac{x}{\overline{\gamma}_1}\right) \frac{m^m}{\Gamma(m)} \sum_{j=0}^{\infty} \frac{K^j d_j}{(j!)^2} \frac{\gamma(j+1, \alpha\gamma_T)}{(2\alpha\sigma^2)^{j+1}}, \tag{4.25}$$

where the relation $F_{\gamma_1}(x-z) = 1 - \overline{\gamma}_1 f_{\gamma_1}(x-z)$ from (4.1)–(4.2) is introduced in (4.23) to obtain (4.24), which is then resolved using [102, eq. (3.381.1)]. Combining (4.4) and (4.25) with (4.20) and grouping terms yields (4.15b), which completes the proof. □

4.3.2 Probability Density Function of the SNR

Theorem 4.3 (PDF of SNR under SC)**.** *The PDF of SNR for the proposed hybrid system under SC is given by*

$$f_{\gamma_{\text{eff}}}(x) = \begin{cases} \dfrac{m^m}{\Gamma(m)} \displaystyle\sum_{j=0}^{\infty} \frac{K^j d_j}{(j!)^2} \left[\frac{1}{\overline{\gamma}_1} \exp\left(-\frac{x}{\overline{\gamma}_1}\right) \gamma\left(j+1, \frac{x}{2\sigma^2}\right) \right. \\ \left. + \left(1 - \exp\left(-\frac{x}{\overline{\gamma}_1}\right)\right) \frac{1}{2\sigma^2} \exp\left(-\frac{x}{2\sigma^2}\right) \left(\frac{x}{2\sigma^2}\right)^j \right], \\ \qquad\qquad x \le \gamma_T, \qquad (4.26a) \\ \dfrac{m^m}{\Gamma(m)} \displaystyle\sum_{j=0}^{\infty} \frac{K^j d_j}{(j!)^2} \left[\frac{1}{2\sigma^2} \exp\left(-\frac{x}{2\sigma^2}\right) \left(\frac{x}{2\sigma^2}\right)^j \right. \\ \left. + \frac{1}{\overline{\gamma}_1} \exp\left(-\frac{x}{\overline{\gamma}_1}\right) \gamma\left(j+1, \frac{\gamma_T}{2\sigma^2}\right) \right], \\ \qquad\qquad x > \gamma_T. \qquad (4.26b) \end{cases}$$

Proof. By differentiation of (4.7), using [102, eq. (8.356.4)]. □

Theorem 4.4 (PDF of SNR under MRC)**.** *The PDF of SNR for the proposed hybrid system under MRC is given by*

$$f_{\gamma_{\text{eff}}}(x)=\begin{cases}\dfrac{1}{\overline{\gamma}_1}\exp\left(-\dfrac{x}{\overline{\gamma}_1}\right)\dfrac{m^m}{\Gamma(m)}\displaystyle\sum_{j=0}^{\infty}\frac{K^j d_j}{(j!)^2}\frac{\gamma(j+1,\alpha x)}{(2\alpha\sigma^2)^{j+1}}, \\ \qquad\qquad x\leq\gamma_T, & \text{(4.27a)}\\ \dfrac{m^m}{\Gamma(m)}\displaystyle\sum_{j=0}^{\infty}\frac{K^j d_j}{(j!)^2}\left[\frac{1}{2\sigma^2}\exp\left(-\frac{x}{2\sigma^2}\right)\left(\frac{x}{2\sigma^2}\right)^j\right. \\ \left.+\dfrac{1}{\overline{\gamma}_1}\exp\left(-\dfrac{x}{\overline{\gamma}_1}\right)\frac{\gamma(j+1,\alpha\gamma_T)}{(2\alpha\sigma^2)^{j+1}}\right], \\ \qquad\qquad x>\gamma_T\ . & \text{(4.27b)}\end{cases}$$

Proof. By differentiation of (4.15), using [102, eq. (8.356.4)]. □

4.4 Performance Analysis

4.4.1 Probabilities of Outage and Link Usage

In the context of URLLC, reliability is defined as the success probability of transmitting a specified amount of bytes within a certain delay target [112]. However, as discussed in Section 4.1, the interest of this chapter lies explicitly in the reliability aspect of URLLC. When delay or latency is not explicitly included, other definitions of reliability can be considered [146], the most common one being the level of link connectivity guarantees, typically quantified in terms of the probability of outage [147]. As pointed out in [115], even when the latency is not explicitly quantified, the use of short packets and the reduction of the outage probability can enable URLLC. Therefore, the outage probability is also a suitable reliability metric for URLLC.

The probability that the proposed hybrid system is in outage is obtained as the probability that the instantaneous effective SNR at the receiver γ_{eff} falls below a given outage threshold γ_{out} that represents the minimum SNR required to ensure that a certain maximum BER is not exceeded. Such probability can be obtained as $P_{\text{out}} = P(\gamma_{\text{eff}} \leq \gamma_{\text{out}}) = F_{\gamma_{\text{eff}}}(\gamma_{\text{out}})$, where $F_{\gamma_{\text{eff}}}(\cdot)$ is the CDF of the effective SNR at the receiver, which is given by (4.7) for SC and (4.15) for MRC.

In the proposed transmission scheme the mm-Wave (FR2) link is used with probability one (i.e., continuously). However, the sub-6 GHz (FR1)

link is used only when the instantaneous channel quality in the FR2 link (in terms of the instantaneous SNR γ_2) falls below a certain threshold (γ_T). The probability that the FR1 link is in use is given by $P_{\text{FR1}} = P(\gamma_2 \leq \gamma_T) = F_{\gamma_2}(\gamma_T)$, which can be evaluated directly from the CDF $F_{\gamma_2}(\cdot)$ given by (4.4). A high P_{FR1} implies that the FR1 link needs to be used often as a backup for the FR2 link, while a low P_{FR1} means that the FR1 link is more often available for other data transmissions.

Note that when $\gamma_T = \gamma_{\text{out}}$ the probability of using the FR1 link coincides with the outage probability of the FR2 link.

4.4.2 Average Bit Error Rate

The Average Bit Error Rate (ABER) over a fading channel, denoted by $\overline{P}_b$, can be obtained as [106, eq. (8.102)]

$$\overline{P}_b = \int_0^\infty P_b(x) f_\gamma(x) dx, \tag{4.28}$$

where $P_b(\gamma)$ represents the conditional bit-error probability for a given SNR γ and $f_\gamma(\cdot)$ is the PDF of the instantaneous SNR per symbol. Without loss of generality, the analysis in this section will consider binary modulations, for which the following general expression can be used [148, eq. (13)]

$$P_b(\gamma) = \frac{\Gamma(b, a\gamma)}{2\Gamma(b)}, \tag{4.29}$$

where $\Gamma(\cdot,\cdot)$ is the upper incomplete gamma function [102, eq. (8.350.2)] and $a, b \in \{\frac{1}{2}, 1\}$ are modulation-specific parameters (see [106, Table 8.1] for details).

Introducing (4.29) in (4.28), integrating by parts [102, 2.02.5] and using [102, 8.356.4], the ABER can be rewritten in the following more convenient form

$$\overline{P}_b = \frac{a^b}{2\Gamma(b)} \int_0^\infty e^{-ax} x^{b-1} F_\gamma(x) dx, \tag{4.30}$$

The solution to the integral in (4.30) for the Rayleigh channel can be obtained with the aid of [102, eq. (3.381.4)], which yields $\overline{P}_b = \frac{1}{2}[1 - (1 + 1/a\overline{\gamma}_1)^{-b}]$. The solution for the FTR channel is provided in [143, eq. (16)] together with [144, eq. (16)]. For the proposed hybrid scheme, (4.30) is calculated as

$$\overline{P}_b = \frac{a^b}{2\Gamma(b)} \int_0^{\gamma_T} e^{-ax} x^{b-1} F_{\gamma_{\text{eff}}}(x) dx \tag{4.31}$$

$$+ \frac{a^b}{2\Gamma(b)} \int_{\gamma_T}^\infty e^{-ax} x^{b-1} F_{\gamma_{\text{eff}}}(x) dx, \tag{4.32}$$

where the expression for $F_{\gamma_{\text{eff}}}(x)$ in each integral is according to the corresponding SNR interval. The result in (4.31)–(4.32) can be used to derive expressions for the ABER of the proposed hybrid transmission scheme under SC and MRC.

Theorem 4.5 (ABER under SC)**.** *The ABER of the proposed hybrid system under SC is given by*

$$\overline{P}_b = \frac{a^b}{2\Gamma(b)} \frac{m^m}{\Gamma(m)} \sum_{j=0}^{\infty} \frac{K^j d_j}{(j!)^2} \left(P_A - P_B - P_C\right), \tag{4.33}$$

where:

$$\begin{aligned} P_A =& \frac{\Gamma(b+j+1)(2\sigma^2)^b}{(j+1)(1+2a\sigma^2)^{b+j+1}} \\ & \times {}_2F_1\left(1, b+j+1; j+2; \frac{1}{1+2a\sigma^2}\right), \end{aligned} \tag{4.34}$$

$$\begin{aligned} P_B =& j! \left[\left(a+\frac{1}{\overline{\gamma}_1}\right)^{-b} \gamma\left(b, \left[a+\frac{1}{\overline{\gamma}_1}\right]\gamma_T\right)\right. \\ & \left. - \sum_{k=0}^{j} \frac{(a+\beta)^{-(k+b)}\,\gamma\left(k+b, [a+\beta]\,\gamma_T\right)}{k!(2\sigma^2)^k}\right], \end{aligned} \tag{4.35}$$

$$P_C = \left(a+\frac{1}{\overline{\gamma}_1}\right)^{-b} \Gamma\left(b, \left[a+\frac{1}{\overline{\gamma}_1}\right]\gamma_T\right) \gamma\left(j+1, \frac{\gamma_T}{2\sigma^2}\right), \tag{4.36}$$

with ${}_2F_1(\cdot,\cdot;\cdot;\cdot)$ *denoting the Gauss hypergeometric function [102, eq. (9.100)] and* $\beta = (2\sigma^2)^{-1} + (\overline{\gamma}_1)^{-1}$.

Proof. Introducing (4.7a) in (4.31) and (4.7b) in (4.32), and expanding all the terms, an expression of the form (4.33) is obtained with

$$P_A = \int_0^{\infty} \exp\left(-ax\right) x^{b-1} \gamma\left(j+1, \frac{x}{2\sigma^2}\right) dx, \tag{4.37}$$

$$P_B = \int_0^{\gamma_T} \exp\left(-\left[a+\frac{1}{\overline{\gamma}_1}\right]x\right) x^{b-1} \gamma\left(j+1, \frac{x}{2\sigma^2}\right) dx, \tag{4.38}$$

$$P_C = \gamma\left(j+1, \frac{\gamma_T}{2\sigma^2}\right) \int_{\gamma_T}^{\infty} \exp\left(-\left[a+\frac{1}{\overline{\gamma}_1}\right]x\right) x^{b-1} dx. \tag{4.39}$$

The integral in (4.37) is resolved by using [102, eq. (6.455.2)], which yields (4.34). The integral in (4.38) is solved by introducing [102, eq. (8.352.1)] and then employing [102, eq. (3.381.1)], which yields (4.35). The integral in (4.39) is resolved with the help of [102, eq. 3.381.3], which yields (4.36). □

Theorem 4.6 (ABER under MRC)**.** *The ABER of the proposed hybrid system under MRC is given by*

$$\overline{P}_b = \frac{a^b}{2\Gamma(b)} \frac{m^m}{\Gamma(m)} \sum_{j=0}^{\infty} \frac{K^j d_j}{j!} \left(\frac{P_D - P_E - P_F}{(2\alpha\sigma^2)^{j+1}} + \frac{P_G - P_H}{j!} \right), \tag{4.40}$$

where

$$P_D = a^{-b}\gamma(b, a\gamma_T), \tag{4.41}$$

$$P_E = \left(a + \frac{1}{\overline{\gamma}_1}\right)^{-b} \gamma\left(b, \left[a + \frac{1}{\overline{\gamma}_1}\right]\gamma_T\right), \tag{4.42}$$

$$P_F = \frac{2\sigma^2}{\overline{\gamma}_1} \sum_{k=0}^{j} (2\alpha\sigma^2)^k \Bigg[a^{-b}\gamma(b, a\gamma_T) - \sum_{l=0}^{k} \frac{\left(a + \frac{1}{2\sigma^2}\right)^{-(l+b)} \gamma\left(l + b, \left[a + \frac{1}{2\sigma^2}\right]\gamma_T\right)}{l!(2\sigma^2)^l} \Bigg], \tag{4.43}$$

$$P_G = (j!) \Bigg[a^{-b}\Gamma(b, a\gamma_T) - \sum_{k=0}^{j} \frac{\left(a + \frac{1}{2\sigma^2}\right)^{-(k+b)} \Gamma\left(k + b, \left[a + \frac{1}{2\sigma^2}\right]\gamma_T\right)}{k!(2\sigma^2)^k} \Bigg], \tag{4.44}$$

$$P_H = \frac{\gamma(j+1, \alpha\gamma_T)}{(2\alpha\sigma^2)^{j+1}} \left(a + \frac{1}{\overline{\gamma}_1}\right)^{-b} \Gamma\left(b, \left[a + \frac{1}{\overline{\gamma}_1}\right]\gamma_T\right), \tag{4.45}$$

with $\alpha = (2\sigma^2)^{-1} - (\overline{\gamma}_1)^{-1}$.

Proof. Introducing (4.15a) in (4.31) and (4.15b) in (4.32), and expanding

terms, an expression of the form (4.40) is obtained with

$$P_D = \int_0^{\gamma_T} \exp(-ax)\, x^{b-1} dx, \tag{4.46}$$

$$P_E = \int_0^{\gamma_T} \exp\left(-\left[a + \frac{1}{\overline{\gamma}_1}\right] x\right) x^{b-1} dx, \tag{4.47}$$

$$P_F = \frac{2\sigma^2}{\overline{\gamma}_1} \sum_{k=0}^{j} \frac{(2\alpha\sigma^2)^k}{k!} \int_0^{\gamma_T} \exp(-ax)\, x^{b-1} \gamma\left(k+1, \frac{x}{2\sigma^2}\right) dx, \tag{4.48}$$

$$P_G = \int_{\gamma_T}^{\infty} \exp(-ax)\, x^{b-1} \gamma\left(j+1, \frac{x}{2\sigma^2}\right) dx, \tag{4.49}$$

$$P_H = \frac{\gamma(j+1, \alpha\gamma_T)}{(2\alpha\sigma^2)^{j+1}} \int_{\gamma_T}^{\infty} \exp\left(-\left[a + \frac{1}{\overline{\gamma}_1}\right] x\right) x^{b-1} dx. \tag{4.50}$$

The integrals in (4.46) and (4.47) can both be resolved by using [102, eq. (3.381.1)], which yields (4.41) and (4.42), respectively. The integral in (4.48) is solved by introducing [102, eq. (8.352.1)] and then making use of [102, eq. (3.381.1)], which yields (4.43). Similarly, the integral in (4.49) is resolved by first introducing [102, eq. (8.352.1)] and then employing [102, eq. (3.381.3)], which yields (4.44). Finally, the integral in (4.50) can be resolved with the assistance of [102, eq. 3.381.3], which yields (4.45). □

4.4.3 Ergodic Capacity

The ergodic capacity C (in bit/s) of a fading channel with bandwidth B (in Hz) for a constant-power transmitter with optimum rate adaptation is given by [106, eq. (15.21)]

$$\begin{aligned} C &= B \int_0^{\infty} \log_2(1+x) f_\gamma(x) dx \\ &= \frac{B}{\ln 2} \int_0^{\infty} \ln(1+x) f_\gamma(x) dx, \end{aligned} \tag{4.51}$$

where $f_\gamma(\cdot)$ is the PDF of the instantaneous SNR per symbol. Solutions to the integral in (4.51) for the Rayleigh and FTR channels are provided in [106, eq. (15.26)] and [143, eq. (12)], respectively. For the proposed scheme,

(4.51) is calculated as

$$C = \frac{B_1}{\ln 2} \int_0^{\gamma_T} \ln(1+x) f_{\gamma_{\text{eff}}}(x) dx \tag{4.52}$$

$$+ \frac{B_2}{\ln 2} \int_{\gamma_T}^{\infty} \ln(1+x) f_{\gamma_{\text{eff}}}(x) dx, \tag{4.53}$$

where B_1 and B_2 are the bandwidths of the FR1 and FR2 links, respectively, and the expression for $f_{\gamma_{\text{eff}}}(x)$ in each integral is according to the corresponding SNR interval. Note that when γ_2 falls below γ_T and the FR1 link is activated, the same bit stream needs to be transmitted in both links (FR1 and FR2) in order to combine them with a diversity technique (SC or MRC) at the receiver. Because the bit stream in both links needs to be identical and the available bandwidth is typically lower in the FR1 link than in the FR2 link[1] (i.e., $B_1 < B_2$), the transmitter needs to reduce the bit rate (by adapting modulation and coding schemes) when the FR1 link is activated. Even though the FR2 link has a higher channel bandwidth, when the FR1 link is activated the bit stream transmitted through the FR2 link only requires a bandwidth B_1, so effectively a bandwidth B_1 is actually used in both links (to transmit the same bit stream) when the FR1 link is activated[2]. Therefore, from the point of view of the ergodic capacity (i.e., maximum amount of bits that can be transmitted per unit time) an effective bandwidth B_1 needs to be considered in (4.52).

This section derives analytical expressions for the ergodic capacity of the proposed hybrid transmission scheme under both SC and MRC diversity techniques based on the general ergodic capacity expression given in (4.52) and taking into account the various considerations discussed above.

[1] If $B_1 \geq B_2$ then mobile operators would have little incentive to use FR2 bands given their poorer propagation characteristics, which combined with a lower bandwidth would provide a much lower capacity than FR1 bands.

[2] In this case, the unused bandwidth in the FR2 link could potentially be utilised for other data transmissions and/or to introduce additional redundancy in the transmitted signal in order to improve the signal decodability (this would require novel diversity techniques specifically designed to this end, which is beyond the scope of this study and is suggested as future work).

Theorem 4.7 (Ergodic capacity under SC)**.** *The ergodic capacity of the proposed hybrid system under SC is given by*

$$C = \frac{1}{\ln 2}\frac{m^m}{\Gamma(m)}\sum_{j=0}^{\infty}\frac{K^j d_j}{j!}\big[B_1(\eta_A - \eta_B + \eta_C - \eta_D) + B_2(\eta_E + \eta_F)\big], \quad (4.54)$$

where η_A, η_B, η_C, η_D, η_E, η_F are given by (4.56)–(4.61) shown on the next page, $E_1(x) = \int_x^\infty e^{-t}t^{-1}\,dt = \int_1^\infty e^{-xt}t^{-1}\,dt$ is the exponential integral function of first order [102, eq. (3.351.5)] and $\beta = (2\sigma^2)^{-1} + (\overline{\gamma}_1)^{-1}$.

Proof. Introducing (4.26a) in (4.52) and (4.26b) in (4.53), replacing the lower incomplete gamma function with its equivalent form in [102, eq. (8.352.1)] and expanding all the terms, integrals of the form $I(s,t) = \int_s^t \ln(1+x)x^p e^{-qx}dx$ are obtained. The solution to $I(0,\infty)$ is given by [149, eq. (A.3)] and the solution to $I(\gamma_T,\infty)$ is given by [149, eq. (A.2)], while $I(0,\gamma_T) = I(0,\infty) - I(\gamma_T,\infty)$. Substituting the equalities $\Gamma(0,x) = E_1(x)$ and $\Gamma(1,x) = e^{-x}$ in the obtained results and grouping terms, (4.54) is obtained. Even though the procedure is tedious, it involves standard mathematical manipulations. □

Theorem 4.8 (Ergodic capacity under MRC)**.** *The ergodic capacity of the proposed hybrid system under MRC is given by*

$$C = \frac{1}{\ln 2}\frac{m^m}{\Gamma(m)}\sum_{j=0}^{\infty}\frac{K^j d_j}{j!}\frac{1}{(2\alpha\sigma^2)^{j+1}}\big[B_1(\eta_A - \eta_G) + B_2\big((2\alpha\sigma^2)^{j+1}\eta_E + \eta_H\big)\big], \quad (4.55)$$

where η_G and η_H are given by (4.62) and (4.63) shown on the next page, respectively, $E_1(x) = \int_x^\infty e^{-t}t^{-1}\,dt = \int_1^\infty e^{-xt}t^{-1}\,dt$ is the exponential integral function of first order [102, eq. (3.351.5)] and $\alpha = (2\sigma^2)^{-1} - (\overline{\gamma}_1)^{-1}$.

Proof. See proof of Theorem 4.7, using (4.27) instead of (4.26). □

$$\eta_A = \exp\left(\frac{1}{\overline{\gamma}_1}\right)\left[E_1\left(\frac{1}{\overline{\gamma}_1}\right) - E_1\left(\frac{1+\gamma_T}{\overline{\gamma}_1}\right)\right] - \ln(1+\gamma_T)\exp\left(-\frac{\gamma_T}{\overline{\gamma}_1}\right) \quad (4.56)$$

$$\begin{aligned}\eta_B =& \frac{1}{\beta\overline{\gamma}_1}\sum_{k=0}^{j}\frac{1}{(2\beta\sigma^2)^k}\left[\sum_{l=0}^{k}\left\{\beta^{k-l}e^{\beta}\Gamma(-k+l,\beta)\right.\right. \\ &\left.\left. -\frac{\Gamma(l,\beta(1+\gamma_T))}{\Gamma(l+1)}\frac{\Gamma(k-l+1,-\beta)}{\Gamma(k-l+1)}\right\} - \ln(1+\gamma_T)\frac{\Gamma(k+1,\beta\gamma_T)}{\Gamma(k+1)}\right]\end{aligned} \quad (4.57)$$

$$\begin{aligned}\eta_C =& \sum_{l=0}^{j}\left\{\frac{\exp(1/2\sigma^2)}{(2\sigma^2)^{j-l}}\Gamma\left(-j+l,\frac{1}{2\sigma^2}\right) - \frac{\Gamma\left(l,\frac{1+\gamma_T}{2\sigma^2}\right)}{\Gamma(l+1)}\frac{\Gamma\left(j-l+1,-\frac{1}{2\sigma^2}\right)}{\Gamma(j-l+1)}\right\} \\ &- \ln(1+\gamma_T)\frac{\Gamma\left(j+1,\frac{\gamma_T}{2\sigma^2}\right)}{\Gamma(j+1)}\end{aligned} \quad (4.58)$$

$$\begin{aligned}\eta_D =& \frac{1}{(2\beta\sigma^2)^{j+l}}\left[\sum_{l=0}^{j}\left\{\beta^{j-l}e^{\beta}\Gamma(-j+l,\beta) - \frac{\Gamma(l,\beta(1+\gamma_T))}{\Gamma(l+1)}\frac{\Gamma(j-l+1,-\beta)}{\Gamma(j-l+1)}\right\}\right. \\ &\left. - \ln(1+\gamma_T)\frac{\Gamma(j+1,\beta\gamma_T)}{\Gamma(j+1)}\right]\end{aligned} \quad (4.59)$$

$$\eta_E = \sum_{l=0}^{j}\frac{\Gamma\left(l,\frac{1+\gamma_T}{2\sigma^2}\right)}{\Gamma(l+1)}\frac{\Gamma\left(j-l+1,-\frac{1}{2\sigma^2}\right)}{\Gamma(j-l+1)} + \ln(1+\gamma_T)\frac{\Gamma\left(j+1,\frac{\gamma_T}{2\sigma^2}\right)}{\Gamma(j+1)} \quad (4.60)$$

$$\eta_F = \frac{\gamma\left(j+1,\frac{\gamma_T}{2\sigma^2}\right)}{\Gamma(j+1)}\left[\exp\left(\frac{1}{\overline{\gamma}_1}\right)E_1\left(\frac{1+\gamma_T}{\overline{\gamma}_1}\right) + \ln(1+\gamma_T)\exp\left(-\frac{\gamma_T}{\overline{\gamma}_1}\right)\right] \quad (4.61)$$

$$\begin{aligned}\eta_G =& \frac{2\sigma^2}{\overline{\gamma}_1}\sum_{k=0}^{j}(2\alpha\sigma^2)^k\left[\sum_{l=0}^{k}\left\{\frac{\exp(1/2\sigma^2)}{(2\sigma^2)^{k-l}}\Gamma\left(-k+l,\frac{1}{2\sigma^2}\right)\right.\right. \\ &\left.\left. -\frac{\Gamma\left(l,\frac{1+\gamma_T}{2\sigma^2}\right)}{\Gamma(l+1)}\frac{\Gamma\left(k-l+1,-\frac{1}{2\sigma^2}\right)}{\Gamma(k-l+1)}\right\} - \ln(1+\gamma_T)\frac{\Gamma\left(k+1,\frac{\gamma_T}{2\sigma^2}\right)}{\Gamma(k+1)}\right]\end{aligned} \quad (4.62)$$

$$\eta_H = \frac{\gamma\left(j+1,\alpha\gamma_T\right)}{\Gamma(j+1)}\left[\exp\left(\frac{1}{\overline{\gamma}_1}\right)E_1\left(\frac{1+\gamma_T}{\overline{\gamma}_1}\right) + \ln(1+\gamma_T)\exp\left(-\frac{\gamma_T}{\overline{\gamma}_1}\right)\right] \quad (4.63)$$

4.5 Results

4.5.1 Evaluation Scenario

The performance of the proposed hybrid transmission technique is evaluated considering band n78 in FR1, which has a central frequency $f_1 = 3.55$ GHz [135, Table 5.2-1], and band n257 in FR2, which has a central frequency $f_2 = 28$ GHz [136, Table 5.2-1]. The User Equipment (UE) channel bandwidth is assumed to be $B_1 = 20$ MHz in the FR1 link [135, Table 5.3.5-1] and $B_2 = 50$ MHz in the FR2 link [136, Table 5.3.5-1].

Rayleigh and FTR ($m = 20$, $K = 5$, $\Delta = 0.1$) fading models are assumed for the FR1 and FR2 bands, respectively. Notice that the average SNR in the FR1 link will be higher than in the FR2 link due to the lower path loss associated with lower propagation frequencies, however both SNR values are not independent since both links are subject to the same physical propagation distance. To ensure realistic pairs of SNR values, the received power in both bands is calculated as $P_R = P_T\, G_T\, G_R\, [c/(4\pi f)]^2\, d^{-\delta}$, where $P_T = 10$ dBm is the transmitted power, $G_T = 40$ dBi and $G_R = 40$ dBi are the gains of the transmitter and receiver antennas, respectively, $c = 3 \cdot 10^8$ m/s is the speed of light, f is the central frequency of each band (f_1 or f_2), $d = 100$ m is the physical distance between the transmitter and receiver antennas, and $\delta = 3.4$ is the path loss exponent (which is an appropriate value for NLOS conditions both in sub-6 GHz and mm-Wave bands [141, 150, 151]). The average SNR of each band ($\overline{\gamma}_1$ or $\overline{\gamma}_2$) is obtained as $\overline{\gamma} = P_R/P_N$, with the receiver's noise power calculated as $P_N = k_B T_0 B F$, where $k_B = 1.38 \cdot 10^{-23}$ J $\cdot$ K^{-1} is the Boltzmann constant, $T_0 = 290$ K is the reference room temperature, B is the bandwidth of the link in each band (B_1 or B_2) and F represents the receiver's noise factor (equivalent to a noise figure of 4 dB). The selected parameters lead to an equivalent noise floor of -110 dBm/MHz.

For evaluation purposes, the general BER model of (4.29) is particularised to $a = b = 1$, which corresponds to a differentially-encoded coherent Binary Phase Shift Keying (BPSK) modulation [106, Table 8.1]. The switching threshold γ_T is set assuming that the maximum tolerable BER for a successful demodulation of the received signal is 10^{-9} (higher values such as 10^{-6} were also evaluated as part of the study presented in this chapter but this was not observed to have a significant impact in the observed trends).

Unless otherwise stated, the parameter values presented in this subsection will be employed by default in the rest of the study presented in this chapter.

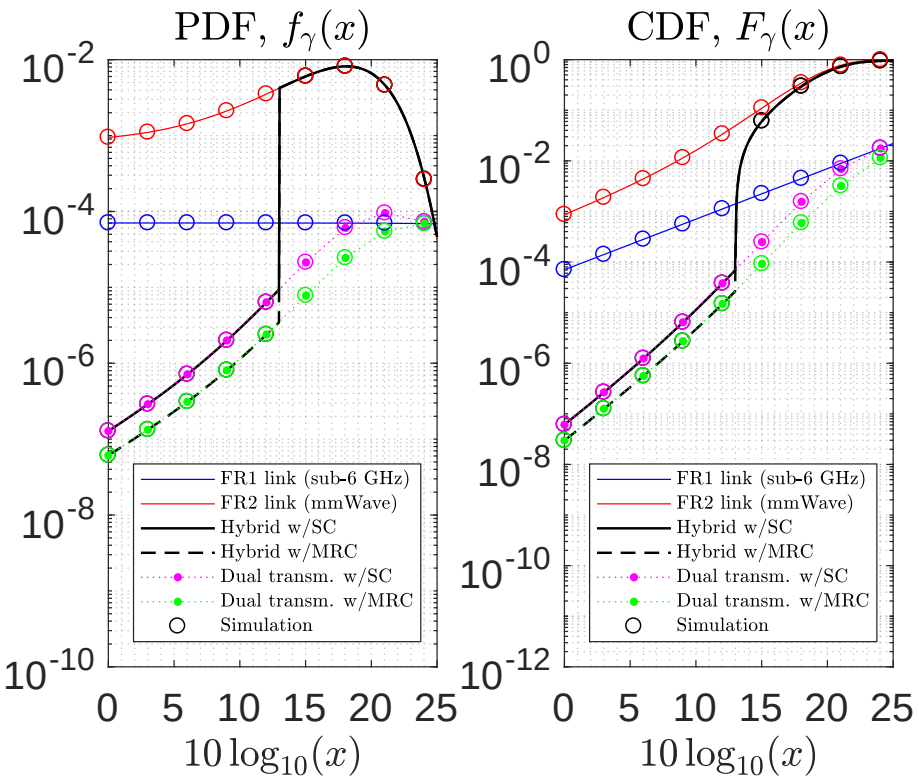

Figure 4.2: Validation of the SNR statistics ($d = 1000$ m).

4.5.2 Validation of the SNR Statistics

Figure 4.2 compares the analytic results presented in Section 4.3 with their Monte Carlo simulation counterparts. Notice that results are plotted in logarithmic axes for a better detail of appreciation in the low SNR regime (around the switching threshold). For the proposed hybrid transmission scheme, the switching threshold is set to $\gamma_T = \gamma_{\text{out}}$, where γ_{out} can be obtained from (4.29). For a target BER of 10^{-9} and $a = b = 1$ the obtained switching threshold is $\gamma_T = 13$ dB. As it can be appreciated, for SNR values above γ_T the effective SNR follows the PDF for the FR2 link while for SNR values below γ_T it follows the PDF of the dual transmission scheme (according to the considered diversity technique). In all cases, analytic and simulation results match perfectly, corroborating the correctness of the results of Section 4.3.

Subsequent results presented later on will be validated in their respective figures either with Monte Carlo simulations (when they relate to the SNR distribution, such as the probabilities of outage and link usage) or by numeric integration (when they relate to the ABER or ergodic capacity).

4.5.3 Performance Evaluation

The performance of the proposed hybrid scheme is evaluated based on the analytic results presented in Section 4.4. The performance is compared with the two limiting cases obtained for $\gamma_T = 0$ (single link transmission scenario where only the FR2 link is used) and $\gamma_T \to \infty$ (dual link transmission scenario where the system transmits continuously in both FR1 and FR2 links). These two cases provide appropriate baseline scenarios for a fair performance evaluation of the proposed hybrid transmission scheme. The performance of transmitting over the FR1 link alone is included for comparison purposes as well. It is worth mentioning that, from a performance point of view, operation in the high SNR regime ($\overline{\gamma}_2 \to \infty$) is equivalent to $\gamma_T = 0$ while operation in the low SNR regime ($\overline{\gamma}_2 \to 0$) is equivalent to $\gamma_T \to \infty$, respectively.

Figure 4.3 shows the probability of outage as a function of the maximum tolerable BER for a differentially-encoded coherent BPSK modulation ($a = b = 1$, [106, Table 8.1]). When the system tolerates a higher BER the associated outage threshold γ_{out}, which can be obtained by solving (4.29) for γ, decreases and so does the probability of outage P_{out}. The highest P_{out} is obtained for the FR2 link alone given its more challenging propagation conditions (i.e., higher path loss and lower average SNR). Transmitting over the FR1 link alone would decrease P_{out}, however the best outage performance is obtained when both links, FR1 and FR2, are used continuously in the dual transmission scenario. The proposed hybrid transmission scheme can achieve that same level of best performance as long as the switching threshold γ_T is greater than the outage threshold ($\gamma_T \geq \gamma_{\text{out}}$) since this allows the activation of the FR1 link before the FR2 link falls in outage; if such condition is met, the proposed hybrid system can only fall in outage when transmitting over both links (i.e., the most reliable transmission approach) falls in outage as well. Under such a scenario, MRC provides a lower outage probability than SC, as expected. On the other hand, if $\gamma_T < \gamma_{\text{out}}$ the FR2 link may temporarily fall in outage before the FR1 link is activated and, even though this still results in a better outage performance than transmission over the FR2 link alone, the outage performance will be worse than when $\gamma_T \geq \gamma_{\text{out}}$ (worse than in the FR1 link alone as well). In this case, the lower the switching threshold γ_T, the higher the outage probability (regardless of which diversity technique is used). Therefore, by properly selecting the switching threshold ($\gamma_T \geq \gamma_{\text{out}}$), the proposed hybrid scheme can deliver the same level of link reliability as continuously transmitting over both links, however using the FR1 link only when it is really needed (and leaving it available for other transmissions otherwise). The discussion above indicates that a suitable choice for the switching threshold from the point of view of the reliability

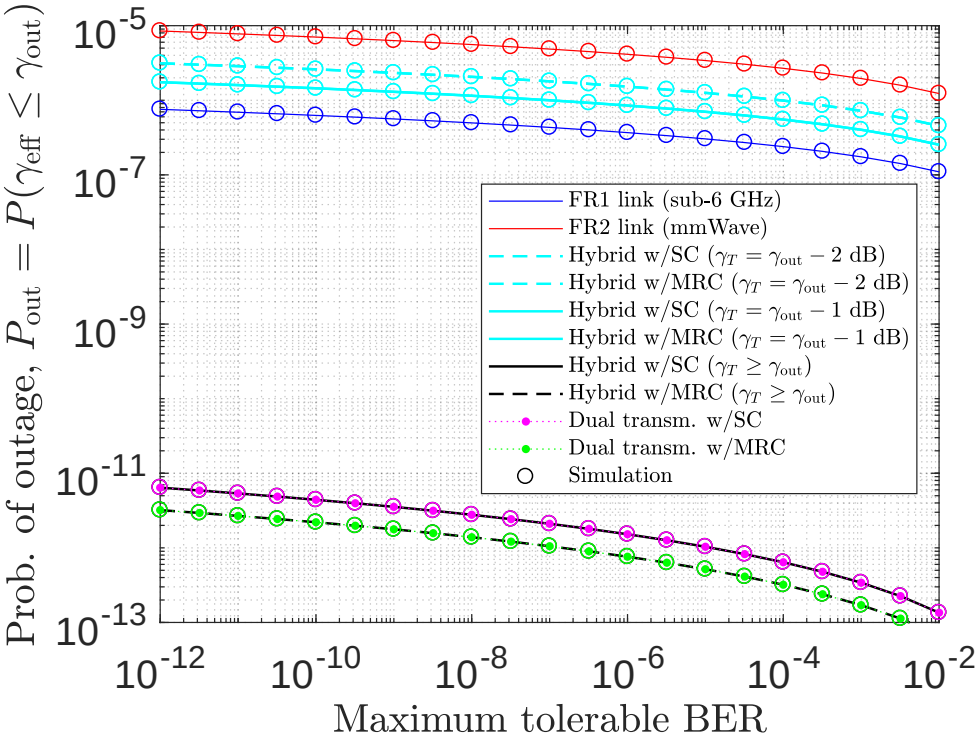

Figure 4.3: Outage probability versus maximum tolerable BER.

performance is any value that meets the condition $\gamma_T \geq \gamma_{\text{out}}$. Selecting lower values of γ_T results in a degradation of the reliability performance. On the other hand, selecting values of γ_T greater than γ_{out} ensures that the proposed hybrid scheme delivers the best reliability that can be attained. It is worth noting that increasing γ_T above γ_{out} does not improve the reliability performance any further, however it affects the extent to which the FR1 link is used (as discussed later on).

Figure 4.4 illustrates the outage performance as a function of the distance between the transmitter and receiver. As it can be observed, for a reliability requirement of $P_{\text{out}} = 10^{-5}$ the FR2 link can provide a maximum communication distance of about 100 m. The proposed hybrid transmission scheme and the dual transmission scheme can both extend the communication distance to about 800 m with SC diversity and 900 m with MRC diversity. However, as shown in Figure 4.5, at those distances the proposed hybrid transmission scheme only needs to use the FR1 link around 2% and 4% of the time, respectively (for $\gamma_T = \gamma_{\text{out}} + 1$ dB), meaning that most of the time the FR1 link would remain available for other data transmissions

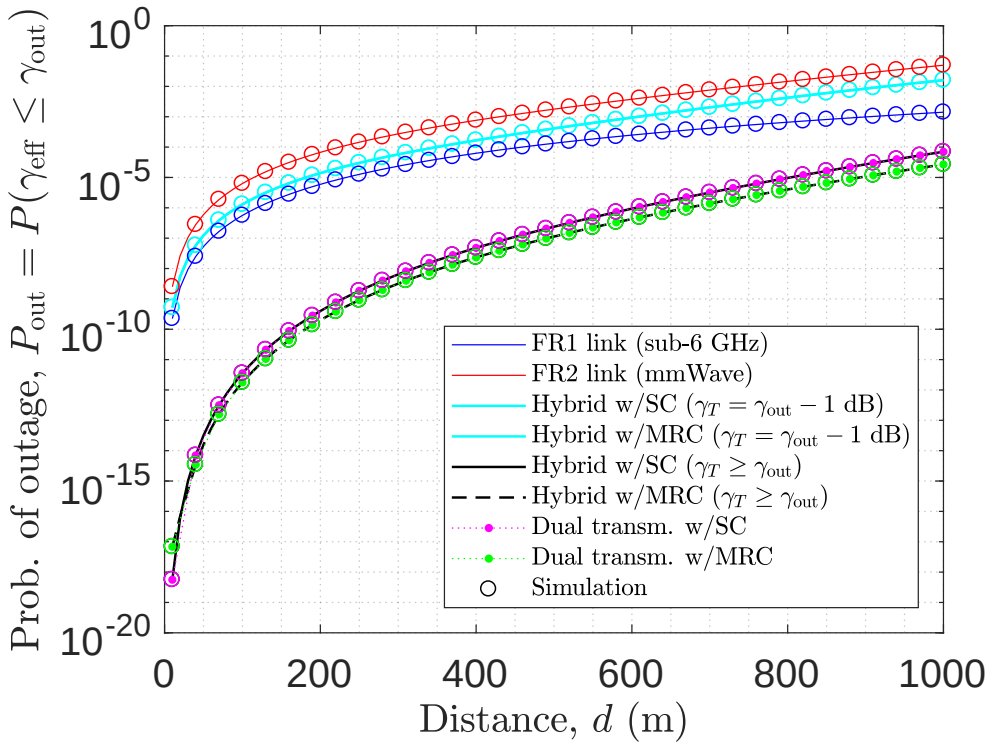

Figure 4.4: Outage probability versus communication distance.

(it would be required to backup the FR2 link only very occasionally). Thus, by only reducing the FR1 link availability by 2%–4%, the proposed hybrid transmission scheme can provide an 8/9-fold increase in the FR2 link communication range. Compared to the dual transmission scheme, which would use the FR1 link 100% of the time as a dedicated (non-shared) resource, the proposed hybrid scheme can improve the link reliability with a dramatically higher level of resource efficiency.

It is worth noting that increasing the switching threshold γ_T above γ_{out} does not further reduce the outage probability (Figure 4.4) but increases the FR1 link usage (Figure 4.5). Therefore, taking into account that the switching threshold γ_T should meet the condition $\gamma_T \geq \gamma_{\text{out}}$ in order to obtain the highest attainable reliability as discussed earlier, it becomes evident that the choice $\gamma_T = \gamma_{\text{out}}$ provides the optimum trade-off between overall system reliability and usage efficiency of radio resources. However, in a practical implementation this choice could potentially lead to momentary outages due to electronic circuit switching delays of practical hardware systems, which could severely degrade the outage performance as it can be appreciated in

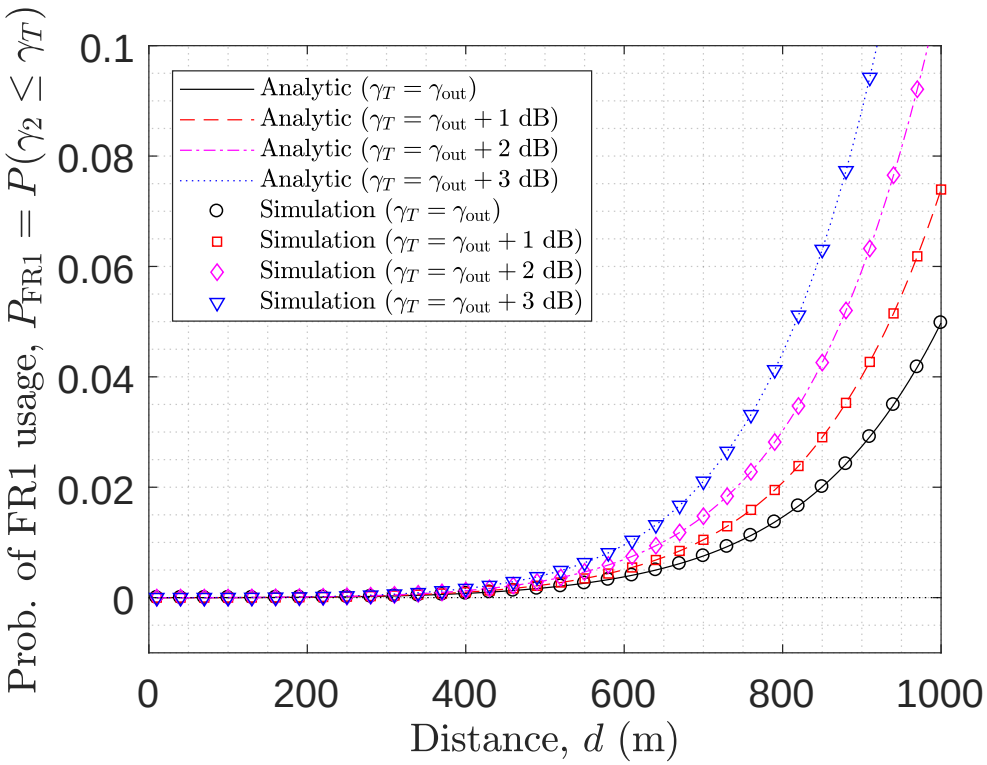

Figure 4.5: FR1 link usage probability versus communication distance.

Figure 4.4 ($\gamma_T < \gamma_{\mathrm{out}}$). Thus, some safety margin should be allowed (e.g., $\gamma_T = \gamma_{\mathrm{out}} + 1$ dB), at the expense of slightly sacrificing some FR1 link availability, to ensure that the FR1 link is activated when needed.

The ABER performance, which is illustrated in Figure 4.6, follows in general a very similar pattern as the outage probability shown in Figure 4.4, hence similar comments are applicable. The most remarkable difference is that the ABER is not degraded as severely as the outage probability when $\gamma_T < \gamma_{\mathrm{out}}$. This can be explained by the fact that $\overline{P}_b$ is an average of probabilities while P_{out} represents the probability that a particular event (outage) occurs. Hence, a slight reduction of the switching threshold γ_T below the outage threshold γ_{out} leads to a significant increase in the occurrence of outages but only a slight increase in the rate of bit-errors at the receiver.

The ergodic capacity performance is shown in Figures 4.7, 4.8 and 4.9 for various antenna gains. Similar to the ABER, the capacity is not significantly affected by small variations of the switching threshold γ_T above or below the outage threshold γ_{out}, hence results are shown only for the case $\gamma_T = \gamma_{\mathrm{out}}$ for the benefit of clarity. Three different configurations of the transmitter

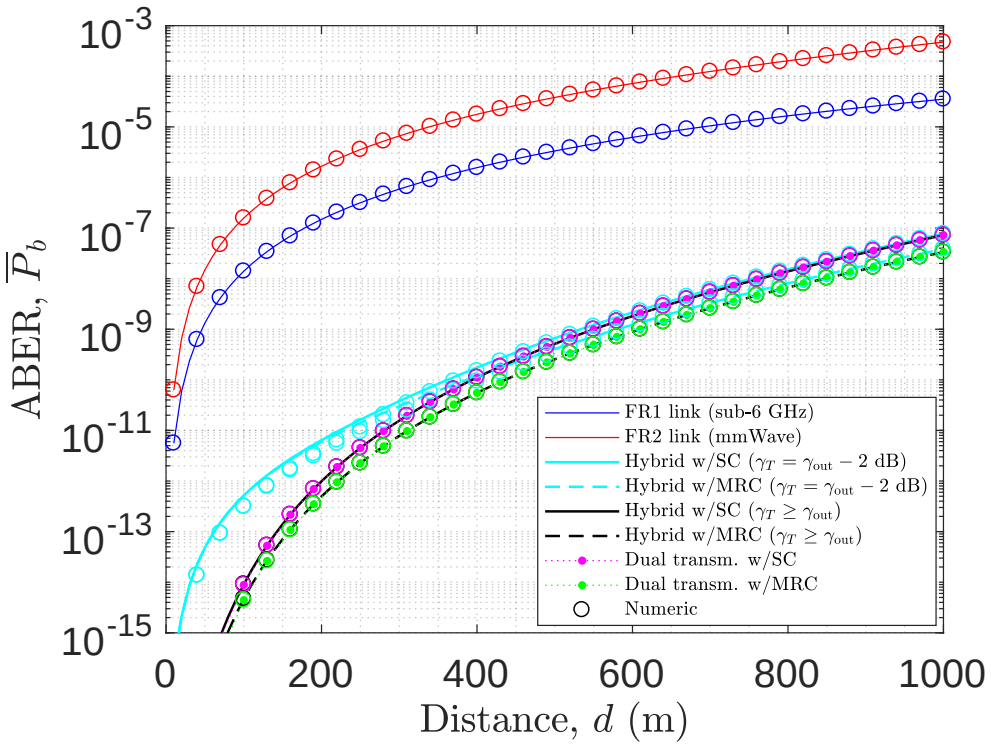

Figure 4.6: ABER versus communication distance.

and receiver antenna gains are considered in order to emulate the effect of various link budgets. Notice that in all cases, the capacity of the dual-link transmission scheme (with both SC and MRC diversity) is very similar to the capacity of the FR1 link alone (indistinguishable in Figures 4.7, 4.8 and 4.9). The explanation for this is that when the system transmits simultaneously in both links (FR1 and FR2), the bit-streams over both links need to be identical in order to combine them at the receiver with a diversity technique (SC or MRC). Since the FR1 link has a lower bandwidth than the FR2 link, the transmitter needs to reduce the bit-rate so that the generated bit-stream can fit within the bandwidth B_1 available in the FR1 link. As a result, the bit-rate of the transmitted signal is constrained by the bandwidth B_1. Therefore, from the point of view of the ergodic capacity, the effective bandwidth used for data transmission by the dual-link scheme is B_1, the same as in the FR1 link alone, hence the resulting capacity is very similar. As a matter of fact, when the dual-link transmission scheme is employed, the MRC capacity is actually slightly higher than the SC capacity, and both are slightly higher than the capacity provided by the FR1 link alone, which

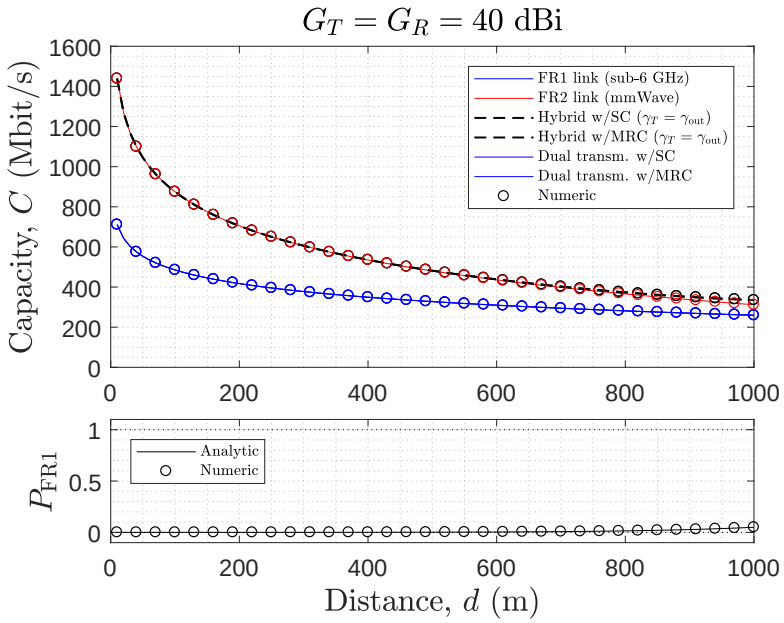

Figure 4.7: Ergodic capacity (top) and FR1 link usage probability (bottom) versus communication distance (transmitter/receiver antenna gains: $G_T = G_R = 40$ dBi.

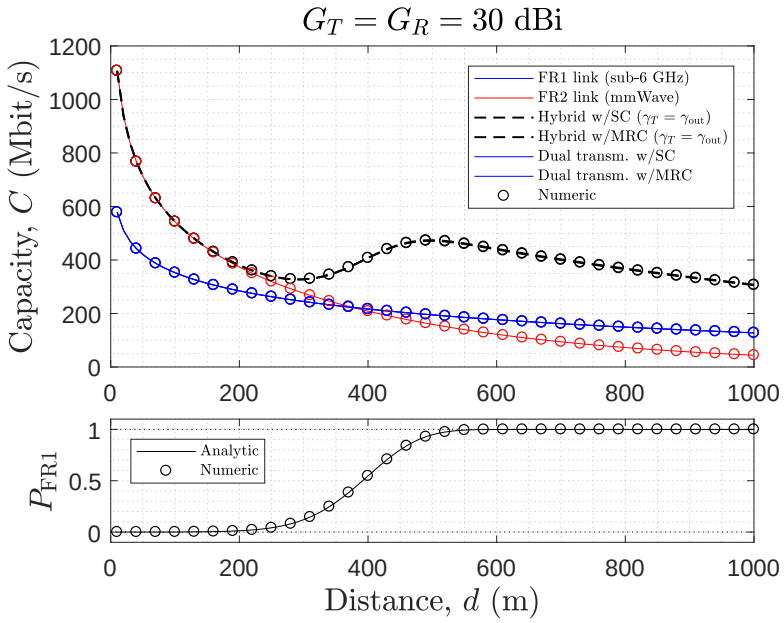

Figure 4.8: Ergodic capacity (top) and FR1 link usage probability (bottom) versus communication distance (transmitter/receiver antenna gains: $G_T = G_R = 30$ dBi.

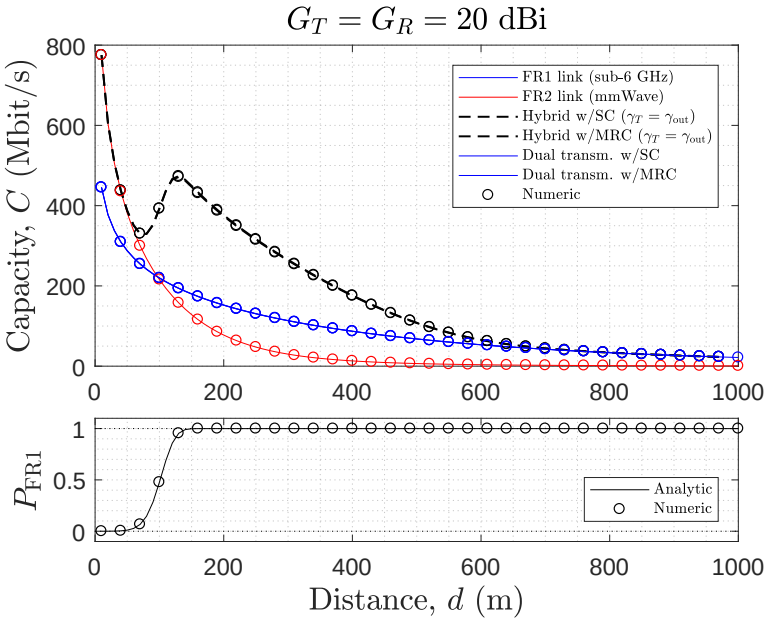

Figure 4.9: Ergodic capacity (top) and FR1 link usage probability (bottom) versus communication distance (transmitter/receiver antenna gains: $G_T = G_R = 20$ dBi.

is due to the SNR gain obtained from diversity. However, the difference is negligible when compared to the other cases. For this reason, the same line type (solid blue line) has been used in Figures 4.7, 4.8 and 4.9 to represent the FR1 link and the dual-link schemes (with both SC and MRC diversity) for the benefit of clarity.

Under a favourable link budget (Figure 4.7), the SNR experienced in the FR2 link is good enough to prescind from the FR1 link and, as a result, the proposed hybrid transmission scheme transmits in the FR2 link most of the time (as observed at the bottom of Figure 4.7). This leads to a channel capacity very similar to that offered by the FR2 link alone, which is higher than the capacity provided by the FR1 link (and the dual transmission scheme) for all the considered distances due to the larger amount of bandwidth available in the FR2 link ($B_2 = 2.5B_1$). When the link budget degrades (Figures 4.8 and 4.9), the experienced channel quality in the FR2 link degrades as well and consequently the proposed hybrid scheme needs to rely more often on the FR1 link as a backup, which can be noticed from the higher FR1 link usage probability (P_{FR1}). As discussed above, when the FR1 link is activated the transmitter needs to reduce the bit-rate so the generated signal can fit within the bandwidth B_1 available in the FR1 link. However, as counter-

intuitive as it may seem, this does not result in a reduction of the channel capacity for the proposed hybrid scheme, which indeed increases when the FR1 link is activated as appreciated in Figures 4.8 and 4.9. Notice that in these two cases the probability of using the FR1 link increases as the FR1 link begins to provide a higher capacity than the FR2 link. Even though the available bandwidth is significantly lower in the FR1 link than in the FR2 link, the FR1 link can provide a higher capacity if the experienced SNR is sufficiently large to compensate the lower amount of bandwidth available (i.e., much higher spectral efficiency). Activating the FR1 link in such cases can significantly increase the resulting capacity, even though the effective transmission bandwidth is lower (but the effective channel quality is comparatively much better). Notice that the capacity of the proposed hybrid transmission system is also noticeably higher than that attained by the dual transmission scheme. This is because the dual link scheme transmits continuously in both links (FR1 and FR2) and therefore is constrained to always do so according to a bandwidth B_1 regardless of the instantaneous channel quality, while the proposed hybrid scheme can benefit from a much higher transmission bandwidth B_2 when the channel quality is good enough, which ends up delivering a much higher capacity. Only when the channel quality is severely degraded due to a very unfavourable link budget (e.g., low antenna gain and long communication distance as in Figure 4.9) the capacity of the proposed scheme falls to match that of the dual transmission scheme, which is still higher than that of the FR2 link alone.

Some interesting insights can be gained from a careful observation of Figure 4.9. Notice that for more favourable link budgets (which in Figure 4.9 can be associated with short communication distances) the proposed hybrid scheme transmits most of the time using the FR2 link only, which allows the system to benefit from the larger bandwidth available in this band in order to achieve a higher channel capacity. On the other hand, for less favourable link budgets (which in Figure 4.9 can be associated with long communication distances) the proposed hybrid scheme relies on the FR1 link as a backup to overcome the degraded channel quality conditions in the FR2 link, which leads to a higher capacity than transmitting in the FR2 link only. For intermediate distances between these two extremes, the proposed hybrid scheme adjusts the FR1 link usage probability proportionally to the experienced channel quality. The dynamic adaptation offered by the hybrid scheme achieves the highest attainable capacity (out of all the considered transmission options/schemes) in all cases. Therefore, it can be concluded that the overall link capacity is positively affected by the application of the proposed scheme.

For a more complete evaluation, Figure 4.10 shows the ergodic capacity

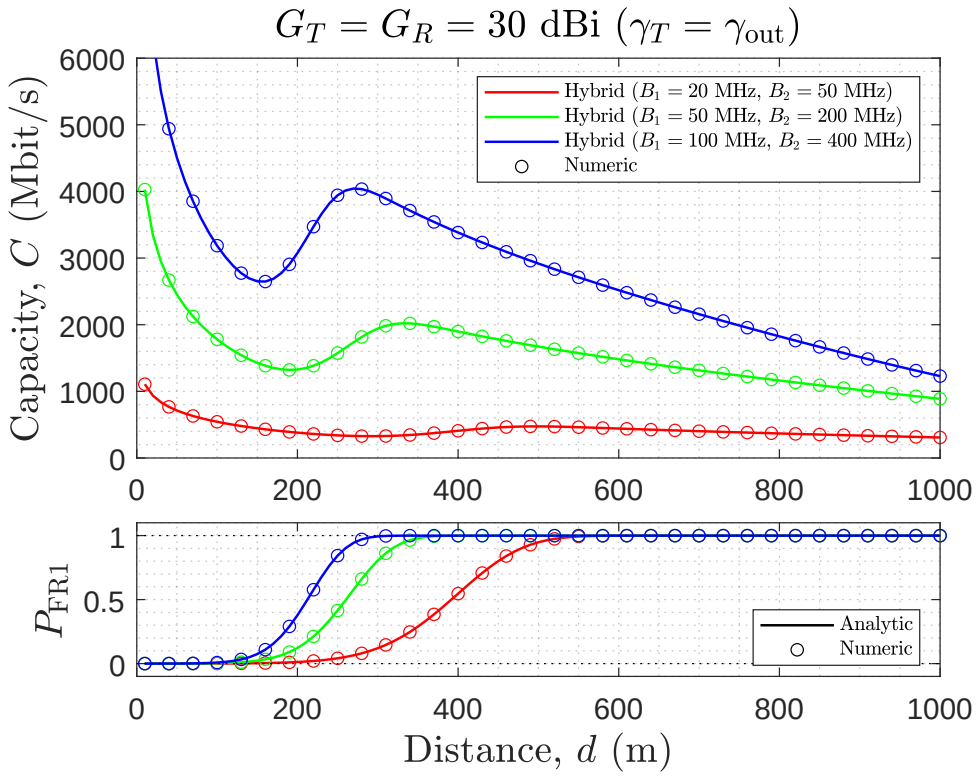

Figure 4.10: Ergodic capacity (top) and FR1 link usage probability (bottom) versus communication distance for various bandwidth configurations with $G_T = G_R = 30$ dBi and $\gamma_T = \gamma_{\text{out}}$.

of the proposed hybrid transmission scheme for various bandwidth configurations. The figure shows the capacity not only for $B_1 = 20$ MHz and $B_2 = 50$ MHz (considered in Figures 4.7, 4.8 and 4.9) but also for the case $B_1 = 50$ MHz and $B_2 = 200$ MHz and the case $B_1 = 100$ MHz and $B_2 = 400$ MHz. As expected, the use of larger bandwidths results in a higher capacity. Moreover, it can also be noticed that increasing the bandwidths also reduces the distance at which the FR1 backup link starts being used more frequently, which determines a trade-off between capacity and usage of the FR1 backup link depending on the selected channel bandwidths.

4.6 Conclusions

This chapter has proposed a dynamic hybrid FR1/FR2 transmission scheme with adaptive combining for improved reliability of wireless communications

in mm-Wave bands. The obtained results demonstrate that the proposed scheme can achieve the same level of reliability (in terms of probability of outage and bit-error rate) as the dual-link transmission scheme where both links (FR1 and FR2) are used continuously, however with a significantly lower level of usage of the FR1 link, thus resulting in a more efficient usage of the available spectral resources. Moreover, the attained high level of link reliability is not obtained at the expense of the link capacity, which is indeed improved by the application of the proposed scheme. These findings suggest that the proposed scheme is a suitable technique to effectively meet the URLLC requirements for 5G/6G in a resource-efficient manner.

Chapter 5

Conclusions and Future Work

5.1 Conclusions

Mobile radio communication systems have become part of our everyday life and their usage is now familiar to most people around the globe. They have enabled communication with the use of radio waves to connect points that could not be connected in the previous wire-constrained networks, making information available within large covered geographical areas. The evolution of mobile communication systems has historically been characterised by increasing demands in data rates, communication reliability and other service requirements, which has made it challenging for mobile operators to meet the ever increasing and heterogeneous demands for quality of service. As a result, several techniques and technological solutions have been proposed to address these challenging requirements. In this context, MC techniques have been proposed to improve the user data rates and the reliability of the wireless communication links, and have been proven to be tremendously successful in enhancing the performance of mobile communication systems in terms of various relevant performance metrics for a wide variety of services and applications. This has motivated the research work presented in this thesis to further explore novel approaches based on the principle of MC. This thesis has proposed novel MC techniques suitable for their use in existing and future mobile communication systems that can improve the performance of existing and new service applications in 5G/6G use case scenarios, in particular to enhance the provision of eMBB and/or URLLC services in 5G/6G networks by means of increased user data rates and/or link reliability to meet the requirements of these services more effectively and more efficiently.

The main scientific contributions and conclusions derived from the work carried out in this thesis are summarised below.

In Chapter 2, the problem of increasing the network capacity and the user data rate through CA has been investigated and a novel framework for CA as a diversity/MC technique has been proposed. The main idea proposed in this chapter is to divide a contiguous block of spectrum (that could in principle be used as a single carrier) into a number of sub-blocks and treat each of them as different CCs that are combined via CA. The motivation for this is to benefit from the frequency diversity experienced by each CC when the spectrum is divided in such a way, given that each aggregated CC runs its own instance of the scheduler, retransmission process, transmission power control, adaptive MCS, etc., and therefore adapts each transmission individually according to the CC's specific propagation conditions. CA was originally proposed as a technique to increase data rates by incorporating additional bandwidth into the system. Therefore, the concept of CA in a traditional sense inherently implies the use of additional bandwidth as a way to increase data rates. On the other hand, the framework proposed in this thesis is based on a different approach that does not require additional bandwidth, but simply splits the existing spectrum into blocks in order to benefit from frequency diversity, thus effectively exploiting CA as an MC technique, which is a novel point of view that, to the best of the author's knowledge, has not been considered in the literature before. The proposed CA-based MC method has been implemented in detail in the ns-3 simulator in order to evaluate its performance based on system level simulations. The performance results obtained under various propagation scenarios have indicated that CA can be effectively exploited as a diversity technique to optimise the overall system performance and increase the network capacity. Moreover, it has been found that the optimum number of CCs into which the spectrum block should be divided depends on the radio propagation distance. Such an optimum number of CCs is determined by the trade-off between the diversity gain (the higher the number of CCs, the higher the diversity gain) and the bandwidth penalty incurred by each CC due to the bandwidth that needs to be sacrificed in order to accommodate guard bands between CCs and to transmit the signalling traffic associated to the processes run individually in each CC (the higher the number of CCs, the higher the bandwidth penalty).

Chapter 3 has explored from an analytical perspective the framework proposed and evaluated with simulations in Chapter 2. More specifically, a mathematical model has been developed aimed at characterising the performance of CA as a diversity technique that can explain the behaviour and performance of the CA-based MC technique presented in Chapter 2. Given the high complexity of this problem, the concept of *effective SNR* has

been proposed. Mathematical models for the effective SNR have been elaborated and then exploited to derive the statistical distribution of the effective SNR under various assumptions. Such statistics have been employed to obtain closed-form expressions for the overall system performance in terms of both ergodic and secrecy capacities as a function of the number of CCs and other relevant configuration parameters. The obtained numerical results have demonstrated that the developed mathematical model can explain and corroborate the findings derived from simulation results in Chapter 2, and can be used to correctly predict the performance of CA as a diversity technique as well as the impact of various relevant configuration parameters. The numerical results have also corroborated that CA can be effectively exploited as a diversity technique to improve the performance of mobile communication systems and increase user data rates without requiring additional spectrum. However, it has also been shown that both the ergodic and secrecy capacities should be jointly taken into account to provide a robust system design. In this context, the mathematical models and expressions presented in Chapter 3 are a useful tool to achieve this end.

In Chapter 4, a novel hybrid transmission scheme for improved link reliability has been proposed. The proposed hybrid system benefits from the range of frequency bands available in mobile communication systems and their complementary characteristics. Higher-frequency bands tend to provide larger bandwidths (i.e., higher data rates) but are also characterised by more challenging propagation conditions (i.e., lower link reliability), while the opposite is true in general for lower-frequency bands. To exploit these complementary characteristics, a hybrid transmission scheme has been proposed that dynamically switches between FR1 and FR2 bands according to the instantaneous channel quality and uses adaptive combining at the receiver to combine the signals received in both bands. The proposed hybrid transmission system has been studied analytically. Concretely, the SNR statistics observed at the receiver have been first determined, which have then been employed to calculate closed-form expressions for relevant system performance metrics including the outage probability, bit-error rate and channel capacity. The obtained results have demonstrated that the proposed hybrid transmission scheme not only dramatically improves the transmission reliability but also has the potential to simultaneously increase the capacity while efficiently exploiting the resources in both bands. In particular, it has been shown that the proposed scheme can achieve the same level of reliability (in terms of probability of outage and bit-error rate) as the dual-link transmission scheme where both links (FR1 and FR2) are used continuously, however with a significantly lower level of usage of the FR1 link, thus resulting in a more efficient usage of the available spectral resources. Moreover,

the attained high level of link reliability is not obtained at the expense of the link capacity, which is indeed improved by the application of the proposed scheme. These findings suggest that the proposed transmission scheme is a suitable technique to effectively meet the URLLC requirements for 5G/6G in a resource-efficient manner without degrading the eMBB performance.

In summary, this thesis has proposed various novel MC techniques suitable for current and future mobile communication systems that can improve the performance of service applications in 5G/6G use case scenarios, in particular to enhance the provision of eMBB and/or URLLC services in 5G/6G networks by means of increased user data rates and/or link reliability to meet the requirements of these services more effectively and more efficiently.

5.2 Future Work

The research work presented in this thesis has contributed some novel ideas to the concept of MC techniques in mobile communication systems, both broadening the author's horizon and opening new questions requiring further investigation and research. Some ideas for consideration as future work to extend the work presented in this thesis are suggested and discussed below.

The concept of CA as a diversity/MC technique was evaluated by means of simulations carried out with the ns-3 simulator. To this end, the ns-3 mm-Wave module was selected. Such a module implements mobile communications in the mm-Wave bands introduced for 5G-NR, however actually using a 4G LTE radio interface. In other words, the ns-3 mm-Wave module implements a 4G LTE system operating in the frequency bands introduced for 5G-NR and, as such, is subject to the constraints and limitations of the 4G LTE specifications. In 4G LTE, the use of CA with up to 5 CCs is allowed and therefore the evaluation of the proposed idea was subject to a limitation of a maximum of 5 CCs. At the time this study was carried out, the ns-3 mm-Wave module was deemed to be the most suitable choice among the options available for the purposes of this research. However, the ns-3 simulator is a popular software platform broadly used by the research community that is in constant maintenance and development. After this research was completed, new features and functionalities were added to the ns-3 simulator within the following two years, including support for the 5G-NR radio interface [152, 153, 154, 155]. In 5G-NR, up to 16 CCs can be aggregated. Therefore, it would be interesting to evaluate the performance of CA as a diversity technique with simulations in the case of a 5G-NR system, in particular taking into account the results shown in Table 2.3, where the impact of the 4G LTE limit of 5 CCs can be clearly appreciated. One possibility

to accomplish this might be to re-consider the new version of the mm-Wave module, which has been maintained and updated to include some 5G-NR features to some extent. Another option could be to use the 5G-LENA module [155], which includes a very detailed implementation of the 5G-NR specifications. In either case, implementing the support for CA required to evaluate the idea proposed in this thesis would require substantial software design and coding work that is beyond the scope of this research, and is therefore suggested as future work. It is worth noting that, although the simulation results presented in this thesis are based on a 4G LTE radio interface, they are sufficient as a proof-of-concept to demonstrate the possibility of using CA as a diversity technique to improve the user data rates without increasing the amount of bandwidth available. The performance evaluation in the context of 5G-NR, and perhaps even in the context of 6G (which theoretically allows up to 32 CCs) once the corresponding 3GPP specifications are finally frozen, would be interesting additional results to investigate in the future.

The performance of CA in a real mobile communication system is determined by a broad range of processes that run at the MAC and PHY layers (packet scheduler, HARQ retransmission process, transmission power control, dynamic adaptation of the MCS, etc.) and the many different algorithms that can be implemented for each of such MAC/PHY processes. As a result, an exact analysis of the performance of CA in the context of the proposed method is actually extremely challenging. To overcome this limitation, the concept of *effective SNR* for CA has been introduced in this thesis. Relying on such concept, two different models for the performance of CA as a diversity technique have been developed, namely an *ideal model* aimed at providing an upper-bound to the real performance and an *average model* aimed at providing a closer approximation to the actual performance. The average model computes the effective SNR as the average of the SNR in each CC. This model can be expected to be more accurate than the ideal model and is sufficient for the purposes of this thesis, where the objective was to validate the possibility of using CA as a diversity technique and understand the qualitative impact of relevant configuration parameters on the resulting performance. Nevertheless, developing more accurate models for the effective SNR would be desirable. However, this is not a trivial task since such models should take into account explicitly the presence of the various processes that run at the MAC and PHY layers and their impact on the performance of CA. Given the complexity and ambitious nature of this challenging problem, this task requires a new specific and dedicated study that is beyond the scope of this thesis and is therefore suggested as future work.

The hybrid transmission scheme proposed in this thesis was analysed mathematically assuming that for each main link in the FR2 band there is a backup link in the FR1 band. In other words, each main link has its own dedicated backup link. This assumption was sufficient to analyse the performance of the proposed hybrid transmission scheme but might not be efficient in a real system implementation given that it would require excessive duplication of spectrum resources, with most of the backup channels remaining idle (i.e., unused and therefore wasted) most of the time – unless they are reallocated to other users when they are not being used as a backup to the main channel. A more interesting possibility, from the point of view of the efficiency of spectral resources, would be to share the same backup channel in the FR1 band among several main links in the FR2 band. This is motivated by the fact that, according to the results obtained in this thesis, the backup link may remain idle most of the time, and therefore it may be used to backup one FR2 link while it is not needed by another FR2 link. The obvious problem with this approach is that it may affect the reliability performance when one FR2 link needs to use the backup channel and it is already being used by another FR2 link. This establishes a trade-off between the number of FR2 links sharing the same FR1 backup link and the resulting reliability performance. This modified version of the hybrid transmission scheme presented in this thesis would add a new degree of complexity to the problem and therefore its mathematical analysis would require a specific study that is beyond the scope of this thesis and is suggested as future work.

Another interesting study would be the application of the hybrid transmission scheme presented in this thesis to improve the reliability of links in the THz bands, which have been recently proposed for 6G mobile communication systems. The THz bands provide even larger bandwidths than mm-Wave bands but are also known to suffer from even more accentuated reliability problems due to the challenging radio propagation conditions at THz frequencies. This paves the way for the application of the proposed hybrid transmission scheme in this scenario, where the THz link would now play the role of the main link and the mm-Wave link would now be the backup link. The FTR fading model for mm-Wave bands would now be used for the backup link and a suitable fading model for THz bands [156] should now be considered for the main link. This new application scenario would be expected to lead to similar conclusions, however a new mathematical analysis of this scenario would be necessary in order to provide a rigorous validation and confirmation of this hypothesis, which is also suggested as future work.

In addition to the specific suggestions provided above for the work presented in this thesis, there are also important challenges broadly in the field that need to be addressed. Some general areas that researchers and industry

experts might focus on in the context of MC techniques for mobile communication systems are discussed below. First, seamless handover and interoperability mechanisms are required to enable smooth transmissions between different connectivity technologies such as 4G/5G/6G, Wi-Fi and others. The use of MC techniques, with multiple simultaneous connections or data paths between the source and the destination of information, provides a new perspective on the important problem of resource management, where sophisticated algorithms are required to efficiently exploit multiple connections for enhanced data rates, improved reliability, reduced latency and higher network capacity. Energy efficiency, an equally important aspect in the performance of mobile communication systems, also requires special consideration in the context of MC solutions in order to minimise their impact on the battery life of mobile devices. Therefore, the investigation of power-aware algorithms to intelligently select and manage connectivity options based on specified energy constraints is required. Security and privacy can benefit tremendously from MC techniques as they are suitable to address potential vulnerabilities associated with the use of a single data path between the source and destination of the information. Finally, MC techniques have traditionally been developed within the realm of specific layers of the protocol stack. As discussed in Section 1.6, different techniques have been proposed at different levels of the protocol stack to embed the MC principles into mobile communication systems, however the existing techniques are limited in scope to individual layers of the protocol stack. In fact, this work has also considered MC techniques for the MAC layer (Chapters 2 and 3) and the PHY layer (Chapter 4). In this context, a promising approach for future work is the investigation of MC techniques from a cross-layer perspective, along with the cross-layer optimisation of existing and new MC techniques that consider interactions between different protocol layers in order to achieve better overall system performance.

5.3 Summary

This thesis has proposed novel MC techniques suitable for their use in existing and future mobile communication systems that can improve the performance of existing and new service applications in 5G/6G use case scenarios, in particular, in the context of eMBB and/or URLLC services in 5G/6G networks by means of increased user data rates and/or link reliability to meet the requirements of these services more effectively and more efficiently.

Firstly, the use of CA as a diversity technique has been proposed. The main proposed idea is to divide a sufficiently large block of contiguous spectrum into a number of smaller adjacent sub-blocks, which are treated as individual CCs and aggregated via regular CA. The motivation for this approach is to benefit from the diversity experienced at different frequencies. Simulation results have demonstrated that CA can effectively be exploited as a diversity technique to increase network capacity, with the optimum number of CCs depending on the radio propagation scenario.

Subsequently, a mathematical model has been developed to characterise the performance of CA as a diversity technique. The model has first been used to characterise the channel capacity as a function of the number of CCs and other relevant parameters, which has been shown to explain and corroborate the findings derived from simulation results. Capitalising on the developed mathematical model, the impact of various relevant configuration parameters on the ergodic and secrecy capacities of CA has then been evaluated. Results have demonstrated that the developed mathematical models can correctly predict the performance of CA as a diversity technique as well as the impact of various relevant configuration parameters.

Finally, a hybrid transmission scheme for improved link reliability has been proposed, which benefits from the range of frequency bands available in mobile communication systems and their complementary characteristics. Such complementary characteristics are exploited by dynamically switching between FR1 and FR2 bands according to the instantaneous channel quality. Results have demonstrated that the proposed hybrid scheme not only dramatically improves the transmission reliability but also has the potential to simultaneously increase the capacity while efficiently exploiting the resources in both bands. These findings suggest that the proposed scheme is a suitable technique to effectively meet the URLLC requirements for 5G/6G in a resource-efficient manner.

In summary, the MC techniques developed in this thesis can provide significant improvements in terms of enhanced data rates and reliability for current and future 5G/6G mobile communication systems.

Appendix

As discussed in Section 2.5.1, the results presented in Chapter 2 were carried out with the ns-3 simulator. In such study, version ns-3.29 (released in September 2018) was employed. To include CA features in the ns-3 simulator, the `mm-Wave` module developed by NYU Wireless and the University of Padova was employed (link: `https://apps.nsnam.org/app/mmwave/`). This is an ns-3 module for the simulation of 5G cellular networks operating at mm-Wave bands. A comprehensive tutorial with a detailed description of the whole module can be found in [95]. The details of the CA implementation are provided in [93]. Version 2.0 of the `mm-Wave` module was employed, which was the latest version available at the time of carrying out the study presented in Chapter 2. The latest version of the module can be downloaded from `https://github.com/nyuwireless-unipd/ns3-mmwave`. The scratch file that served as the baseline for the simulations carried out for Chapter 2 is `mmwave-ca-same-bandwidth.cc`, which can be found in the `/src/mmwave/examples/` folder of the `mm-Wave` module's source code. The specific version of such scratch file from version 2.0 of the `mm-Wave` module is reproduced below for the reader's convenience, and the latest version can be downloaded from `https://github.com/nyuwireless-unipd/ns3-mmwave/blob/new-handovermmwave-ca-same-bandwidth.cc`.

To carry out the simulations for Chapter 2, the base code was configured with the different simulation parameters shown in Table 2.1. Concretely, `--useCa` was set to `true`, `--ueDist` was set to the desired simulated distance between UE and BS, and the corresponding carrier frequencies were set to the values shown in Table 2.2 for the different numbers of CCs simulated. The baseline code shown below supports two CCs; larger numbers of CCs were implemented by adding new `MmWavePhyMacCommon` and `MmWaveComponentCarrier` objects (one per CC) and configuring the corresponding parameters accordingly. The DL and UL RLC statistics were obtained using the `read_traces.pl` Perl script provided in the `/scripts/` folder of the `mm-Wave` module, which served to produce the final results.

```
/* -*-  Mode: C++; c-file-style: "gnu"; indent-tabs-mode:nil;
    ↪ -*- */

#include "ns3/core-module.h"
#include "ns3/network-module.h"
#include "ns3/mobility-module.h"
#include "ns3/config-store.h"
#include "ns3/mmwave-helper.h"
#include <ns3/buildings-helper.h>
#include "ns3/global-route-manager.h"
#include "ns3/ipv4-global-routing-helper.h"
#include "ns3/internet-module.h"
#include "ns3/applications-module.h"
#include "ns3/log.h"
#include <map>

using namespace ns3;
using namespace mmwave;

/*
 * In this example a single UE is connected with a single
 * MmWave BS. The UE is placed at distance ueDist from
 * the BS and it does not move. The system bandwidth is
 * fixed at 1GHz. If CA is enabled, 2 CCs are used and
 * each of them uses half of the total bandwidth.
*/

int main (int argc, char *argv[])
{
        bool useCa = true;
        double ueDist = 50;
        bool blockage0 = false;
        bool blockage1 = false;
```

```
int numRefSc = 864;
uint32_t chunkPerRb0 = 72;
uint32_t chunkPerRb1 = 72;
double frequency0 = 28e9;
double frequency1 = 73e9;
double simTime = 5;
uint32_t runSet = 1;
std::string filePath;

CommandLine cmd;
cmd.AddValue("useCa", "If enabled use 2 CC", useCa);
cmd.AddValue("ueDist", "Distance between Enb and Ue [m]"
    , ueDist);
cmd.AddValue("blockage0", "If enabled, PCC blockage =
    true", blockage0);
cmd.AddValue("blockage1", "If enabled, SCC blockage =
    true", blockage1);
cmd.AddValue("frequency0", "CC 0 central frequency",
    frequency0);
cmd.AddValue("frequency1", "CC 1 central frequency",
    frequency1);
cmd.AddValue("simTime", "Simulation time", simTime);
cmd.AddValue("filePath", "Where to put the output files"
    , filePath);
cmd.AddValue("runSet", "Run number", runSet);
cmd.Parse (argc, argv);

if(useCa)
{
        // use half BW per carrier
        chunkPerRb0 = chunkPerRb0/2;
        chunkPerRb1 = chunkPerRb1/2;
        numRefSc = numRefSc/2;
```

```
}

// RNG
uint32_t seedSet = 1;
RngSeedManager::SetSeed (seedSet);
RngSeedManager::SetRun (runSet);

// set output file names
std::cout << "File path: " << filePath << std::endl;
Config::SetDefault("ns3::MmWaveBearerStatsCalculator::
    ↪ DlRlcOutputFilename", StringValue(filePath + "
    ↪ DlRlcStats.txt"));
Config::SetDefault("ns3::MmWaveBearerStatsCalculator::
    ↪ UlRlcOutputFilename", StringValue(filePath + "
    ↪ UlRlcStats.txt"));
Config::SetDefault("ns3::MmWaveBearerStatsCalculator::
    ↪ DlPdcpOutputFilename", StringValue(filePath + "
    ↪ DlPdcpStats.txt"));
Config::SetDefault("ns3::MmWaveBearerStatsCalculator::
    ↪ UlPdcpOutputFilename", StringValue(filePath + "
    ↪ UlPdcpStats.txt"));
Config::SetDefault("ns3::MmWavePhyRxTrace::
    ↪ OutputFilename", StringValue(filePath + "
    ↪ RxPacketTrace.txt"));
Config::SetDefault("ns3::LteRlcAm::BufferSizeFilename",
    ↪ StringValue(filePath + "RlcAmBufferSize.txt"));

// CC 0
// 1. create MmWavePhyMacCommon object
Config::SetDefault("ns3::MmWavePhyMacCommon::CenterFreq"
    ↪ ,DoubleValue(frequency0));
Config::SetDefault("ns3::MmWavePhyMacCommon::
    ↪ ComponentCarrierId", UintegerValue(0));
```

```
Config::SetDefault("ns3::MmWavePhyMacCommon::ChunkPerRB"
    ↪ , UintegerValue(chunkPerRb0));
Ptr<MmWavePhyMacCommon> phyMacConfig0 = CreateObject<
    ↪ MmWavePhyMacCommon> ();
phyMacConfig0->SetNumRefScPerSym( numRefSc );
double bandwidth0 = phyMacConfig0->GetNumRb() *
    ↪ phyMacConfig0->GetChunkWidth() * phyMacConfig0->
    ↪ GetNumChunkPerRb();

// 2. create the MmWaveComponentCarrier object
Ptr<MmWaveComponentCarrier> cc0 = CreateObject<
    ↪ MmWaveComponentCarrier> ();
cc0->SetConfigurationParameters(phyMacConfig0);
cc0->SetAsPrimary(true);

// CC 1
Ptr<MmWaveComponentCarrier> cc1;
if(useCa)
{
        // 1. create MmWavePhyMacCommon object
        Config::SetDefault("ns3::MmWavePhyMacCommon::
            ↪ CenterFreq",DoubleValue(frequency1));
        Config::SetDefault("ns3::MmWavePhyMacCommon::
            ↪ ComponentCarrierId", UintegerValue(1));
        Config::SetDefault("ns3::MmWavePhyMacCommon::
            ↪ ChunkPerRB", UintegerValue(chunkPerRb1));
        Ptr<MmWavePhyMacCommon> phyMacConfig1 =
            ↪ CreateObject<MmWavePhyMacCommon> ();
        phyMacConfig1->SetNumRefScPerSym( numRefSc );

        // 2. create the MmWaveComponentCarrier object
        cc1 = CreateObject<MmWaveComponentCarrier> ();
        cc1->SetConfigurationParameters(phyMacConfig1);
```

```
        cc1->SetAsPrimary(false);

}

// create the CC map
std::map<uint8_t, MmWaveComponentCarrier> ccMap;
ccMap[0] = *cc0;
if(useCa)
{
        ccMap[1] = *cc1;
}

// set the blockageMap
std::map<uint8_t, bool> blockageMap;
blockageMap[0] = blockage0;
if(useCa)
{
        blockageMap[1] = blockage1;
}

// print CC parameters
for(uint8_t i = 0; i < ccMap.size(); i++)
{
        std::cout << "Component Carrier " << (uint32_t)(
            ↪ ccMap[i].GetConfigurationParameters()->
            ↪ GetCcId())
        << " frequency : " << ccMap[i].
            ↪ GetConfigurationParameters()->
            ↪ GetCenterFrequency()/1e9 << " GHz,"
        << " bandwidth : " << bandwidth0/1e6 << " MHz,"
        << " blockage : " << blockageMap[i]
        << std::endl;
}
```

```
// create and set the helper
// first set UseCa = true, then
    ↪ NumberOfComponentCarriers
Config::SetDefault("ns3::MmWaveHelper::UseCa",
    ↪ BooleanValue(useCa));
if(useCa)
{
        Config::SetDefault("ns3::MmWaveHelper::
            ↪ NumberOfComponentCarriers",UintegerValue
            ↪ (2));
        Config::SetDefault("ns3::MmWaveHelper::
            ↪ EnbComponentCarrierManager",StringValue ("
            ↪ ns3::MmWaveRrComponentCarrierManager"));
}
Config::SetDefault("ns3::MmWaveHelper::ChannelModel",
    ↪ StringValue("ns3::MmWave3gppChannel"));
Config::SetDefault("ns3::MmWaveHelper::PathlossModel",
    ↪ StringValue("ns3::MmWave3gppPropagationLossModel")
    ↪ );

// The available channel scenarios are 'RMa', 'UMa', '
    ↪ UMi-StreetCanyon', 'InH-OfficeMixed', 'InH-
    ↪ OfficeOpen', 'InH-ShoppingMall'
std::string scenario = "UMa";
std::string condition = "n"; // n = NLOS, l = LOS
Config::SetDefault ("ns3::MmWave3gppPropagationLossModel
    ↪ ::ChannelCondition", StringValue(condition));
Config::SetDefault ("ns3::MmWave3gppPropagationLossModel
    ↪ ::Scenario", StringValue(scenario));
Config::SetDefault ("ns3::MmWave3gppPropagationLossModel
    ↪ ::OptionalNlos", BooleanValue(false));
```

```
Config::SetDefault ("ns3::MmWave3gppPropagationLossModel
    ↪ ::Shadowing", BooleanValue(false)); // enable or
    ↪ disable the shadowing effect
Config::SetDefault ("ns3::MmWave3gppPropagationLossModel
    ↪ ::InCar", BooleanValue(false)); // enable or
    ↪ disable the shadowing effect

Config::SetDefault ("ns3::MmWave3gppChannel::
    ↪ UpdatePeriod", TimeValue (MilliSeconds (100))); //
    ↪  Set channel update period, 0 stands for no update
    ↪ .
Config::SetDefault ("ns3::MmWave3gppChannel::DirectBeam"
    ↪ , BooleanValue(true)); // Set true to perform the
    ↪ beam in the exact direction of receiver node.
Config::SetDefault ("ns3::MmWave3gppChannel::
    ↪ PortraitMode", BooleanValue(true)); // use
    ↪ blockage model with UT in portrait mode
Config::SetDefault ("ns3::MmWave3gppChannel::
    ↪ NumNonselfBlocking", IntegerValue(4)); // number
    ↪ of non-self blocking obstacles
Config::SetDefault ("ns3::MmWave3gppChannel::
    ↪ BlockerSpeed", DoubleValue(1)); // speed of non-
    ↪ self blocking obstacles

Ptr<MmWaveHelper> helper = CreateObject<MmWaveHelper> ()
    ↪ ;
helper->SetCcPhyParams(ccMap);
helper->SetBlockageMap(blockageMap);


// create the enb node
NodeContainer enbNodes;
enbNodes.Create(1);
```

```
// set mobility
Ptr<ListPositionAllocator> enbPositionAlloc =
    ↪ CreateObject<ListPositionAllocator> ();
enbPositionAlloc->Add (Vector (0.0, 0.0, 15.0));

MobilityHelper enbmobility;
enbmobility.SetMobilityModel ("ns3::
    ↪ ConstantPositionMobilityModel");
enbmobility.SetPositionAllocator(enbPositionAlloc);
enbmobility.Install (enbNodes);
BuildingsHelper::Install (enbNodes);

// install enb device
NetDeviceContainer enbNetDevices = helper->
    ↪ InstallEnbDevice (enbNodes);
std::cout<< "eNB device installed" << std::endl;

// create ue node
NodeContainer ueNodes;
ueNodes.Create(1);

// set mobility
std::cout << "Distance : " << (uint32_t)ueDist << " m"
    ↪ << std::endl;
MobilityHelper uemobility;
uemobility.SetMobilityModel ("ns3::
    ↪ ConstantPositionMobilityModel");
Ptr<ListPositionAllocator> uePositionAlloc =
    ↪ CreateObject<ListPositionAllocator> ();
uePositionAlloc->Add (Vector (ueDist, 0.0, 1.6));
uemobility.SetPositionAllocator(uePositionAlloc);
uemobility.Install (ueNodes.Get (0));
```

```
        BuildingsHelper::Install (ueNodes);

        // install ue device
        NetDeviceContainer ueNetDevices = helper->
            ↪ InstallUeDevice(ueNodes);
        std::cout<< "UE device installed" << std::endl;

        helper->AttachToClosestEnb (ueNetDevices, enbNetDevices)
            ↪ ;
        helper->EnableTraces();

        // activate a data radio bearer
        enum EpsBearer::Qci q = EpsBearer::GBR_CONV_VOICE;
        EpsBearer bearer (q);
        helper->ActivateDataRadioBearer (ueNetDevices, bearer);

        BuildingsHelper::MakeMobilityModelConsistent ();

        Simulator::Stop (Seconds (simTime));
        Simulator::Run ();
        Simulator::Destroy ();

        return 0;
}
```

References

[1] J. Lundberg, "Evolution of Wireless Communication Technologies," 5 2020, last accessed 19/10/2023. [Online]. Available: https://www.researchgate.net/publication/341625780

[2] ITU-R, "M.2370-0, IMT Traffic Estimates for the Years 2020 to 2030," 2015.

[3] ITU-R, "M.2083-0, IMT Vision-Framework and Overall Objectives of the Future Development of IMT for 2020 and Beyond," 9 2015.

[4] Samsung, "The Next Hyper Connected Experience for All. Issued by Samsung Research," 2020.

[5] A. Gupta and R. K. Jha, "A Survey of 5G Network: Architecture and Emerging Technologies," pp. 1206–1232, 2015.

[6] G. A. Akpakwu, B. J. Silva, G. P. Hancke, and A. M. Abu-Mahfouz, "A Survey on 5G Networks for the Internet of Things: Communication Technologies and Challenges," *IEEE Access*, vol. 6, pp. 3619–3647, 12 2017.

[7] T. S. Rappaport, *Wireless Communications: Principles and Practice*. New Jersey: Prentice Hall PTR, 2002.

[8] R. Frenkiel, "A Brief History of Mobile Communications," *IEEE Vehicular Technology Society News*, 2002.

[9] J. Jain, "Mobile Communication: From 1G to 4G - Electronics For You," 2 2019, last accessed 19/10/2023. [Online]. Available: https://www.electronicsforu.com/technology-trends/mobile-communication-1g-4g

[10] N. Tripathi and J. Reed, *Cellular Communications*. New Jersey: Wiley-IEEE Press, 2014.

[11] J. Eberspächer and H.-J. V. C. Bettstetter, *GSM Switching, Services and Protocols*, 2nd ed. Chichester: Wiley, 2001.

[12] M. Y. Rhee, *Mobile Communication Systems and Security*. Singapore: Wiley-IEEE Press, 2009.

[13] V. Pereira and T. Sousa, "Evolution of Mobile Communications: from 1G to 4G," University of Coimbra, Tech. Rep., 7 2004.

[14] T. Mshvidobadze, "Evolution Mobile Wireless Communication and LTE Networks," in *2012 6th International Conference on Application of Information and Communication Technologies, AICT 2012 - Proceedings*, 2012.

[15] 3rd Generation Partnership Project, "Technical Specification Group Radio Access Network; Overview of 3GPP (Release 10)," 3GPP, Tech. Rep. 3GPP, 6 2014, v0.2.1.

[16] Nidhi, A. Mihovska, and R. Prasad, "Overview of 5G New Radio and Carrier Aggregation: 5G and Beyond Networks," in *International Symposium on Wireless Personal Multimedia Communications, WPMC*, vol. 2020-October. IEEE Computer Society, 10 2020.

[17] M. Iwamura, K. Etemad, M. H. Fong, R. Nory, and R. Love, "Carrier Aggregation Framework in 3GPP LTE-Advanced," *IEEE Communications Magazine*, vol. 48, pp. 60–67, 8 2010.

[18] H. S. Kamath, H. Singh, and A. Khanna, "Carrier Aggregation in LTE," *Proceedings of the International Conference on Intelligent Computing and Control Systems, ICICCS 2020*, pp. 135–138, 5 2020.

[19] D. Feng, C. She, K. Ying, L. Lai, Z. Hou, T. Q. Quek, Y. Li, and B. Vucetic, "Toward Ultrareliable Low-Latency Communications: Typical Scenarios, Possible Solutions, and Open Issues," *IEEE Vehicular Technology Magazine*, vol. 14, pp. 94–102, 6 2019.

[20] H. Chen, R. Abbas, P. Cheng, M. Shirvanimoghaddam, W. Hardjawana, W. Bao, Y. Li, and B. Vucetic, "Ultra-Reliable Low Latency Cellular Networks: Use Cases, Challenges and Approaches," *IEEE Communications Magazine*, vol. 56, pp. 119–125, 12 2018.

[21] U. B. Shukurillaevich, R. O. Sattorivich, and R. U. Amrillojonovich, "5G Technology Evolution," in *2019 International Conference on Information Science and Communications Technologies (ICISCT)*, 2019, pp. 1–5.

[22] L. Chettri and R. Bera, "A Comprehensive Survey on Internet of Things (IoT) Toward 5G Wireless Systems," *IEEE Internet of Things Journal*, vol. 7, pp. 16–32, 1 2020.

[23] A. Sutton, "5G Network Architecture," *The ITP (Institute of Telecommunications Professionals) Journal*, vol. 12, 2018.

[24] F. Rinaldi, A. Raschellà, and S. Pizzi, "5G NR System Design: A Concise Survey of Key Features and Capabilities," *Wireless Networks*, vol. 27, pp. 5173–5188, 11 2021.

[25] P. Marsch, Ömer Bulakci, O. Queseth, and M. Boldi, *5G System Design: Architectural and Functional Considerations and Long Term Research*. Wiley, 2018.

[26] S. Sinha, "State of IoT 2023: Number of Connected IoT Devices Growing 16% to 16.7 Billion Globally," 5 2023, last accessed 15/11/2023. [Online]. Available: https://iot-analytics.com/number-connected-iot-devices/

[27] T. Insights, "Current IoT Forecast Highlights," 11 2023, last accessed 15/11/2023. [Online]. Available: https://transformainsights.com/research/forecast/highlights

[28] Ericsson, "IoT Connections Outlook," last accessed 15/11/2023. [Online]. Available: https://www.ericsson.com/en/reports-and-papers/mobility-report/dataforecasts/iot-connections-outlook

[29] ITU-R, "M.2410-0, Minimum Requirements Related to Technical Performance for IMT-2020 Radio Interface(s)," 2017.

[30] 3rd Generation Partnership Project, "Technical Specification Group Radio Access Network; 5G; Study on Scenarios and Requirements for Next Generation Access Technologies (Release 17)," 3GPP, Tech. Rep. 3GPP TR 38.913, 5 2022, v17.0.0.

[31] A. Dogra, R. K. Jha, and S. Jain, "A Survey on Beyond 5G Network with the Advent of 6G: Architecture and Emerging Technologies," *IEEE Access*, vol. 9, pp. 67 512–67 547, 2021.

[32] R. N. Esa, A. Hikmaturokhman, and A. R. Danisya, "5G NR Planning at Frequency 3.5 GHz: Study Case in Indonesia Industrial Area," in *Proceeding - 2020 2nd International Conference on Industrial Electrical and Electronics, ICIEE 2020*. Institute of Electrical and Electronics Engineers Inc., 10 2020, pp. 187–193.

[33] P. Popovski, K. F. Trillingsgaard, O. Simeone, and G. Durisi, "5G Wireless Network Slicing for eMBB, URLLC, and mMTC: A Communication-Theoretic View," *IEEE Access*, vol. 6, pp. 55 765–55 779, 2018.

[34] S. Parkvall, E. Dahlman, A. Furuskar, and M. Frenne, "NR: The New 5G Radio Access Technology," *IEEE Communications Standards Magazine*, vol. 1, pp. 24–30, 12 2017.

[35] D. Erik, P. Stefa, and J. Skold, *5G NR The Next Generation Wireless Access Technology*, 2nd ed. London: Elsevier-Academic press, 2021.

[36] M. T. Moayyed, F. Restuccia, and S. Basagni, "Comparative Performance Evaluation of mmWave 5G NR and LTE in a Campus Scenario," *IEEE Vehicular Technology Conference*, vol. 2020-November, 11 2020.

[37] M. Shafi, A. F. Molisch, P. J. Smith, T. Haustein, P. Zhu, P. D. Silva, F. Tufvesson, A. Benjebbour, and G. Wunder, "5G: A Tutorial Overview of Standards, Trials, Challenges, Deployment, and Practice," *IEEE Journal on Selected Areas in Communications*, vol. 35, pp. 1201–1221, 6 2017.

[38] O. Semiari, W. Saad, M. Bennis, and M. Debbah, "Integrated Millimeter Wave and Sub-6 GHz Wireless Networks: A Roadmap for Joint Mobile Broadband and Ultra-Reliable Low-Latency Communications," *IEEE Wireless Communications*, vol. 26, pp. 109–115, 4 2019.

[39] P. Popovski, C. Stefanovic, J. J. Nielsen, E. de Carvalho, M. Angjelichinoski, K. F. Trillingsgaard, and A.-S. Bana, "Wireless Access in Ultra-Reliable Low-Latency Communication (URLLC)," *IEEE Transactions on Communications*, vol. 67, pp. 5783–5801, 5 2019.

[40] K. B. Letaief, W. Chen, Y. Shi, J. Zhang, and Y. J. A. Zhang, "The Roadmap to 6G: AI Empowered Wireless Networks," *IEEE Communications Magazine*, vol. 57, pp. 84–90, 8 2019.

[41] T. Nakamura, "5G Evolution and 6G," in *Digest of Technical Papers - Symposium on VLSI Technology*, vol. 2020-June. Honolulu: Institute of Electrical and Electronics Engineers Inc., 6 2020.

[42] W. Saad, M. Bennis, and M. Chen, "A Vision of 6G Wireless Systems: Applications, Trends, Technologies, and Open Research Problems," *IEEE Network*, vol. 34, pp. 134–142, 5 2020.

[43] R. Shafin, L. Liu, V. Chandrasekhar, H. Chen, J. Reed, and J. C. Zhang, "Artificial Intelligence-Enabled Cellular Networks: A Critical Path to Beyond-5G and 6G," *IEEE Wireless Communications*, vol. 27, pp. 212–217, 4 2020.

[44] "Key Drivers and Research Challenges for 6G Ubiquitous Wireless Intelligence ," 2019, last accessed 19/10/2023. [Online]. Available: http://jultika.oulu.fi/files/isbn9789526223544.pdf

[45] K. David and H. Berndt, "6G Vision and Requirements: Is There Any Need for Beyond 5G?" *IEEE Vehicular Technology Magazine*, vol. 13, pp. 72–80, 9 2018.

[46] X. Xu, H. Li, W. Xu, Z. Liu, L. Yao, and F. Dai, "Artificial Intelligence for Edge Service Optimization in Internet of Vehicles: A Survey," *Tsinghua Science and Technology*, vol. 27, pp. 270–287, 4 2022.

[47] "UN projects world population to reach 8.5 billion by 2030, driven by growth in developing countries — UN News," last accessed 19/10/2023. [Online]. Available: https://news.un.org/en/story/2015/07/505352

[48] M. López-Benítez and J. Zhang, "Comments and corrections to "new results on the fluctuating two-ray model with arbitrary fading parameters and its applications"," *IEEE Transactions on Vehicular Technology*, vol. 70, no. 2, pp. 1938–1940, Feb. 2021.

[49] E. N. Papasotiriou, A.-A. A. Boulogeorgos, K. Haneda, M. F. de Guzman, and A. Alexiou, "An experimentally validated fading model for thz wireless systems," *Scientific Reports*, vol. 11, no. 1, p. 18717, Sep. 2021.

[50] Samsung, "Spectrum Expanding the Frontier 6G. Issued by Samsung Research," May 2022.

[51] T. S. Rappaport, Y. Xing, O. Kanhere, S. Ju, A. Madanayake, S. Mandal, A. Alkhateeb, and G. C. Trichopoulos, "Wireless Communications and Applications Above 100 GHz: Opportunities and Challenges for 6G and Beyond," *IEEE Access*, vol. 7, pp. 78 729–78 757, 2019.

[52] H. Viswanathan and P. E. Mogensen, "Communications in the 6G Era," *IEEE Access*, vol. 8, pp. 57 063–57 074, 2020.

[53] M.-T. Suer, C. Thein, H. Tchouankem, and L. Wolf, "Multi-Connectivity as an Enabler for Reliable Low Latency Communications

– An Overview," *IEEE Commun. Surveys Tuts.*, vol. 22, no. 1, pp. 156–169, First Quarter 2020.

[54] S. A. Buari, R. Mumtaz, and J. Gonzalez, "Multi-connectivity in 5G New Radio Standards — IEEE Standards University," 11 2020, last accessed 19/10/2023. [Online]. Available: https://www.standardsuniversity.org/e-magazine/december-2020/multi-connectivity-in-5g-new-radio-standards/

[55] M. Majamaa, H. Martikainen, L. Sormunen, and J. Puttonen, "Adaptive Multi-Connectivity Activation for Throughput Enhancement in 5G and Beyond Non-Terrestrial Networks," *2022 30th International Conference on Software, Telecommunications and Computer Networks, SoftCOM 2022*, 2022.

[56] 3rd Generation Partnership Project, "Technical Specification Group Radio Access Network; Coordinated multi-point operation for LTE physical layer aspects (Release 11)," 3GPP, Tech. Rep. 3GPP TR 36.819, 9 2013, v11.2.0.

[57] S. Bassoy, H. Farooq, M. A. Imran, and A. Imran, "Coordinated Multi-Point Clustering Schemes: A Survey," *IEEE Communications Surveys and Tutorials*, vol. 19, pp. 743–764, 4 2017.

[58] M. T. Suer, C. Thein, H. Tchouankem, and L. Wolf, "Multi-Connectivity as an Enabler for Reliable Low Latency Communications - An Overview," *IEEE Communications Surveys and Tutorials*, vol. 22, pp. 156–169, 1 2020.

[59] S. Ahmadi, *LTE-Advanced. A Practical Systems Approach to Understanding 3GPP LTE Release 10 and 11 Radio Access Technologies.* Academic Press, 2014.

[60] K. S. R. S. Jyothsna and T. A. Babu, "Enhanced CoMP Technique for Interference Cancellation in HETNets of LTE," *International Journal of Scientific & Engineering Research*, vol. 7, 2016.

[61] N. Lassoued, N. Boujnah, and R. Bouallegue, "Enhancing Energy Efficiency in Wireless Heterogeneous Networks using Coordinated Multipoint and eNB Parameters Tuning," *2019 15th International Wireless Communications and Mobile Computing Conference, IWCMC 2019*, pp. 1650–1655, 6 2019.

[62] F. Irram, M. Ali, Z. Maqbool, F. Qamar, and J. J. Rodrigues, "Coordinated Multi-Point Transmission in 5G and Beyond Heterogeneous Networks," *Proceedings - 2020 23rd IEEE International Multi-Topic Conference, INMIC 2020*, 11 2020.

[63] H. Al-Hraishawi, N. Maturo, E. Lagunas, and S. Chatzinotas, "Scheduling Design and Performance Analysis of Carrier Aggregation in Satellite Communication Systems," *IEEE Transactions on Vehicular Technology*, vol. 70, pp. 7845–7857, 8 2021.

[64] P. U. Adamu and M. Lopez-Benitez, "Performance Evaluation of Carrier Aggregation as a Diversity Technique in mmWave Bands," *IEEE Vehicular Technology Conference*, vol. 2021-April, 4 2021.

[65] J. Parikh and A. Basu, "Scheduling Schemes for Carrier Aggregation in LTE-Advanced Systems," *IJRET: International Journal of Research in Engineering and Technology*, pp. 2321–7308, 8 2014.

[66] 3rd Generation Partnership Project, "Technical Specification Group Radio Access Network; LTE; 5G; NR; Multi-connectivity; Overall description; Stage-2 (3GPP TS 37.340 version 15.5.0 Release 15)," 3GPP, Tech. Rep. 3GPP TS 137 340, 5 2019, v15.5.0.

[67] J. F. Monserrat, F. Bouchmal, D. Martin-Sacristan, and O. Carrasco, "Multi-Radio Dual Connectivity for 5G Small Cells Interworking," *IEEE Communications Standards Magazine*, vol. 4, pp. 30–36, 9 2020.

[68] J. Elias, F. Martignon, and S. Paris, "Multi-Connectivity in 5G New Radio: Optimal Resource Allocation for Split Bearer and Data Duplication," *Elsevier*, 3 2023.

[69] P. U. Adamu, M. Lopez-Benitez, and J. Zhang, "Hybrid Transmission Scheme for Improving Link Reliability in mmWave URLLC Communications," *IEEE Transactions on Wireless Communications*, 2023.

[70] F. Boccardi, R. Heath, A. Lozano, T. L. Marzetta, and P. Popovski, "Five Disruptive Technology Directions for 5G," *IEEE Communications Magazine*, vol. 52, pp. 74–80, 2014.

[71] W. Gao, L. Ma, and G. Chuai, "Energy Efficient Power Allocation Strategy for 5G Carrier Aggregation Scenario," *Eurasip Journal on Wireless Communications and Networking*, vol. 2017, pp. 1–10, 12 2017.

[72] R. Vidhya and P. Karthik, "Dynamic Carrier Aggregation in 5G network scenario," *2015 International Conference on Computing and Network Communications, CoCoNet 2015*, pp. 936–940, 2 2016.

[73] 3rd Generation Partnership Project, "Technical Specification Group Radio Access Network; Overview of 3GPP (Release 10)," 3GPP, Tech. Rep. 3GPP, 6 2014, v0.2.1.

[74] C. S. Park, L. Sundström, A. Wallén, and A. Khayrallah, "Carrier aggregation for LTE-advanced: Design challenges of terminals," *IEEE Communications Magazine*, vol. 51, pp. 76–84, 2013.

[75] P. Lin, C. Hu, X. Li, J. Yu, and W. Xie, "Research on Carrier Aggregation of 5G NR," in *IEEE International Symposium on Broadband Multimedia Systems and Broadcasting, BMSB*, vol. 2022-June. Bilbao: IEEE Computer Society, 2022.

[76] I. Shayea, M. Ismail, and R. Nordin, "Capacity Evaluation of Carrier Aggregation Techniques in LTE-Advanced System," in *Proceedings - 2012 International Conference on Computer and Communication Engineering, ICCCE 2012*. Kuala Lumpur: Institute of Electrical and Electronics Engineers Inc., 2012, pp. 99–103.

[77] V. W. S. Wong, R. Schober, D. W. K. Ng, and L.-C. Wang, "Overview of New Technologies for 5G Systems," *Key Technologies for 5G Wireless Systems*, pp. 1–24, 4 2017.

[78] Nidhi, B. Khan, A. Mihovska, R. Prasad, and F. J. Velez, "A Study on Cross-Carrier Scheduler for Carrier Aggregation in Beyond 5G Networks," *2022 3rd URSI Atlantic and Asia Pacific Radio Science Meeting, AT-AP-RASC 2022*, 2022.

[79] W. Roh, J. Y. Seol, J. H. Park, B. Lee, J. Lee, Y. Kim, J. Cho, K. Cheun, and F. Aryanfar, "Millimeter-wave Beamforming as an Enabling Technology for 5G Cellular Communications: Theoretical Feasibility and Prototype Results," *IEEE Communications Magazine*, vol. 52, pp. 106–113, 2014.

[80] S. Sun, T. S. Rappaport, R. W. Heath, A. Nix, and S. Rangan, "MIMO for Millimeter-wave Wireless Communications: Beamforming, Spatial Multiplexing, or Both?" *IEEE Communications Magazine*, vol. 52, pp. 110–121, 2014.

[81] S. Sun, T. S. Rappaport, M. Shafi, P. Tang, J. Zhang, and P. J. Smith, "Propagation Models and Performance Evaluation for 5G Millimeter-Wave Bands," *IEEE Transactions on Vehicular Technology*, vol. 67, pp. 8422–8439, 9 2018.

[82] T. S. Rappaport, S. Sun, R. Mayzus, H. Zhao, Y. Azar, K. Wang, G. N. Wong, J. K. Schulz, M. Samimi, and F. Gutierrez, "Millimeter Wave Mobile Communications for 5G Cellular: It Will Work!" *IEEE Access*, vol. 1, pp. 335–349, 2013.

[83] S. Rangan, T. S. Rappaport, and E. Erkip, "Millimeter-wave Cellular Wireless Networks: Potentials and Challenges," *Proceedings of the IEEE*, vol. 102, pp. 366–385, 2014.

[84] H. Shokri-Ghadikolaei, C. Fischione, G. Fodor, P. Popovski, and M. Zorzi, "Millimeter Wave Cellular Networks: A MAC Layer Perspective," *IEEE Transactions on Communications*, vol. 63, pp. 3437–3458, 2015.

[85] M. Polese, M. Giordani, M. Mezzavilla, S. Rangan, and M. Zorzi, "Improved Handover Through Dual Connectivity in 5G mmWave Mobile Networks," *IEEE Journal on Selected Areas in Communications*, vol. 35, pp. 2069–2084, 9 2017.

[86] M. Polese, R. Jana, and M. Zorzi, "TCP and MP-TCP in 5G mmWave Networks," *IEEE Internet Computing*, vol. 21, pp. 12–19, 2017.

[87] B. Khan, A. Rocha Ramos, R. Paulo, and F. Velez, "Deployment of Beyond 4G Wireless Communication Networks with Carrier Aggregation," in *Proceedings of the International Conference on Electronics and Electrical Engineering (ICEEE 2020)*, 02 2020.

[88] R. Joda, M. Elsayed, H. Abou-Zeid, R. Atawia, A. B. Sediq, G. Boudreau, and M. Erol-Kantarci, "Carrier Aggregation With Optimized UE Power Consumption in 5G," *IEEE Networking Letters*, vol. 3, pp. 61–65, 4 2021.

[89] B. Khan, A. Mihovska, R. Prasad, and F. J. Velez, "A Study on Cross-Carrier Scheduler for Carrier Aggregation in Beyond 5G Networks," in *Proceedings - 2022 3rd URSI Atlantic and Asia Pacific Radio Science Meeting (AT-AP-RASC)*. Gran Canaria: Institute of Electrical and Electronics Engineers Inc., 2022.

[90] S. M. Rayavarapu, S. D. Amuru, and K. Kiran, "Dynamic Control of Packet Duplication in 5G-NR Dual Connectivity Architecture," in *2020 International Conference on COMmunication Systems and NETworkS, COMSNETS 2020*. Institute of Electrical and Electronics Engineers Inc., 1 2020, pp. 539–542.

[91] A. Wulandari, M. Hasan, A. Hikmaturokhman, Ashamdono, L. Damayanti, and Damelia, "5G Stand Alone Inter-Band Carrier Aggregation Planning in Kelapa Gading Jakarta Utara," in *Proceeding - 2021 2nd International Conference on ICT for Rural Development, IC-ICTRuDev 2021*. Jogjakarta: Institute of Electrical and Electronics Engineers Inc., 2021.

[92] Yoko, R. Munadi, Syahrial, Y. Away, T. Y. Arif, and R. Adriman, "The Investigation of Carrier Aggregation in LTE Advanced System using Systematic Literature Review Approach," in *Proceedings of the International Conference on Electrical Engineering and Informatics*, vol. 2022-September. Banda Aceh: Institute of Electrical and Electronics Engineers Inc., 2022, pp. 121–124.

[93] T. Zugno, M. Polese, and M. Zorzi, "Integration of Carrier Aggregation and Dual Connectivity for the NS-3 mmWave Module," *ACM International Conference Proceeding Series*, vol. 9, pp. 45–52, 2 2018.

[94] R. Ford, M. Zhang, S. Dutta, M. Mezzavilla, S. Rangan, and M. Zorzi, "A Framework for End-to-End Evaluation of 5G mmWave Cellular Networks in NS-3," *ACM International Conference Proceeding Series*, vol. Part F132163, pp. 85–92, 2 2016.

[95] M. Mezzavilla, M. Zhang, M. Polese, R. Ford, S. Dutta, S. Rangan, and M. Zorzi, "End-to-End Simulation of 5G mmWave Networks," *IEEE Communications Surveys and Tutorials*, vol. 20, pp. 2237–2263, 7 2018.

[96] M. Zhang, M. Polese, M. Mezzavilla, S. Rangan, and M. Zorzi, "NS-3 Implementation of the 3GPP MIMO Channel Model for Frequency Spectrum above 6 GHz," *ACM International Conference Proceeding Series*, vol. Part F128360, pp. 71–78, 2 2017.

[97] 3rd Generation Partnership Project, "Technical Specification Group Radio Access Network; LTE; 5G; Study on Channel Model for Frequency Spectrum Above 6 GHz (Release 14)," 3GPP, Tech. Rep. 3GPP TR 138 900, 2017, v14.2.0.

[98] M. Mezzavilla, M. Zhang, M. Polese, R. Ford, S. Dutta, S. Rangan, and M. Zorzi, "End-to-end simulation of 5G mmWave networks," *IEEE Communications Surveys and Tutorials*, vol. 20, no. 3, pp. 2237–2263, 2018.

[99] T. Zugno, M. Polese, and M. Zorzi, "Integration of carrier aggregation and dual connectivity for the ns-3 mmWave module," in *Proceedings of the 2018 Workshop on Ns-3*, ser. WNS3 '18. New York, NY, USA: Association for Computing Machinery, 2018, p. 45–52.

[100] C. G. Tsinos, F. Foukalas, T. Khattab, and L. Lai, "On channel selection for carrier aggregation systems," *IEEE Transactions on Communications*, vol. 66, no. 2, pp. 808–818, 2018.

[101] F. Foukalas, R. Shakeri, and T. Khattab, "Distributed power allocation for multi-flow carrier aggregation in heterogeneous cognitive cellular networks," *IEEE Transactions on Wireless Communications*, vol. 17, no. 4, pp. 2486–2498, 2018.

[102] I. Gradshteyn and I. Ryzhik, *Table of Integrals, Series, and Products*, 7th ed. London, UK: Academic Press, 2007.

[103] M. Evans, N. Hastings, and B. Peacock, *Statistical Distributions*, 3rd ed. John Wiley & Sons Inc, 2000.

[104] M. Bibinger, "Notes on the sum and maximum of independent exponentially distributed random variables with different scale parameters," 2013, last accessed 19/10/2023. [Online]. Available: https://arxiv.org/abs/1307.3945

[105] M. Abramowitz and I. A. Stegun, *Handbook of mathematical functions with formulas, graphs, and mathematical tables*, 10th ed. Dover, 1972.

[106] M. K. Simon and M.-S. Alouini, *Digital Communications Over Fading Channels*, 2nd ed. New Jersey: Wiley-IEEE Pres, 2005.

[107] M. Bloch, J. Barros, M. R. D. Rodrigues, and S. W. McLaughlin, "Wireless information-theoretic security," *IEEE Transactions on Information Theory*, vol. 54, no. 6, pp. 2515–2534, 2008.

[108] O. S. Badarneh, P. C. Sofotasios, S. Muhaidat, S. L. Cotton, K. M. Rabie, and N. Aldhahir, "Achievable physical-layer security over composite fading channels," *IEEE Access*, vol. 8, pp. 195 772–195 787, 2020.

[109] H. Chen, R. Abbas, P. Cheng, M. Shirvanimoghaddam, W. Hardjawana, W. Bao, Y. Li, and B. Vucetic, "Ultra-Reliable Low Latency Cellular Networks: Use Cases, Challenges and Approaches," *IEEE Commun. Mag.*, vol. 56, no. 12, pp. 119–125, Dec. 2018.

[110] G. Pocovi, H. Shariatmadari, G. Berardinelli, K. Pedersen, J. Steiner, and Z. Li, "Achieving Ultra-Reliable Low-Latency Communications: Challenges and Envisioned System Enhancements," *IEEE Netw.*, vol. 32, no. 2, pp. 8–15, Mar. 2018.

[111] D. Feng, C. She, K. Ying, L. Lai, Z. Hou, T. Q. S. Quek, Y. Li, and B. Vucetic, "Toward Ultrareliable Low-Latency Communications: Typical Scenarios, Possible Solutions, and Open Issues," *IEEE Veh. Technol. Mag.*, vol. 14, no. 2, pp. 94–102, Jun. 2019.

[112] 3rd Generation Partnership Project, "Technical Specification Group Radio Access Network; Study on Scenarios and Requirements for Next Generation Access Technologies (Release 17)," 3GPP, Tech. Rep. 3GPP TR 38.913, Mar. 2022, v17.0.0.

[113] M. Bennis, M. Debbah, and H. V. Poor, "Ultrareliable and Low-Latency Wireless Communication: Tail, Risk, and Scale," *Proc. IEEE*, vol. 106, no. 10, pp. 1834–1853, Oct. 2018.

[114] P. Popovski, J. J. Nielsen, C. Stefanovic, E. d. Carvalho, E. Strom, K. F. Trillingsgaard, A.-S. Bana, D. M. Kim, R. Kotaba, J. Park, and R. B. Sorensen, "Wireless Access for Ultra-Reliable Low-Latency Communication: Principles and Building Blocks," *IEEE Netw.*, vol. 32, no. 2, pp. 16–23, Mar. 2018.

[115] P. Popovski, C. Stefanović, J. J. Nielsen, E. de Carvalho, M. Angjelichinoski, K. F. Trillingsgaard, and A.-S. Bana, "Wireless Access in Ultra-Reliable Low-Latency Communication (URLLC)," *IEEE Trans. Commun.*, vol. 67, no. 8, pp. 5783–5801, Aug. 2019.

[116] H. Ji, S. Park, J. Yeo, Y. Kim, J. Lee, and B. Shim, "Ultra-Reliable and Low-Latency Communications in 5G Downlink: Physical Layer Aspects," *IEEE Wireless Commun.*, vol. 25, no. 3, pp. 124–130, Jun. 2018.

[117] T.-K. Le, U. Salim, and F. Kaltenberger, "An Overview of Physical Layer Design for Ultra-Reliable Low-Latency Communications in 3GPP Releases 15, 16, and 17," *IEEE Access*, vol. 9, pp. 433–444, Jan. 2021.

[118] H. Lee and Y.-C. Ko, "Physical Layer Enhancements for Ultra-Reliable Low-Latency Communications in 5G New Radio Systems," *IEEE Commun. Stand. Mag.*, vol. 5, no. 4, pp. 112–122, Dec. 2021.

[119] G. J. Sutton, J. Zeng, R. P. Liu, W. Ni, D. N. Nguyen, B. A. Jayawickrama, X. Huang, M. Abolhasan, Z. Zhang, E. Dutkiewicz, and T. Lv, "Enabling Technologies for Ultra-Reliable and Low Latency Communications: from PHY and MAC Layer Perspectives," *IEEE Commun. Surveys Tuts.*, vol. 21, no. 3, pp. 2488–2524, Third Quarter 2019.

[120] G. Pocovi, K. I. Pedersen, and P. Mogensen, "Joint Link Adaptation and Scheduling for 5G Ultra-Reliable Low-Latency Communications," *IEEE Access*, vol. 6, pp. 28 912–28 922, May 2018.

[121] C. She, C. Yang, and T. Q. S. Quek, "Joint Uplink and Downlink Resource Configuration for Ultra-Reliable and Low-Latency Communications," *IEEE Trans. Commun.*, vol. 66, no. 5, pp. 2266–2280, May 2018.

[122] J. Cheng and C. Shen, "Relay-Assisted Uplink Transmission Design of URLLC Packets," *IEEE Internet Things J.*, vol. 9, no. 19, pp. 18 839–18 853, Oct. 2022.

[123] S. Kurma, P. K. Sharma, S. Dhok, K. Singh, and C.-P. Li, "Adaptive AF/DF Two-way Relaying in FD Multi-User URLLC System with User Mobility," *IEEE Trans. Wireless Commun.*, vol. 21, no. 12, pp. 10 224–10 241, Dec. 2022.

[124] Y. Zhang, W. Tang, and Y. Liu, "Multi-Cell Grant-Free Uplink IoT Networks with Hard Deadline Services in URLLC," *IEEE Wireless Commun. Lett.*, vol. 11, no. 7, pp. 1448–1452, Jul. 2022.

[125] M. C. Lucas-Estañ and J. Gozalvez, "Sensing-Based Grant-Free Scheduling for Ultra Reliable Low Latency and Deterministic Beyond 5G Networks," *IEEE Trans. Veh. Technol.*, vol. 71, no. 4, pp. 4171–4183, Apr. 2022.

[126] K. Jiang, H. Zhou, X. Chen, and H. Zhang, "Mobile Edge Computing for Ultra-Reliable and Low-Latency Communications," *IEEE Commun. Stand. Mag.*, vol. 5, no. 2, pp. 68–75, Jun. 2021.

[127] D. Van Huynh, S. R. Khosravirad, A. Masaracchia, O. A. Dobre, and T. Q. Duong, "Edge Intelligence-Based Ultra-Reliable and Low-Latency Communications for Digital Twin-Enabled Metaverse," *IEEE Wireless Commun. Lett.*, vol. 11, no. 8, pp. 1733–1737, Aug. 2022.

[128] B. Kharel, O. L. A. López, N. H. Mahmood, H. Alves, and M. Latva-Aho, "Fog-RAN Enabled Multi-Connectivity and Multi-Cell Scheduling Framework For Ultra-Reliable Low Latency Communication," *IEEE Access*, vol. 10, pp. 7059–7072, Jan. 2022.

[129] Y. Wang, W. Chen, and H. V. Poor, "Ultra-Reliable and Low-Latency Wireless Communications in the High SNR Regime: A Cross-layer Tradeoff," *IEEE Trans. Commun.*, vol. 70, no. 1, pp. 149–162, Jan. 2022.

[130] G. Pocovi, T. Kolding, and K. I. Pedersen, "On the Cost of Achieving Downlink Ultra-Reliable Low-Latency Communications in 5G Networks," *IEEE Access*, vol. 10, pp. 29 506–29 513, Mar. 2022.

[131] A. Anand, G. de Veciana, and S. Shakkottai, "Joint Scheduling of URLLC and eMBB Traffic in 5G Wireless Networks," *IEEE/ACM Trans. Netw.*, vol. 28, no. 2, pp. 477–490, Apr. 2020.

[132] Y. Prathyusha and T.-L. Sheu, "Coordinated Resource Allocations for eMBB and URLLC in 5G Communication Networks," *IEEE Trans. Veh. Technol.*, vol. 71, no. 8, pp. 8717–8728, Aug. 2022.

[133] M. Alsenwi, N. H. Tran, M. Bennis, S. R. Pandey, A. K. Bairagi, and C. S. Hong, "Intelligent Resource Slicing for eMBB and URLLC Coexistence in 5G and Beyond: A Deep Reinforcement Learning Based Approach," *IEEE Trans. Wireless Commun.*, vol. 20, no. 7, pp. 4585–460, Jul. 2021.

[134] Y. Zhao, X. Chi, L. Qian, Y. Zhu, and F. Hou, "Resource Allocation and Slicing Puncture in Cellular Networks with eMBB and URLLC Terminals Coexistence," *IEEE Internet Things J.*, vol. 9, no. 19, pp. 18 431–18 444, Oct. 2022.

[135] 3rd Generation Partnership Project, "Technical Specification Group Radio Access Network; NR; User Equipment (UE) radio transmission and reception; Part 1: Range 1 Standalone (Release 17)," 3GPP, Tech. Rep. 3GPP TS 38.101-1, Mar. 2022, v17.5.0.

[136] 3rd Generation Partnership Project, "Technical Specification Group Radio Access Network; NR; User Equipment (UE) radio transmission and reception; Part 2: Range 2 Standalone (Release 17)," 3GPP, Tech. Rep. 3GPP TS 38.101-2, Mar. 2022, v17.5.0.

[137] Z. Pi and F. Khan, "An Introduction to Millimeter-wave Mobile Broadband Systems," *IEEE Commun. Mag.*, vol. 49, no. 6, pp. 101–107, Jun. 2011.

[138] I. A. Hemadeh, K. Satyanarayana, M. El-Hajjar, and L. Hanzo, "Millimeter-wave Communications: Physical Channel Models, Design Considerations, Antenna Constructions, and Link-budget," *IEEE Commun. Surveys Tuts.*, vol. 20, no. 2, pp. 870–913, Second Quarter 2018.

[139] T. S. Rappaport, R. W. Heath, R. C. Daniels, and J. N. Murdock, *Millimeter Wave Wireless Communication*. New Jersey, USA: Prentice-Hall, 2015.

[140] D. Ohmann, A. Awada, I. Viering, M. Simsek, and G. P. Fettweis, "Diversity Trade-offs and Joint Coding Schemes for Highly Reliable Wireless Transmissions," in *Proceedings of the 84th IEEE Vehicular Technology Conference (VTC-Fall 2016)*, Sep. 2016, pp. 1–6.

[141] G. L. Stüber, *Principles of Mobile Communication*, 4th ed. Cham: Springer, 2017, vol. 9781461403.

[142] J. M. Romero-Jerez, F. J. Lopez-Martinez, J. F. Paris, and A. J. Goldsmith, "The Fluctuating Two-Ray Fading Model: Statistical Characterization and Performance Analysis," *IEEE Trans. Wireless Commun.*, vol. 16, no. 7, pp. 4420–4432, Jul. 2017.

[143] J. Zhang, W. Zeng, X. Li, Q. Sun, and K. P. Peppas, "New Results on the Fluctuating Two-Ray Model with Arbitrary Fading Parameters and its Applications," *IEEE Trans. Veh. Technol.*, vol. 67, no. 3, pp. 2766–2770, Mar. 2018.

[144] M. López-Benítez and J. Zhang, "Comments and Corrections to New Results on the Fluctuating Two-Ray Model with Arbitrary Fading Parameters and its Applications," *IEEE Trans. Veh. Technol.*, vol. 70, no. 2, pp. 1938–1940, Feb. 2021.

[145] A. Papoulis and S. U. Pillai, *Probability, Random Variables and Stochastic Processes*, 4th ed. Singapore: McGraw Hill, 2001.

[146] T. K. Vu, M. Bennis, M. Debbah, M. Latva-aho, and C. S. Hong, "Ultra-Reliable Communication in 5G mmWave Networks: A Risk-Sensitive Approach," *IEEE Commun. Lett.*, vol. 22, no. 4, pp. 708–711, Apr. 2018.

[147] A. Wolf, P. Schulz, M. Dörpinghaus, J. C. S. Santos Filho, and G. Fettweis, "How Reliable and Capable is Multi-Connectivity?" *IEEE Trans. Commun.*, vol. 67, no. 2, pp. 1506–1520, Feb. 2019.

[148] A. H. Wojnar, "Unknown Bounds on Performance in Nakagami Channels," *IEEE Trans. Commun.*, vol. 34, no. 1, pp. 22–24, Jan. 1986.

[149] E. D. Vagenas, P. Karadimas, and S. A. Kotsopoulos, "Ergodic Capacity for the SIMO Nakagami-m Channel," *EURASIP J. Wireless Commun. Netw.*, vol. 2009, no. 802067, pp. 1–9, Aug. 2009.

[150] A. I. Sulyman, A. T. Nassar, M. K. Samimi, G. R. MacCartney, T. S. Rappaport, and A. Alsanie, "Radio Propagation Path Loss Models for 5G Cellular Networks in the 28 GHz and 38 GHz Millimeter-wave Bands," *IEEE Commun. Mag.*, vol. 52, no. 9, pp. 78–86, Sep. 2014.

[151] M. K. Samimi, T. S. Rappaport, and G. R. MacCartney, "Probabilistic Omnidirectional Path Loss Models for Millimeter-wave Outdoor Communications," *IEEE Wireless Commun. Lett.*, vol. 4, no. 4, pp. 357–360, Aug. 2015.

[152] M. Polese, M. Giordani, A. Roy, S. Goyal, D. Castor, and M. Zorzi, "End-to-end simulation of integrated access and backhaul at mmwaves," *IEEE*, Sept 2018.

[153] K. Koutlia, B. Bojovic, Z. Ali, and S. Lagén, "Calibration of the 5g-lena system level simulator in 3gpp reference scenarios," *Simulation Modelling Practice and Theory*, vol. 119, p. 102580, Sept 2022.

[154] N. Patriciello, S. Lagén, B. Bojović, and L. Giupponi, "Nr-u and ieee 802.11 technologies coexistence in unlicensed mmwave spectrum: Models and evaluation," *IEEE Access*, vol. 8, pp. 71 254–71 271, Apr 2020.

[155] N. Patriciello, S. Lagen, B. Bojovic, and L. Giupponi, "An E2E simulator for 5G NR networks," *Simulation Modelling Practice and Theory*, vol. 96, p. 101933, Nov 2019.

[156] E. N. Papasotiriou, A.-A. A. Boulogeorgos, K. Haneda, M. F. de Guzman, and A. Alexiou, "An experimentally validated fading model for THz wireless systems," *Scientific Reports*, vol. 11, p. 18717, 2021.